THERMAL ANALYSIS OF DRY SPENT FUEL TRANSPORTATION AND STORAGE CASKS

by

XINHUI CHEN

B.E., Engineering Physics (1989)
Tsinghua University, Beijing

M.E., Engineering Physics (1991)
Tsinghua University, Beijing

SUBMITTED TO THE DEPARTMENT OF
NUCLEAR ENGINEERING
IN PARTIAL FULFILLMENT OF THE REQUIREMENTS
FOR THE DEGREE OF
MASTER OF SCIENCE IN NUCLEAR ENGINEERING

at the

MASSACHUSETTS INSTITUTE OF TECHNOLOGY

April 1996

Signature of Author ____________________
Department of Nuclear Engineering
April 18, 1996

Certified by ____________________
Professor Neil E. Todreas, Nuclear Engineering
Thesis Supervisor

Accepted by ____________________
Professor Jeffrey P. Freidberg
Chairman, Department Committee on Graduate Students

THERMAL ANALYSIS OF DRY SPENT FUEL TRANSPORTATION AND STORAGE CASKS

by
XINHUI CHEN

Submitted to the Department of Nuclear Engineering
on April 18, 1996 in partial fulfillment of the requirements
for the Degree of Master of Science in Nuclear Engineering

ABSTRACT

Three heat transfer mechanisms exist in the dry spent fuel transportation and storage cask: conduction, radiation, and convection. The methodologies for predicting the first two mechanisms in both the COBRA-SFS/RADGEN codes and the MIT Method are studied and compared. Conduction length factors are determined as those values which result in COBRA-SFS calculations generating the same peak clad temperatures for the same heat conduction problem as the MIT effective conductivity method. The functional dependence of these factors on pitch to diameter and wall to diameter ratios, fill gas and bundle size are derived theoretically. Then, radiative heat transfer is modeled along with conductive heat transfer. Studies of rod segments of 15° and 90° show that their effect on the peak clad temperature is within 3.2°C. In addition, a bundle-lumping method is developed which makes it feasible for small computers to simulate large fuel bundles. In this method, a radiation factor, $F_{\varepsilon r}$, is introduced to compensate for excess radiative heat transfer when a large fuel bundle is homogenized into a smaller bundle. Furthermore, sensitivity studies of fuel rod emissivity, wall emissivity, and wall temperature, are undertaken to quantify the effect of these significant parameters on the peak clad temperature. Finally, an analytical heat transfer model is developed for the spent fuel cask and the solution procedure to find the maximum clad temperature is also provided.

Thesis Supervisor:	Dr. Neil E. Todreas
Title:	Professor of Nuclear Engineering and Mechanical Engineering
Thesis Reader:	Dr. Michael J. Driscoll
Title:	Professor Emeritus of Nuclear Engineering

ACKNOWLEDGMENT

I would like to express my sincere appreciation to the Korea Atomic Energy Research Institute (KAERI) for sponsoring this project.

I would like to thank Professor Neil E. Todreas, my thesis supervisor, for his supervision and assistance during the period of completing the thesis and beyond. Additionally, my appreciation and admiration go to Professor Michael J. Driscoll, my thesis reader. Thanks also go to Professor Mujid S. Kazimi, Head of the Department, for his review of Appendix 8.

My appreciation also goes to Judith M. Cuta of Pacific Northwest Laboratory for her prompt response to many code-related questions. Randall D. Manteufel and Phyllis M. Lovett are acknowledged for providing their coded MIT Method. I am also grateful to Tsu-Mu Kao for his appreciable Conduction-only calculations and evaluation of results from the pre-released Cycle 2 of COBRA-SFS.

The deepest of all, I would like to thank my wife, Shuying, for her continuous understanding and encouragement, especially for her sacrifice before and after our son Kevin (who makes my life so colorful and meaningful) was born. Many thanks go to my mom and dad for their living with us to take care of Kevin and my brother for his care-taking at home while my parents are here in the U. S. A..

TABLE OF CONTENTS

LIST OF TABLES

LIST OF FIGURES

CHAPTER 1

INTRODUCTION

One of the most important objectives for a spent fuel transportation and storage cask design is to remove decay heat from the fuel array and maintain the peak clad temperature below certain design limits, i.e., ~ 380°C*. Regulations pertinent to spent fuel transportation and storage require that the spent fuel cladding be protected from degradation (10CFR71.43d for transportation casks and 10CFR72.122h for storage casks). This peak temperature is generally not accessible to measurement, hence these design limits are established far below the material's melting point.

Two methods are reviewed and compared in order to study thermal analysis in a spent fuel transportation and storage cask. One is the COBRA-SFS/RADGEN [1] codes developed at Pacific Northwest Laboratory. The other is the MIT Method [2,3] developed at MIT by Randall D. Manteufel and Neil E. Todreas.

COBRA-SFS (Spent Fuel Storage) is a computer code designed and specialized to predict thermal-hydraulic parameters, e.g., fluid and rod temperatures as well as the fluid velocities, by modeling conductive, radiative, and convective heat transfer for spent fuel transportation and storage systems.

Its Users' Manual [1] generally explains each group of input data, but does not elaborate upon how to select proper values for these parameters. This research project is to provide accurate input parameters for cask configurations of interest to the Korea Atomic Energy Research Institute (KAERI) based on the MIT physical cask modeling work of Manteufel and Todreas [2,3].

The MIT Method is based on the lumped k_{eff}/h_{edge} model and is applicable only to a single square or hexagonal bundle.

The purpose of this study is to calibrate COBRA-SFS against the MIT Method using thermal analysis of standard PWR bundles. Then users (designers and/or reviewers) will have confidence in the code with respect to their thermal analyses of spent fuel transportation and storage cask where the MIT Method is not applicable.

Note that:

(1) unless otherwise specified, COBRA-SFS results in the study are based on Cycle 1 version of the code.

(2) gas properties used in this study and provided in the Appendices are for pure gas, i.e., zero humidity.

---

* This design limit is obtained from [2] and [3].

CHAPTER 2

SCOPE OF THE STUDY

This study is designed to provide improved input parameters in the heat transfer calculation in COBRA-SFS code, to obtain best estimate peak clad temperature in dry spent fuel storage cask. Four major tasks are accomplished within this study and are listed as follows.

2.1 Improved Input Parameters for COBRA-SFS

- Develop improved major input parameters for the description of radiation and conduction in the COBRA-SFS code for analysis of the Korean Standard Cask (KSC-7). These parameters will cover the following conditions and be based on the MIT effective thermal conductivity modeling work.
  - Typical PWR fuel bundles,
  - Backfill gases: Nitrogen and helium,
  - Horizontal orientation,
  - Different boundary conditions, i.e., bundle wall temperatures.
- Review radiation factor including emissivities for cask geometry.
- Review convection factor for cask geometry

2.2 Lumped Effective Conductivity

This task is to simulate typical PWR fuel bundles, i.e., 17x17 array, using a lumped fuel model, i.e., 8x8 array. It is motivated by the intention to reduce computer hardware requirements, i.e., memory and storage space, and to shorten computation time while achieving adequate accuracy. Hence computational expenses will be reduced dramatically.

- Develop a lumped effective conductivity for the fuel bundles within a KSC-7 cask for the following conditions:
  - Typical PWR fuel bundles,
  - Backfill gases: Nitrogen and helium,
  - Horizontal orientation.

2.3 Lumped Effective Conductivity Thermal Analysis of the KSC-7 Cask

- To provide analytic solution equations for the KSC-7 quarter geometry. This solution approximates the geometry and inputs the appropriate bundle powers. The equation set can be coded for solution.

2.4 Comments on KAERI's COBRA-SFS Thermal Analysis of the KSC-7 Cask

- Guidance and review of a COBRA-SFS thermal analysis using inputs developed in 2.1 above.
- Inputs for thermal analysis of the quarter symmetry full cask compared to Korea Atomic Energy Research Institute / Nuclear Environment Management Center (KAERI/ NEMAC) inputs.
- KSC-7 quarter cask input to COBRA-SFS and RADGEN will be reviewed with attention to input for cavity region between fuel basket and inner shell.
- We will examine the KAERI's KSC-7 quarter cask analysis results and offer comments on their character as well as attempt to provide suggestions to resolve problems that are apparent.

CHAPTER 3

COMPUTATIONAL TOOLS

3.1 COBRA-SFS

COBRA-SFS is a generally used thermal-hydraulic analysis code developed at Pacific Northwest Laboratory to predict the fuel temperatures, fluid temperatures and fluid velocities under a wide variety of flow conditions in spent fuel shipping and storage casks. It is a single-phase flow computer code in which the mass, momentum, and energy conservation equations [4] are solved using the semi-implicit method. Its specific features for spent fuel storage cask analysis include:

- A solution method that models 3-D conductive heat transfer through a solid structure network such as a spent fuel cask basket.
- A detailed radiation heat transfer model that simulates radiation on a rod-to-rod basis, e.g., connection with RADGEN, a radiation exchange factor generator for rod bundles.
- Boundary conditions to model radiation and natural convection heat transfer between the cask surface and the ambient air.
- A total flow boundary condition that automatically adjusts the pressure–flow relation.

The conservation equations for mass, momentum and energy are presented in [4]. Note that for the Cycle 1 code of COBRA-SFS, there is no gravity term in the lateral momentum equation. This is why THETA = 90.0 (CHAN.2) (horizontal orientation) [1] represents a case without convective heat transfer in the fill gas region. (THETA is the angle between spent fuel axial direction and the vertical direction, hence THETA = 90.0 specifies a horizontal cask orientation.)

3.2 RADGEN

The Code RADGEN is an ancillary radiation exchange factor generator for COBRA-SFS that uses these exchange factors to describe the net energy transferred from one surface to any other surfaces in an enclosure (See Figure 3-1). RADGEN has the capability to handle rod patterns of square and triangular (or hexagonal) pitch as well as open channel geometries. Specifications for RADGEN can be found in [5]. Be warned that:

(1) RADGEN is only valid for pitch-to-diameter ratio $1.0 \leq p/d \leq \sqrt{2}$, which is applicable to typical PWR fuel bundles,

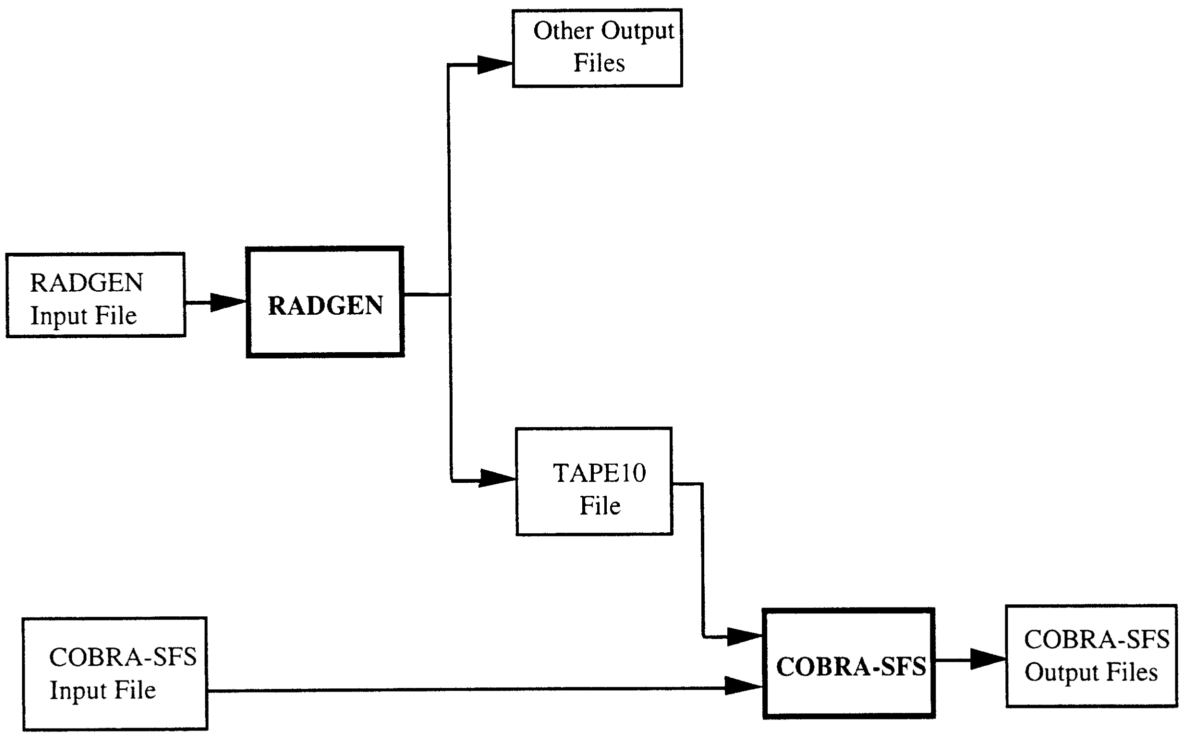

Figure 3-1 Schematic Block Diagram of COBRA-SFS / RADGEN Code

(2) In the current version of RADGEN, Groups RADGEN.3 and RADGEN.4 are input in a combined fashion in one line instead of two separate lines as wrongly described in its User's Manual [5].

3.3 The MIT Method

The MIT Method is based on the lumped k_{eff}/h_{edge} model by Randall D. Manteufel and Neil E. Todreas [2,3]. As described in Reference [3], the lumped k_{eff}/h_{edge} model is expressed using a set of two coupled algebraic equations. The first equation applies to the interior region:

$$\frac{Q \cdot F_{peak}}{L_a \cdot S} = F_{cond} \cdot k_{gas} \,(T_m - T_e) + C_{rad}\, \sigma \pi d \cdot (T_m^4 - T_e^4) \qquad (3\text{-}1)$$

while the second equation is used in the edge region within the enclosing wall:

$$\frac{Q \cdot F_{peak}}{L_a \cdot L_c} = \frac{F_{cond,w} \cdot k_{gas}}{(1 - f/2) \cdot w} \cdot (T_e - T_w) + \frac{C_{rad,w,2}\, \sigma \pi d}{(1 - f/2) \cdot p} \cdot (T_e^4 - T_w^4) \qquad (3\text{-}2)$$

where

Q	= total assembly decay power
F_{peak}	= axial power peaking factor
L_a	= assembly active axial length
L_c	= assembly cross-sectional circumferential length
S	= assembly cross-sectional conduction shape factor (13.5738 for square, 12.8365 for hexagonal and 4.0π for circular shape assemblies)
k_{gas}	= fill gas conductivity
F_{cond}	= conduction factor (interior)
$F_{cond,w}$	= wall conduction factor
T_m	= maximum fuel rod temperature
T_e	= extrapolated wall temperature (imaginary)
T_w	= average enclosing wall temperature (true)
C_{rad}	= radiative heat transfer coefficient for the interior region
$C_{rad,w,1}$	= first wall radiative heat transfer coefficient for the edge region
$C_{rad,w,2}$	= second wall radiative heat transfer coefficient for the edge region
d	= clad outside diameter of the fuel rod
p	= rod-to-rod pitch
w	= edge rod center-to-wall distance
f	= edge-to-interior heat transfer ratio.

A code package of three individual programs has been prepared [6] to solve these two equations using Macintosh software *Mathematica* [7,8]. These three programs are:

(1) Program "gas.m" which provides the thermal properties, i.e., thermal conductivity, specific heat capacity, of four media, air/nitrogen (N_2), argon (Ar), helium (He) and vacuum.

(2) Program "keff.m" which provides the source for the lumped k_{eff}/h_{edge} model.

The first two programs are generic and contain undefined variables of the lumped k_{eff}/h_{edge} model.

(3) Program "MIT14X14.m" which contains problem-specific input data and, after running, provides the maximum differential temperature between the boundary wall and the rod clad or the maximum rod clad temperature depending on user's preference. It is not restricted to 14x14 arrays as the program title may imply.

These three programs are executed individually but in series (See Figure 3-2.). First "gas.m" is executed which may take about 0.8 second, then "keff.m" is executed which may need about 0.6 second, and finally "MIT14X14.m" is executed whose execution needs approximately 8.9 seconds. The output of "MIT14X14.m" is tabulated with the fill medium in the first column, power (in watt) in the second column and predicted differential temperature $\Delta T = T_m - T_w$ (in °C) in the third column. More specialized output, i.e., $\Delta T_w = T_e - T_w$ (°C), k_c/k_{eff}, h_{cw}/h_{edge}, can be found in the output of "keff.m" by eliminating "(*" and "*)" in the "Print"-related statements.

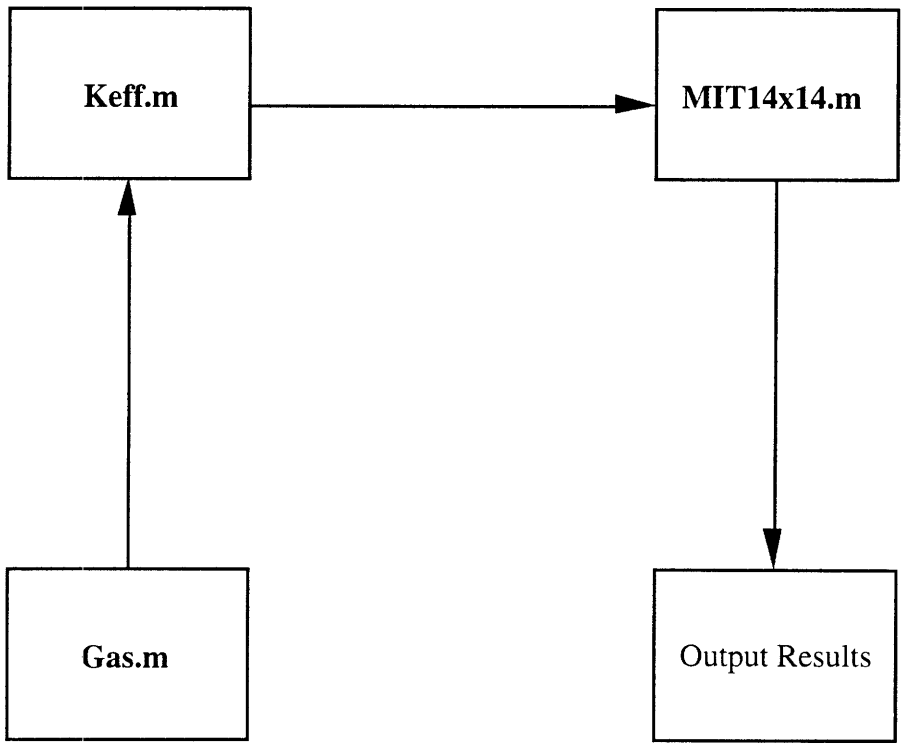

Figure 3-2 Schematic Block Diagram of the MIT Method

CHAPTER 4

SUMMARY OF THE APPROACH

The MIT Method [2,3] is to be used as the technical basis to adjust the COBRA-SFS input parameters affecting conduction, radiation and convection (if possible) heat transfer to provide state-of-the-art thermal-hydraulic analyses for the Korean KSC-4 and KSC-7 casks. The modeling of each heat transfer process is discussed next.

4.1 Conduction Modeling

4.1.1 COBRA-SFS Conduction Model

The COBRA-SFS fluid conduction model simulates one-dimensional fluid conduction and accommodates lateral constriction in this 1-D geometry by an input factor, GK. In the derivation of the equations, the potential and kinetic energies are assumed to be negligible.

Basically, the COBRA-SFS fluid conduction model is based on Fick's First Law (Refer to Equation 7-11), that is, the heat flux is proportional to the temperature gradient. This gradient is expressed as the quotient of the temperature difference ΔT and the effective conduction length, ℓ_c, which is the rod-to-rod or wall-to-rod pitch, ℓ_i, divided by the conduction length factor, GK.

Specifically, the conduction-only calculation in COBRA-SFS is achieved using a combination of the following parameters:

THETA	= 90.0	(CHAN.2)
NFCON	= 1	(HEAT.1)
AHL1(I)	= 0.0	(HEAT.2)
AHL2(I)	= 0.0	(HEAT.2)
AHL3(I)	= 0.0	(HEAT.2)
AHL4(I)	= 1.0	(HEAT.2)
GK	= suitable value	(HEAT.5)
ISCHEME	= 1	(CALC.1)
C1(I)	> 0.0	(BDRY.2)
C2(I)	= 0.0	(BRDY.2)
C3(I)	= 0.0	(BDRY.2)

Omitting Group RADG

4.1.2 The MIT Conduction Model

The MIT conduction model uses the effective conductivity of a composite region representing fuel rods immersed in the medium (fluid or vacuum). The effective conductivity is defined differently for the interior and edge bundle regions:

$$k_{eff} = F_{cond}\, k_{gas} \qquad \text{(for the interior)} \qquad (4\text{-}1)$$

$$h_{cond} = F_{cond,w}\, k_{gas}/[(1 - f/2)\, w] \qquad \text{(for the edge)} \qquad (4\text{-}2)$$

where F_{cond} is the conduction factor which compensates for heat transfer through the rods and constriction in the fluid conduction path due to the presence of the fuel rods. The factor F_{cond} is a function of:

(1) Array configuration pattern, square (SQ) or hexagonal (HX).

(2) Volume fraction, f.

(3) Core-to-gas conductivity ratio, k_{core}/k_{gas}.

(4) Tube-to-gas conductivity ratio, k_{tube}/k_{gas}.

(5) Inner-to-outer radius ratio, r_i/r_o.

The two regions are connected to each other by an extrapolated wall temperature T_e (see Figure 4-1). For solid fuel rods, $r_i = 0$, $k_{core} = k_{tube} = k_{rod}$, so that F_{cond} can be reduced to a function of the following variables:

$$F_{cond} = \text{function}\ (\{SQ\} \text{ or } \{HX\},\ f,\ k_{rod}/k_{gas}) \qquad (4\text{-}3)$$

Complete numerical values of F_{cond} under different conditions are listed in Tables 3.2-1 to 3.2-4 of Reference [2]. For our standard bundle, the appropriate values of F_{cond} are summarized in Table 4-1.

4.1.3 Isothermal Rod (Clad)

Compared with the gas conductivities ($k_{He} = 0.2$ W/m°C, $k_{N2} = 0.04$ W/m°C, hence $k_{He} / k_{N2} = 5.0$), fuel rod materials have much higher conductivities ($k_{Zr} = 15$W/m°C, $k_{UO2} = 5$W/m°C). Hence heat conduction is a more significant process in the rods than in the fill gas. Consequently, the azimuthal temperature variation in each rod is almost negligible at nominal decay heat power level. Hence fuel rods can be treated as isothermal rods. This assertion can further be confirmed by the Biot Criterion.

Biot Criterion is a criterion to determine whether isothermal temperature distribution assumption in the solid is valid in the solid-fluid heat transfer situation, i.e., to determine whether the Lumped Parameter Method (LPM) is applicable to the solid. If the solid is isothermal, then its temperature is uniformly distributed and we can treat the solid as if it were a single point. The Biot number is defined by Equation 4-4.

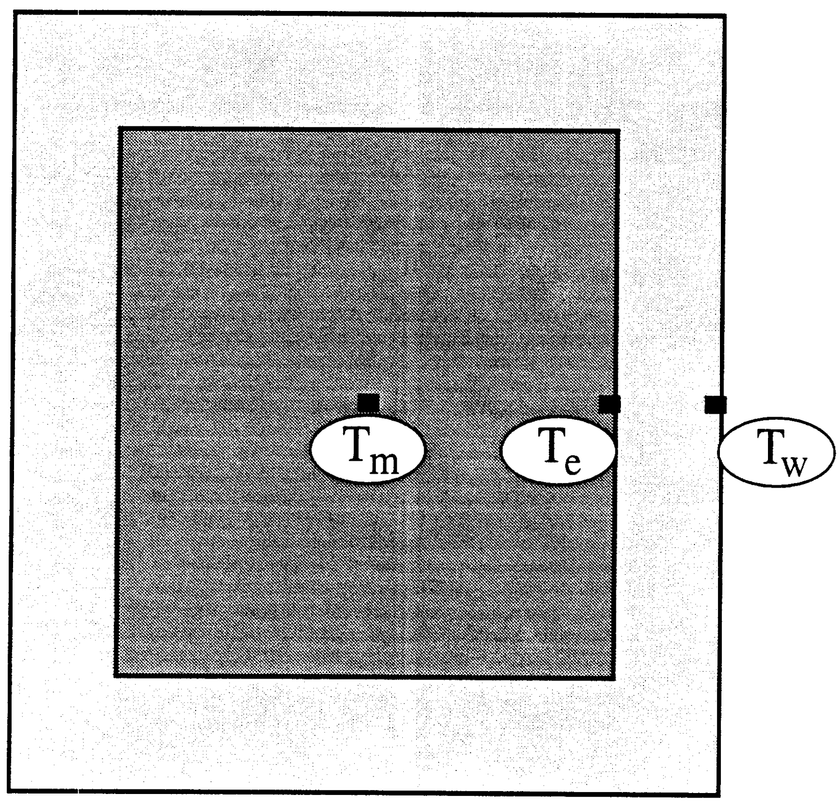

Figure 4-1. MIT Model – Locations of T_m, T_e and T_w.

Table 4-1. F_{cond} as a Function of p/d for Square Array [2]

p/d	Isothermal	He		N_2	
		w/c&f *	w/c **	w/c&f	w/c
1.32	2.680	2.504	2.168	2.642	2.555
1.326*	**2.651**	2.479	2.151	2.614	2.530
1.33	2.632	2.463	2.140	2.596	2.513

* w/c&f ----- zero fuel-clad contact resistance

** w/c ----- infinite fuel-clad contact resistance

*** Results of p/d = 1.326 are interpolated from those of p/d = 1.32 and 1.33.

$$Bi = \frac{h\ D}{k_s} \tag{4-4}$$

where

h = heat transfer coefficient between solid and fluid, W/m^2°C

D = geometry dimension, i.e., diameter of the solid, m

k_s = thermal conductivity of the solid, i.e., zircaloy cladding, W/m°C

If Bi << 1 (i.e., k_s is very large and h is small), then heat conduction in the solid is very fast and effective, and isothermal assumption in the solid is valid.

Biot number differs from Nusselt number (defined in Equation 4-5) in that in Nusselt number, k_f is the thermal conductivity of the fluid, i.e., that of He or N_2 while in Biot number, k_s is the thermal conductivity of the solid.

$$Nu = \frac{h\ D}{k_f} \tag{4-5}$$

Dividing Equation 4-4 by Equation 4-5 and rearranging, we get

$$Bi = \frac{k_f}{k_s}\ Nu \tag{4-6}$$

A set of Biot numbers is calculated for Nusselt numbers ranging from 1.0 to 10.0 using Equation 4-6. The result is listed in Table 4-2. From the Table, the following conclusions can be drawn:

(1) For a wide range of Nusselt number, i.e., from 1.0 to 10.0, Biot number is much smaller than unity. Hence the isothermal cladding assumption is valid;

(2) If other conditions are the same, Biot numbers are five times smaller for N_2 than for He. Hence, the isothermal cladding assumption is more valid for N_2 than for He. This fact explains why the GK model developed in Chapter 7 are more accurate for N_2 than for He. (See Table 7-2.)

4.1.4 Temperature Gradient in Pellet, Gap and Clad

Under nominal power operation conditions (i.e., average linear power density $\overline{q'}$ = 16 kW/m) in the reactor core, the temperature gradient in the pellet and gap is very large compared with that in the cladding. Typical values at hot spot are 1200°C from the fuel centerline to fuel outside surface (pellet), 350°C from fuel outside surface to clad inside surface (gap), and 60°C from clad inside surface to its outside surface (clad).

Table 4-2. Biot Numbers for Zircaloy Cladding-Fluid Pairs vs. Nusselt Number

Nu *	Bi	
	He	N_2
1.0	0.0133	0.00267
3.66	0.0488	0.00976
10.0	0.133	0.0267

* Nusselt numbers ranging from 1.0 to 10.0 cover a wide spectrum of convective heat transfer. (Refer to Table 8-1.)

In dry storage spent fuel cask, the spent fuel bundles have been discharged out of reactor core for several years, their decay heat generation rate is 3 to 4 orders of magnitude smaller (i.e., $\overline{q'}$ = 5W/m for bundles discharged out of the core for 1.5 years in this study). Hence the temperature gradient is 3 to 4 orders of magnitude smaller than that under power operation. This characteristic will be demonstrated below by examining KAERI's typical spent fuel bundles stored in KSC-7 cask.

There are seven spent fuel bundles in KAERI's KSC-7 cask (see Figure 5-3) with a total decay power of 32.3 kW. On average, each bundle has a power of 4614 W.

1) Calculate linear power density

Average linear power density

$$\overline{q'} = \frac{\text{Bundle Power}}{(\text{\# of Rods/Bundle}) \times (\text{Active Core Height})} \qquad (4\text{-}7)$$

$$= \frac{4614 \text{ W}}{(17\text{x}17)\text{x}(365.76 \text{ cm})}$$

$$= 4.365 \text{ x}10^{-2} \text{ W / cm}$$

Maximum Linear Power Density

$q'_{max} = \overline{q'} \text{ x } F_{peak} = 4.365 \text{ x } 10^{-2}\text{x}1.206 = 5.264 \text{ x } 10^{-2}$ W/cm.

where

F_{peak} = (axial) power peaking factor

2) Obtain geometric and physical data from input file

We obtain geometric and physical data, i.e., material properties, from KAERI's input file and these fundamental data are incorporated into our input deck for COBRA-SFS.

Geometric data (See Figure 4-2.):

Radius of fuel pellet, r_f	= 0.4095 cm
Radius of clad inside surface, r_{ci}	= 0.4178 cm
Radius of clad outside surface, r_{co}	= 0.4750 cm
Average gap radius, $r_g = (r_f + r_{ci}) / 2$	= 0.4136 cm

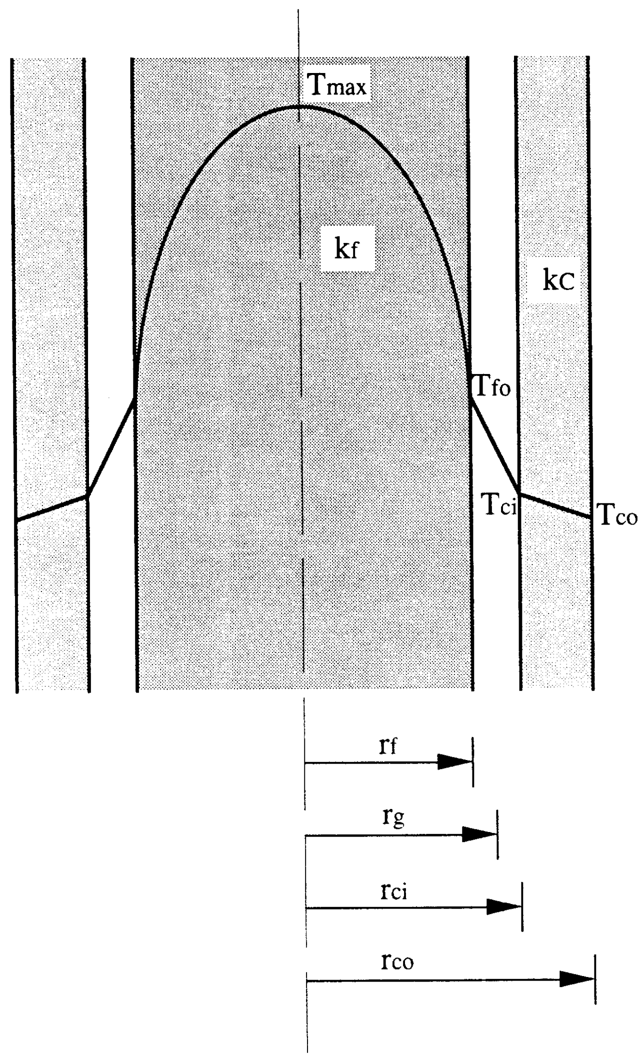

Figure 4-2 Schematic Diagram of a Typical Fuel Rod Section

Physical data:

Conductivity of pellet, k_f	= 3.0 Btu / (h ft °F) = 5.275 W / (m °C)
Conductivity of clad , k_c	= 10.0 Btu / (h ft °F) = 17.58 W / (m °C)
Gap conductance, h_g	= 1000.0 Btu / (h ft^2 °F) = 5861.1 W / (m^2 °C)

3) Calculate temperature gradient (Refer to [9])

Temperature gradient in fuel pellet can be expressed as

$$T_{max} - T_{fo} = \frac{q'_{max}}{4\pi k_f} \qquad (4\text{-}8)$$

Plugging above data into Equation 4-8 yields

$$T_{max} - T_{fo} = \frac{5.264 \times 10^{-2}\,\mathrm{W/cm}}{4 \times 3.14 \times 5.275\mathrm{W/(m \cdot °C)}} = 0.080°\mathrm{C}$$

Temperature gradient in gap can be expressed as

$$T_{fo} - T_{ci} = \frac{q'_{max}}{2\pi r_f h_g} \qquad (4\text{-}9)$$

Plugging above data into Equation 4-9 yields

$$T_{fo} - T_{ci} = \frac{5.264 \times 10^{-2}\,\mathrm{W/cm}}{2 \times 3.14 \times 0.4136\mathrm{cm} \times 5861.1\mathrm{W/(m^2 \cdot °C)}} = 0.035°\mathrm{C}$$

Temperature gradient in cladding can be expressed as

$$T_{ci} - T_{co} = \frac{q'_{max}}{2\pi k_c} \cdot \left(\frac{r_{co}}{r_{ci}}\right) \qquad (4\text{-}10)$$

Plugging above data into Equation 4-10 yields

$$T_{ci} - T_{co} = \frac{5.264 \times 10^{-2}\,\mathrm{W/cm}}{2 \times 3.14 \times 17.58\mathrm{W/(m°C)}} \cdot \ln\left(\frac{r_{co}}{r_{ci}}\right) = 0.006°\mathrm{C}$$

Total temperature drop from centerline of pellet to cladding outside surface is

$$T_{max} - T_{co} = 0.080\ °\mathrm{C} + 0.035°\mathrm{C} + 0.006°\mathrm{C} \approx 0.12°\mathrm{C}$$

From the above calculation, it is believed that temperature gradient across the fuel pin is virtually negligible in spent fuels. This is why the design limit, in thermal calculation of the spent fuel cask, is placed on the cladding temperature rather than the fuel centerline temperature as under power operation conditions.

4.2 Radiation Modeling

4.2.1 COBRA-SFS Radiation Model

The COBRA-SFS radiative heat transfer model is based on the Stefan-Boltzmann black body model multiplied by the gray body radiation exchange factor, F_{ij}. Means to compensate for the error from the non-uniform radiosity effect introduced by the finite rod segment length used by COBRA-SFS is not provided for by definition of user-specified input parameters. The radiation heat transfer from one surface to another is calculated using Equation 4-11.

$$q''_{rad} = \sigma F_{ij} \left(T^4_i - T^4_j\right) \tag{4-11}$$

where

q''_{rad} = the radiative heat flux

σ = the Stefan-Boltzmann constant

F_{ij} = the gray body radiation exchange factor (between surfaces i and j) based on geometry and surface emissivity.

With Group RADG included in the input file, COBRA-SFS has two different ways to model radiative heat transfer:

(1) By reading gray body exchange factors and emissivities via I/O Unit 10 from a file generated by the auxiliary code called RADGEN; or

(2) By supplying blackbody view factors and emissivities in Groups RADG.2 and RADG.3.

Although both options can be used for the same problem, Option (2) is preferential in simple cases with a few surfaces while Option (1) is effective in more complex cases where many surfaces are present. When Option (1) is used, the walls of the assembly must be modeled with eight solid structure nodes, two on each side, and they must be numbered after all fuel rods have been counted.

4.2.2 The MIT Radiation Model

The MIT Method of radiation modeling uses one radiative coefficient (C_{rad}) for radiative heat transfer in the interior region and two wall radiative coefficients ($C_{rad,w,1}$ and $C_{rad,w,2}$) for radiative heat transfer in the edge region. The two regions are related to each other by an imaginary wall temperature T_e to connect the real wall temperature T_w and the peak rod temperature T_m. Numerically, the values for C_{rad}, $C_{rad,w,1}$ and $C_{rad,w,2}$ under different conditions can be found in Appendix H of Reference [2]. The non-uniform radiosity effect has been accommodated by developing the radiative coefficients from Monte Carlo simulations using 15° circumferential rod segments.

4.3 Convection Modeling

4.3.1 COBRA-SFS Convection Model

Convective heat transfer model in COBRA-SFS is based on the Nusselt Number Nu (= h D/k) from which the heat transfer coefficient h (= Nu k/D) between the solid surface and the medium is obtained. In the fluid energy equation, the surface-averaged convective heat flux, q''_{conv}, is modeled using the expression:

$$q''_{conv} = h\,(T_s - T_{gas}) \qquad (4\text{-}12)$$

where

q''_{conv} = the convective heat flux
T_s = the rod or slab surface temperature
T_{gas} = the medium temperature.

COBRA-SFS models convective heat transfer in Groups HEAT.1, HEAT.2 (for the interior) and BDRY.2 (for the edge boundary) by the following parameter values:

AHL1(I)	= 0.0	(HEAT.2)
AHL2(I)	= 0.0	(HEAT.2)
AHL3(I)	= 0.0	(HEAT.2)
AHL4(I)	> 1.0, i.e., 3.66	(HEAT.2)
C1(I)	> 0.0	(BDRY.2)
C2(I)	> 0.0	(BRDY.2)
C3(I)	> 0.0	(BDRY.2)

4.3.2 The MIT Convection Model

The MIT Method defines the Critical Rayleigh Number Ra_{crit} to model the convective heat transfer. For Rayleigh Numbers below Ra_{crit}, the fill gas is regarded as stagnant and, hence, the convective heat transfer mechanism can be ignored. For Rayleigh Numbers above Ra_{crit}, the flow of the fill gas will enhance heat exchange. This mechanism is modeled by increasing the conduction factor F_{cond} by a factor of $(Ra/Ra_{crit})^{1/4}$ (See Equation 4-13). The major obstacle is to determine the value of the parameter Ra_{crit} which defines the transition from the conduction to the convection regime.

$$k_{cond} = \begin{cases} F_{cond}\,k_{gas} & (Ra \le Ra_{crit}) \\ F_{cond}\,k_{gas}\,(Ra/Ra_{crit})^{1/4} & (Ra > Ra_{crit}) \end{cases} \qquad (4\text{-}13)$$

CHAPTER 5

CONFIGURATIONS OF INTEREST AND BOUNDARY CONDITIONS

Several configurations have been set up to study the heat transfer mechanisms in the KSC-7 spent fuel cask:

(1) A 17x17 square fuel array with surrounding walls on four sides (Figure 5-1).

(2) An 8x8 square lumped fuel array (Figure 5-2).

(3) A quarter of the Korean KSC-7 cask (Figure 5-4) extracted from Figure 5-3 based on Reference [10]. The cask body is comprised of fuel baskets, inner shell, intermediate shell and outer shell made of stainless steel. Fuel baskets are located inside the inner shell cavity. The space between the inner and intermediate shells is cast with pure lead to shield gamma rays. The neutron shield is cast from a silicone mixture and located between the intermediate and outer shells. There are 80 copper plates attached in silicone mixture to enhance heat transfer effectiveness in the neutron shielding layer. Eighty external cooling fins (not shown in Figure 5-3) are attached to the outer shell to increase heat transfer into the environment.

The first configuration, the 17x17 array, is designed to evaluate COBRA-SFS's heat transfer models, including conduction, radiation, and convection against the respective MIT models. Its geometrical parameters are:

fuel rod height	L_a	= 144" (total height = 160")
rod diameter	d	= 0.3740"
array pitch	p	= 0.4961"
edge rod center-to-wall distance	w	= 0.5591"
wall thickness	δ	= 0.3937"

The second configuration is an 8x8 lumped fuel array. The geometry of this array is established as follows:

fuel rod height	L_a	= 144" (total height = 160")
rod diameter	d	= 0.7948"
array pitch	p	= 1.0539"
edge rod center-to-wall distance	w	= 0.8389"
wall thickness	δ	= 0.3937"

These 8x8 array values are obtained using our homogenization method which will be discussed later in Chapter 7.

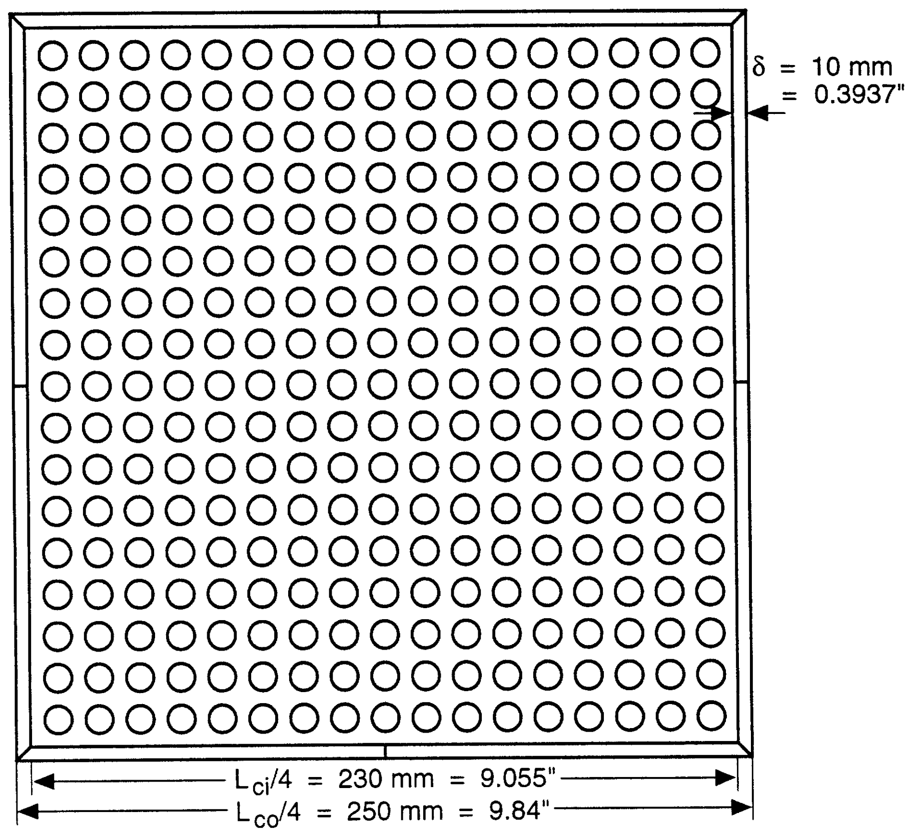

Figure 5-1 17x17 Array Configuration.

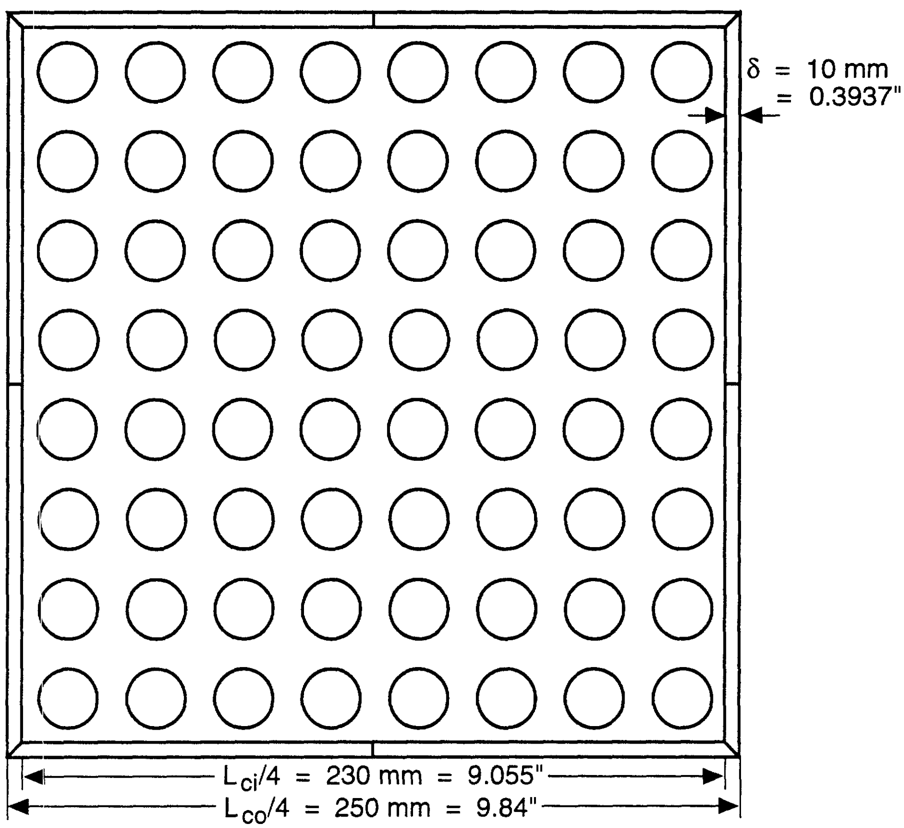

Figure 5-2 8x8 Lumped Fuel Array.

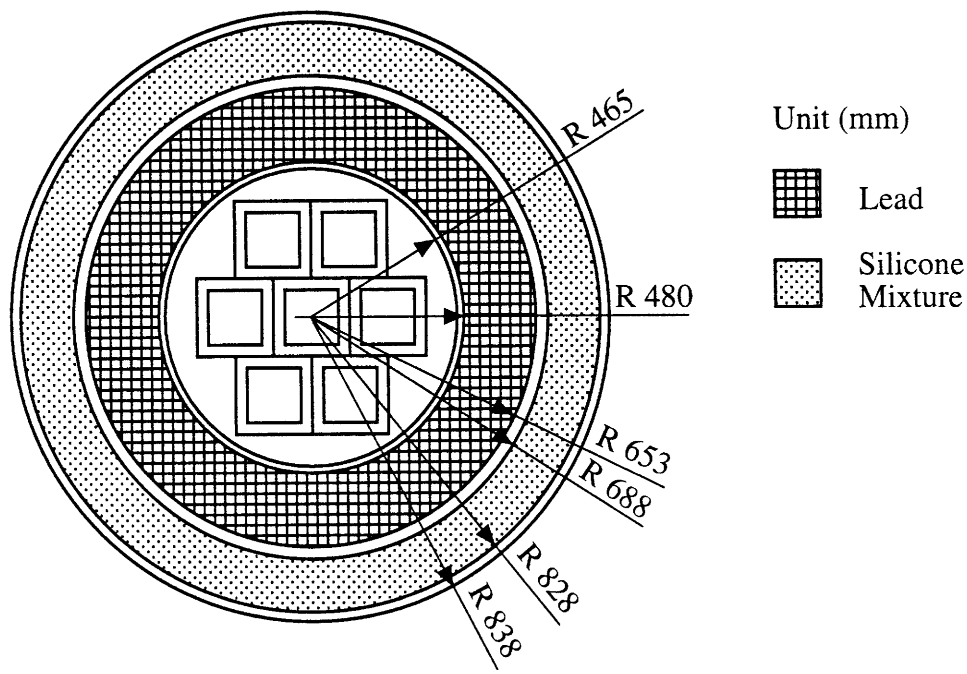

Figure 5-3 Cross-Section of Fuel Basket for KSC-7 Cask (adapted from KAERI).

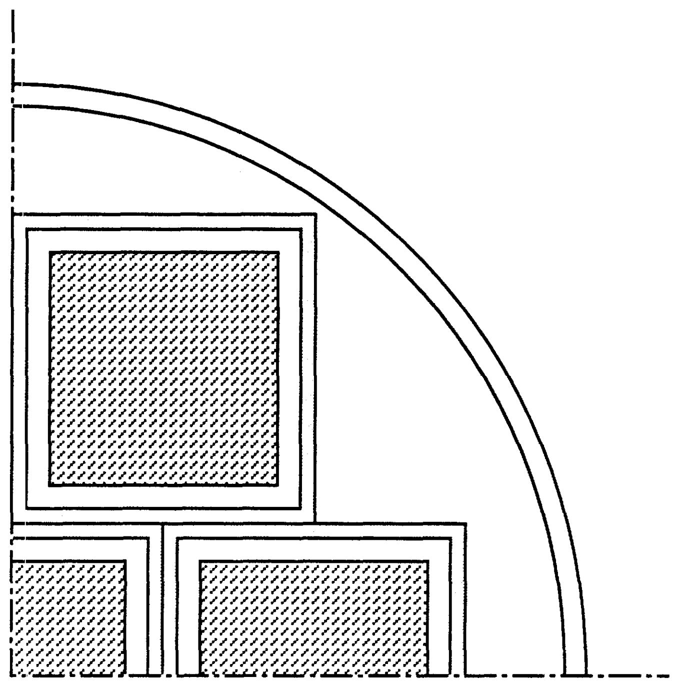

Figure 5-4 Quarter Sector of KSC-7 Cask to be Analyzed

The final configuration is a quarter sector of the KSC-7 cask. The full cross-section is shown in Figure 5-3 and the quarter sector in Figure 5-4.

The KSC-7 cask contains seven 17x17 fuel assemblies with two in the first row, three in the second row and two in the third row (see Figure 5-3). Each of the assemblies is identical to the one shown in Figure 5-1, whose outer side length is 250 mm (9.84"). The inner diameter of the inner shell is 930 mm (36.90"), and the inner shell wall thickness is 15 mm (0.60").

CHAPTER 6

PREDICTED TEMPERATURES FOR 17X17 ARRAY BY COBRA-SFS PRECEDING THIS STUDY

The goal of this project is to enhance COBRA-SFS predictions by providing evaluated input parameters. Hence, it is instructive to record the COBRA-SFS base case for later comparison with results using recommended enhanced input. We define two base cases—Nitrogen and Helium fill gases—with Conduction (GK = 1) and Radiation (RADGEN Modeling, i.e., 90° rod segments, $\varepsilon_r = 0.8$, $\varepsilon_w = 0.3$) models employed.

In each case the spent fuel bundle's operating power is 4684 W (rounded upper bound value from a 32.3 kW cask load from seven bundles) and the geometry is that of the 17x17 square array as defined in Chapter 5. The base cases are summarized in Table 6-1.

Table 6-1. Maximum Clad Temperature for Standard Square Array under Base Case COBRA-SFS Modeling—Conduction and Radiation, 17x17 Bundle, 4684 W

Conditions	Nitrogen	Helium
GK = 1		
90° segments		
$\varepsilon_r = 0.8$, $\varepsilon_W = 0.3$	428.0°C	368.4°C

CHAPTER 7

RESULTS OF THE STUDY

7.1 Improved Input Parameters for COBRA-SFS

7.1.1 Conduction

COBRA-SFS and the MIT Method deal with conduction differently. COBRA-SFS uses a conduction length factor GK (= $1/Z_k$) to generate an effective conduction length $\ell_c = \ell * Z_k = \ell/GK$ while the MIT Method employs the conduction factor, F_{cond}, which differs for the interior region and the edge region to compensate for the enhancement of the conductive heat transfer due to the fuel rod and bundle wall surfaces.

For the same heat conduction problem, however, the two methods should produce the same (or comparable) results. This concept links GK in COBRA-SFS and F_{cond} in the MIT Method. Thus it is possible to find an appropriate GK value for COBRA-SFS input using the MIT Method.

Heat conduction in the plane of the real bundle is two-dimensional (2D), whereas it is possible analytically to relate GK and F_{cond} by considering a one-dimensional (1D) strip model for conduction heat transfer. Hence, the true relationship between GK and F_{cond} needs to be built from comparative 2D COBRA-SFS and MIT Method calculation results. Nevertheless, it is instructive to perform 1D strip model comparisons to confirm the approximate range of GK values which match the MIT Method.

In deriving GK expressions, the difference between the maximum clad temperature and the bundle wall temperature, i.e., $T_m - T_w$, is expressed as a function of geometry, physical parameters, power deposition, and Conduction Factor (F_{cond}) using the MIT Method. Then, the same temperature difference is expressed in terms of geometry, physical parameters, power deposition, and conduction length factor (GK) using COBRA-SFS strategy. By equating the two temperature differences, relationships for the GK factors are obtained. Note that, for cases of odd number of rods per row and even number of rods per row, the GK formula are slightly different.

The following is the implementation of the 1D strip model assessment. From the MIT Method [2] (See Figure 7-1):

$$\bar{q}''' = \frac{\left(\frac{n}{2}\right)\left(\frac{\pi d_f^2}{4}\right) q'''_{rod}}{L \cdot p} = \frac{\left(\frac{n}{2}\right) q'_{rod}}{L \cdot p} \tag{7-1}$$

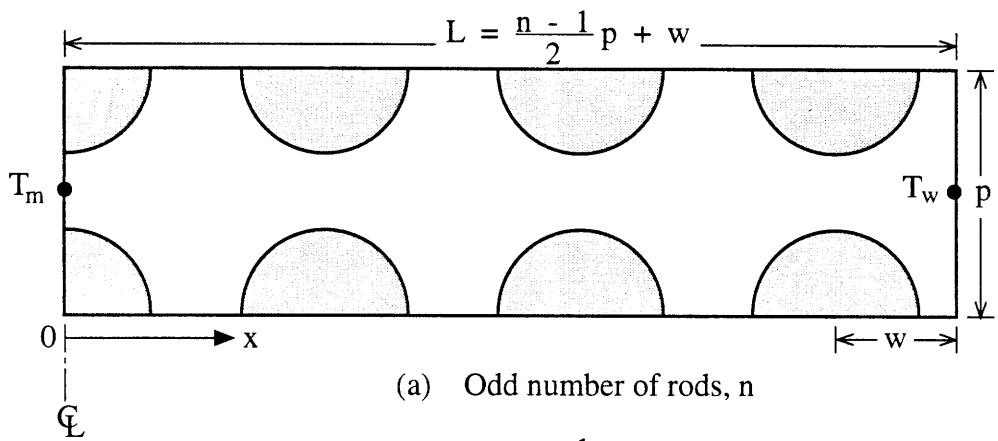

(a) Odd number of rods, n

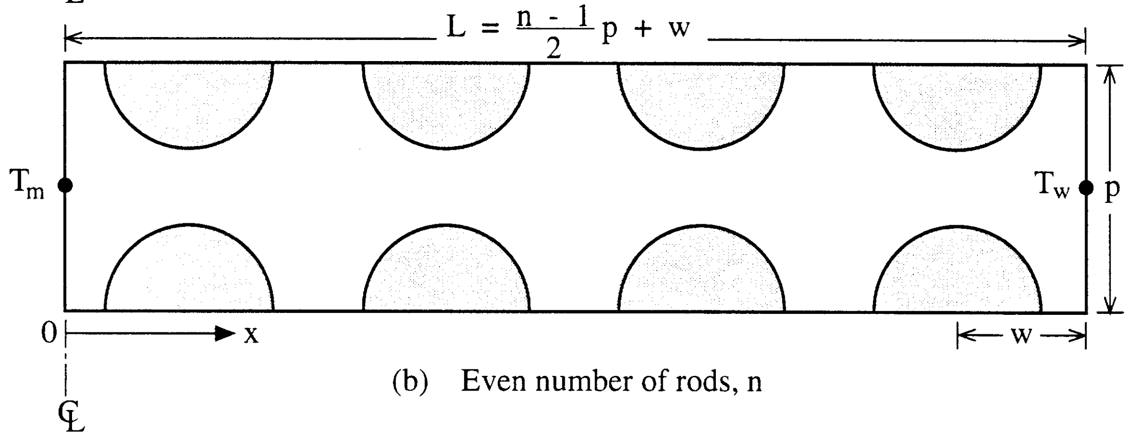

(b) Even number of rods, n

Figure 7-1. The MIT Conduction Model.

where

$\bar{q}'''$ = average volumetric energy generation rate in the whole rectangle, W/m^3

n = number of rods per row in the square array

d_f = fuel pellet diameter

p = pitch of the square array, m

L = half of the square array inner side length, m

q'''_{rod} = rod volumetric energy generation rate, W/m^3

q'_{rod} = rod linear power rate (= $\frac{1}{4}\pi d_f^2 q'''_{rod}$), W/m

The steady state heat conduction equation [9] is:

$$\nabla \cdot k_{eff} \nabla T + \bar{q}''' = 0 \tag{7-2}$$

where

k_{eff} = effective conductivity.

Assuming k_{eff} is constant, Equation 7-2 can be written as

$$k_{eff} \nabla^2 T = -\bar{q}''' \tag{7-3}$$

For the one-dimensional heat transfer problem (Figure 7-1), Equation 7-3 can be reduced to

$$\frac{d^2T}{dx^2} = -\frac{\bar{q}'''}{k_{eff}} \tag{7-4}$$

Integrate Equation 7-4 once

$$\frac{dT}{dx} = -\frac{\bar{q}'''}{k_{eff}} x + C_1 \tag{7-5}$$

where

C_1 = first integration constant

Applying Boundary Condition 1: $\left.\frac{dT}{dx}\right|_{x=0} = 0$ to solve for C_1, we get $C_1 = 0$.

With another integration, Equation 7-5 becomes

$$T(x) = -\frac{\bar{q}'''}{2k_{eff}} x^2 + C_2 \tag{7-6}$$

where

C_2 = second integration constant

Applying Boundary Condition 2: $T(L) = T_w$ to solve for C_2, we get

$$C_2 = T_w + \frac{\overline{q}'''}{2k_{eff}} L^2$$

Hence the temperature distribution is

$$T(x) = T_w + \frac{\overline{q}'''}{2k_{eff}}(L^2 - x^2) \tag{7-7}$$

The maximum temperature, T_m, occurs at x = 0 and is

$$T_m = T_w + \frac{\overline{q}'''}{2k_{eff}} L^2 \tag{7-8}$$

or equivalently

$$T_m - T_w = \frac{\overline{q}'''}{2k_{eff}} L^2 \tag{7-9}$$

Substituting for $\overline{q}'''$ from Equation 7-1 yields

$$T_m - T_w = \frac{\left(\frac{n}{2}\right) \cdot q'_{rod}}{2k_{eff}} \cdot \frac{L}{p} \tag{7-10}$$

For COBRA-SFS, the conduction model is illustrated in Figure 7-2. Hence,

$$q'_i = k_{gas,COBRA} \frac{S(T_{Hi} - T_{Li})}{\ell_i / GK} \tag{7-11}$$

Solve for T_{Hi} from Equation 7-11

$$T_{Hi} = T_{Li} + \frac{q'_i \cdot \ell_i}{k_{gas,COBRA} \cdot S \cdot GK} \tag{7-12}$$

where

i	=	cell sequential number from center to edge
T_{Hi}	=	higher temperature in cell i, K
T_{Li}	=	lower temperature in cell i, K
q'_i	=	linear power rate in cell i, W/m
$k_{gas,COBRA}$	=	thermal conductivity used in COBRA-SFS input deck W/m°C
S	=	gap between rods (= p-d), m
d	=	outside clad diameter of fuel rod, m
p	=	pitch, m
ℓ_i	=	conduction length in cell i, m
GK	=	cell conduction length factor, assumed constant for all cells

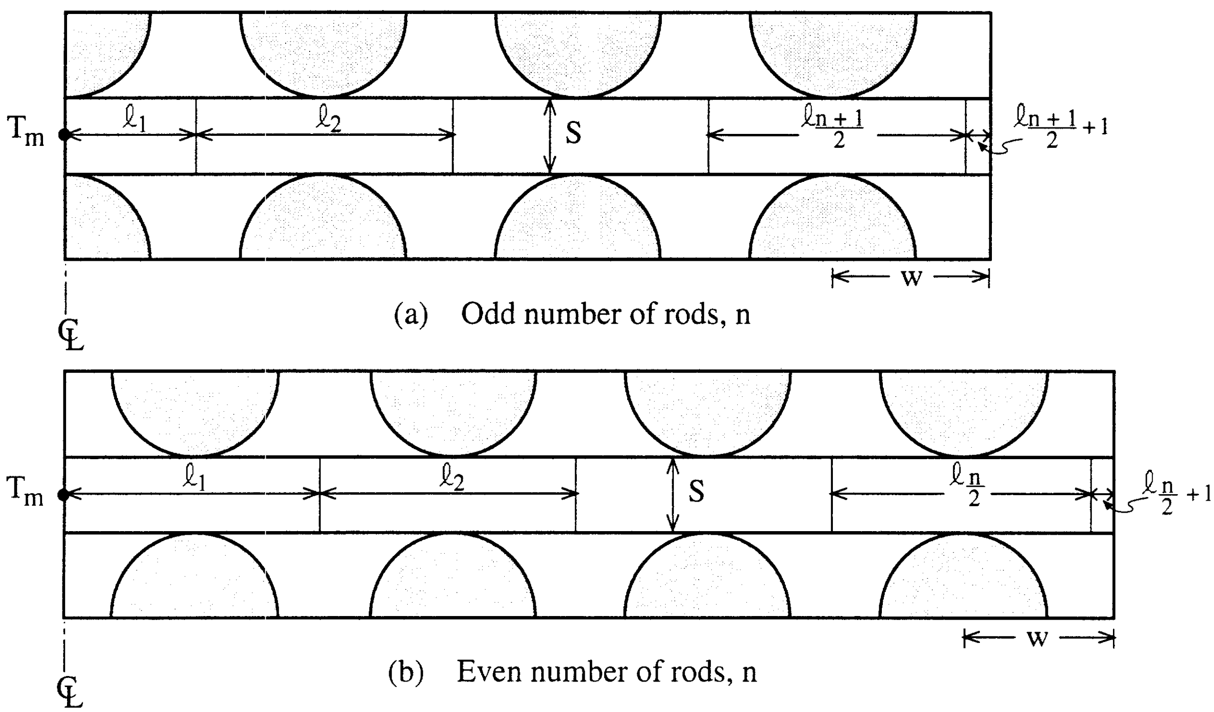

Figure 7-2. COBRA-SFS Conduction Model.

Performing a summation over all *i*'s yields

$$T_m = T_w + \frac{\sum_i q_i' \cdot \ell_i}{k_{gas,COBRA} \cdot S \cdot GK} \tag{7-13}$$

Since the fuel bundle is symmetric, i.e., heat flux at the center of the bundle is zero, it is reasonable to assume that T_m, the gas temperature in the center subchannel in Figures 7-1 and 7-2, is equal to clad temperature of rods which form this subchannel. The latter is the peak cladding temperature.

For Figure 7-2a, where there is odd number of rods per row, i.e., n = odd, Equation 7-13 becomes

$$T_m - T_w = \frac{1}{k_{gas,COBRA} \cdot S \cdot GK} \cdot \sum_{i=1}^{\frac{n+1}{2}+1} q_i' \cdot \ell_i \tag{7-14}$$

$$= \frac{1}{k_{gas,COBRA} \cdot S \cdot GK} \underbrace{\left(q'_1 \ell_1 + \sum_{i=2}^{\frac{n+1}{2}} q'_i \ell_i + q'_{\frac{n+1}{2}+1} \ell_{\frac{n+1}{2}+1} \right)}_{\equiv Q} \tag{7-15}$$

where

ℓ_1 = p/2, m

ℓ_i = p (i = 2, 3, ..., $\frac{n+1}{2}$), m

$\ell_{\frac{n+1}{2}+1}$ = w - (p/2), (w = distance from the edge rod center to wall), m

q'_1 = 1/2 q'_{rod}, W/m

q'_i = [1/2 + (i - 1)] q'_{rod} = (i - 1/2) q'_{rod} (i = 2, 3, ..., $\frac{n+1}{2}$), W/m
(From the center to the edge of the bundle, linear power density and heat flux across cell boundary will increase monotonically.)

$q'_{\frac{n+1}{2}+1}$ = (n/2) q'_{rod} , W/m

Using the above relations, we get

$$Q = \frac{q'_{rod}}{2} \cdot \frac{p}{2} + pq'_{rod} \sum_{i=2}^{\frac{n+1}{2}} \left(i - \frac{1}{2}\right) + \left(w - \frac{p}{2}\right)\frac{n}{2} q'_{rod}$$

$$= pq'_{rod} \left[\frac{1}{4} + \frac{n+3}{4} \cdot \frac{n-1}{2} + \left(\frac{w}{p} - \frac{1}{2}\right)\frac{n}{2}\right]$$

$$= pq'_{rod} \left(\frac{n^2 - 1}{8} + \frac{n}{2}\frac{w}{p}\right) \tag{7-16}$$

Substituting Equation 7-16 into Equation 7-15 yields

$$T_m - T_w = \frac{pq'_{rod}}{k_{gas,COBRA} \cdot S \cdot GK}\left(\frac{n^2 - 1}{8} + \frac{n}{2} \cdot \frac{w}{p}\right) \tag{7-17}$$

Equating Equation 7-10 and Equation 7-17 yields

$$\frac{\left(\frac{n}{2}\right) q'_{rod}}{2k_{eff}} \cdot \frac{L}{p} = \frac{pq'_{rod}}{k_{gas,COBRA} \cdot S \cdot GK}\left(\frac{n^2 - 1}{8} + \frac{n}{2} \cdot \frac{w}{p}\right) \tag{7-18}$$

From definition of k_{eff} in Equation 4-1

$$k_{eff} = F_{cond} \cdot k_{gas,MIT} \tag{7-19}$$

where

$k_{gas,MIT}$ = gas thermal conductivity used in the MIT Method

Referring to the geometry in Figure 7-1, the following equation is obvious for both odd and even number of rods per row.

$$L = \frac{n-1}{2} p + w \tag{7-20a}$$

Divided by p on both sides, Equation (7-20a) can be rewritten as

$$\frac{L}{p} = \frac{n-1}{2} + \frac{w}{p} \tag{7-20b}$$

Substituting Equation 7-19 and Equation 7-20b into Equation 7-18 and rearranging yields

$$GK = 2\frac{p}{s} \cdot F_{cond} \cdot \frac{k_{gas,MIT}}{k_{gas,COBRA}} \cdot \frac{\frac{n^2 - 1}{8} + \frac{n}{2} \cdot \frac{w}{p}}{\left(\frac{n-1}{2} + \frac{w}{p}\right) \cdot \frac{n}{2}}$$

or for odd number of rod per row,

$$GK = 2F_{cond} \frac{k_{gas,MIT}}{k_{gas,COBRA}} \cdot \frac{p}{S} \cdot \frac{\frac{n - \frac{1}{n}}{4} + \frac{w}{p}}{\frac{n - 1}{2} + \frac{w}{p}} \tag{7-21}$$

Note:

(1) Theoretically, gas thermal conductivity in the MIT Method $k_{gas,MIT}$, should be identical to that in COBRA-SFS, $k_{gas,COBRA}$ since both methods are used to solve the same heat conduction problem;

(2) In practice, there is a slight difference between the two conductivities. In the MIT Method, the thermal conductivity of gas is fitted as a polynomial function of absolute temperature [6] described as follows:

$$k_{gas,MIT} = a_0 + a_1 \cdot T + a_2 \cdot T^2 + a_3 \cdot T^3 + a_4 \cdot T^4 \tag{7-22}$$

where

a_i = coefficients (i = 0, 1, 2, 3, 4)

T = gas temperature, K

while in COBRA-SFS, thermal conductivity of backfill gas, together with other physical quantities is input as a tabular function of Fahrenheit temperature in Card PROP (see Appendix 1). By interpolation, thermal conductivity at each specific temperature is obtained in COBRA-SFS. This minor difference between the two methods is compensated for by introducing the thermal conductivity ratio in Equation 7-21.

These thermal conductivity ratios at relevant temperatures of column 4 in Table 7-2 are shown in Table 7-1.

In particular, utilizing the thermal conductivity ratios listed in Table 7-1, together with KSC-7 fuel bundle parameters, i.e., n = 17, w/p = 1.1262, p/d = 1.326, F_{cond} = 2.651, theoretical GK values from Equation 7-21 are obtained and listed in Table 7-2.

For Figure 7-2b, where there is an even number of rods per row (n = even), Equation 7-13 is written as

$$T_m - T_w = \frac{1}{k_{gas,COBRA} \cdot S \cdot GK} \cdot \sum_{i=1}^{\frac{n}{2}+1} q_i' \cdot \ell_i \tag{7-23a}$$

Table 7-1 Thermal Conductivities and Their Ratios at Relevant Temperatures

Gas Type	Power (W)	Temperature (°C)	$k_{gas,MIT}$ (Btu / hr ft °F)	$k_{gas,COBRA}$ (Btu / hr ft °F)	$k_{gas,MIT}/k_{gas,COBRA}$ (from [11])
N_2	4684	1089.0	0.04574	0.04792	0.9545
	1750	568.4	0.0323	0.03225	1.002
He	4684	359.3	0.1475	0.1326	1.112
	1750	207.3	0.1187	0.1118	1.062

or

$$T_m - T_w = \frac{1}{k_{gas,COBRA} \cdot S \cdot GK} \underbrace{\left(\sum_{i=1}^{\frac{n}{2}} q'_i \ell_i + q'_{\frac{n}{2}+1} \ell_{\frac{n}{2}+1} \right)}_{\equiv R} \tag{7-23b}$$

where

ℓ_i = p (i = 1, 2, 3, ..., $\frac{n}{2}$), m

$\ell_{\frac{n}{2}+1}$ = w - p/2, m

q'_i = $i \cdot q'_{rod}$ (i = 1, 2, 3, ..., $\frac{n}{2}$), W/m

(From the center to the edge of the bundle, linear power density and heat flux across cell boundary will increase monotonically.)

$q'_{\frac{n}{2}+1}$ = $\left(\frac{n}{2}\right) q'_{rod}$, W/m

Using these relations yields

$$\begin{aligned} R &= pq'_{rod} \sum_{i=1}^{\frac{n}{2}} i + \left(w - \frac{p}{2}\right) \frac{n}{2} q'_{rod} \\ &= pq'_{rod} \left[\frac{1 + \frac{n}{2}}{2} \cdot \frac{n}{2} + \left(\frac{w}{p} - \frac{1}{2}\right) \frac{n}{2} \right] \\ &= pq'_{rod} \left(\frac{n^2}{8} + \frac{n}{2} \frac{w}{p} \right) \end{aligned} \tag{7-24}$$

Substituting Equation 7-24 into Equation 7-23b yields

$$T_m - T_w = \frac{pq'_{rod}}{k_{gas,COBRA} \cdot S \cdot GK} \left(\frac{n^2}{8} + \frac{n}{2} \cdot \frac{w}{p} \right) \tag{7-25}$$

Equating Equation 7-10 and Equation 7-25 yields

$$\frac{\left(\frac{n}{2}\right) q'_{rod}}{2k_{eff}} \cdot \frac{L}{p} = \frac{pq'_{rod}}{k_{gas,COBRA} \cdot S \cdot GK} \left(\frac{n^2}{8} + \frac{n}{2} \cdot \frac{w}{p} \right) \tag{7-26}$$

Substituting Equations 7-19 and 7-20b into 7-26 and rearranging, we get the GK expression for even n

$$GK = 2\frac{p}{s}\cdot F_{cond}\cdot\frac{k_{gas,MIT}}{k_{gas,COBRA}}\cdot\frac{\frac{n^2}{8}+\frac{n}{2}\cdot\frac{w}{p}}{\left(\frac{n-1}{2}+\frac{w}{p}\right)\cdot\frac{n}{2}}$$

or equivalently,

$$GK = 2F_{cond}\ \frac{k_{gas,MIT}}{k_{gas,COBRA}}\cdot\frac{p}{S}\cdot\frac{\frac{n}{4}+\frac{w}{p}}{\frac{n-1}{2}+\frac{w}{p}} \qquad (7\text{-}27)$$

These analytic relations, Equations 7-21 and 7-27, for GK not only yield numerical predictions, but as importantly give the functional dependence of GK. We see that in both cases

$$GK = f\,(F_{cond},\ p/S,\ w/p,\ n,\ k_{gas,MIT}/k_{gas,COBRA})$$

Since F_{cond} per Table 4-1 is a function of array type, p/d and a weak function of fill gas, we have

GK = f (array type, size through n, geometry, and weakly fill gas).

Ideally, GK should not be a function of assembly power level and only a weak function of fill gas.

Next, the true values of GK are assessed by comparative COBRA-SFS (Cycle 2) and MIT Model calculations for this 17x17 square array of interest.

Equivalent Boundary Condition In COBRA-SFS, the environmental (air) temperature is assumed to be the boundary temperature (see Section 2.10.1 [1]), while the temperature distribution in the solid boundary, i.e., fuel basket (Figure 5-1) is calculated using boundary surface heat transfer coefficients (see Section 2.10.1 [1]), and the thermal conductivity of the solid material in property group PROP.3 (see Section 2.2 [1]). The MIT Method, however, defines the temperature at the outmost boundary surface as the boundary temperature (Figure 4-1). These two boundary temperatures are equalized by assuming extremely large values for C_1 (heat transfer coefficient on the outer surface) in group BDRY.2 and CONSOL (thermal conductivity of the wall) in group PROP.3. The recommended value is 1.0×10^8.

Table 7-2 summarizes the results of the two methods and compares the theoretical and actual GK values calculated by COBRA-SFS for conduction-only in each case. In the table, Cycle 1 and Cycle 2 represent Cycle 1 and pre-released Cycle 2 of COBRA-SFS code, respectively.

Table 7-2. Comparison between COBRA-SFS and the MIT Method —Conduction Only, 17x17 Bundle

Fill Gases	Powers (W)	Methods	$T_{clad,max}$ (°C)	F_{cond} *or* Actual GK (Cycle 1/ Cycle 2)	Theoretical GK (Eq. 7-21)	Relative Error
N_2	4684	MIT	1088.6	2.65	-	
		COBRA-SFS	1088.4	17.1 / 12.3	12.1	1.6%
	1750	MIT	568.3	2.65	-	
		COBRA-SFS	568.2	14.3 / 14.2	12.7	11%
He	4684	MIT	359.4	2.65	-	
		COBRA-SFS	359.4	17.8 / 17.8	14.1	21%
	1750	MIT	207.1	2.65	-	
		COBRA-SFS	207.1	17.9 / 17.8	13.5	24%

Note that $\dot{Q}$ = 4684 W is the nominal power for a KSC-7 spent fuel bundle while $\dot{Q}$ = 1750 W is an alternate power assumed to study the effect of power on the GK factor. From Table 7-2, actual GK's match theoretical GK's reasonably well, i.e. maximum error is 24% and minimum error is 1.6%. Further, these errors will be shown inconsequential when conduction and radiation are both operative. (Compare Tables 6-1, 7-2 and 7-5.)

7.1.2 Radiation

The MIT Method uses three radiation coefficients—namely, C_{rad}, $C_{rad,w,1}$, $C_{rad,w,2}$—to model radiation heat transfer. Monte Carlo simulations were performed to provide these radiative coefficients for 15° circumferential rod segments and the results are listed in Appendix H of Reference [2].

The MIT Method was derived by assuming infinite numbers of rows or columns of rod. (See Figure 7-3.). Hence, special attention should be paid in the edge regions where the boundary condition plays a more important role than in the internal region. But, practically, as shown later, the edge effect disappears several rows away from the edges. The data in the interior region from COBRA-SFS/RADGEN are compared with the MIT Method.

The RADGEN source code was carefully studied, and the strategy to calculate rod gray body exchange factors was identified. First, the quarter-rod (90° segment) gray body exchange factors are calculated (See Figure 7-4.). Then they are combined to obtain the full-rod (360°) gray body exchange factors using Equation 7-28

$$F_{ij} = \frac{1}{4}\sum_{n=1}^{4}\sum_{m=1}^{4} F_{nm} \qquad (7\text{-}28)$$

where

F_{ij} = full-rod gray body exchange factor from rod i to rod j

F_{nm} = quarter-rod gray body exchange factor from quarters n to m

n, m = sequential number of each quarter in rods i and j, respectively.

Figure 7-5 illustrates the exchange factors of the center rod of row 8 (rod 128) to rods in other rows.

Though the quarter-rod exchange factor, F_{nm}, is not part of the standard output file in RADGEN, we extracted it as part of the output at MIT. The full-rod exchange factors, F_{ij}, which are necessary to simulate radiative heat transfer in COBRA-SFS, are in file TAPE10 after RADGEN execution is completed.

Table 7-3 gives the exchange factors of rods in the 8-th row to rows 9, 10, 11, and 12 based on TAPE10 file of KSC-7 fuel assembly (17x17 array) with rod emissivity ε_r = 0.8 and wall emissivity ε_w = 0.3. Note that in F_{k-L}, k stands for the sequential number of rods, while L

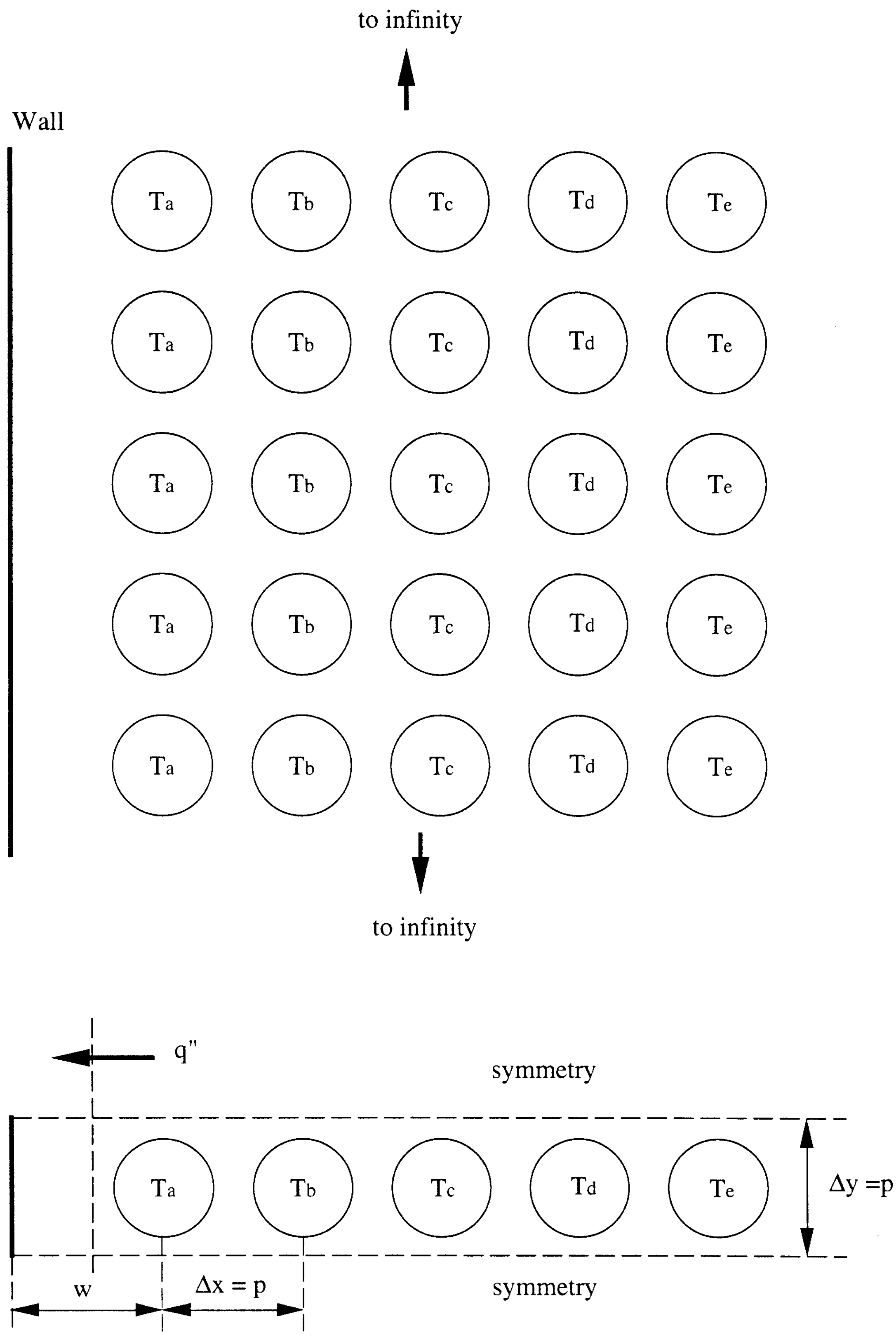

Figure 7-3 The MIT Method Derived from Infinite Array (after [2])

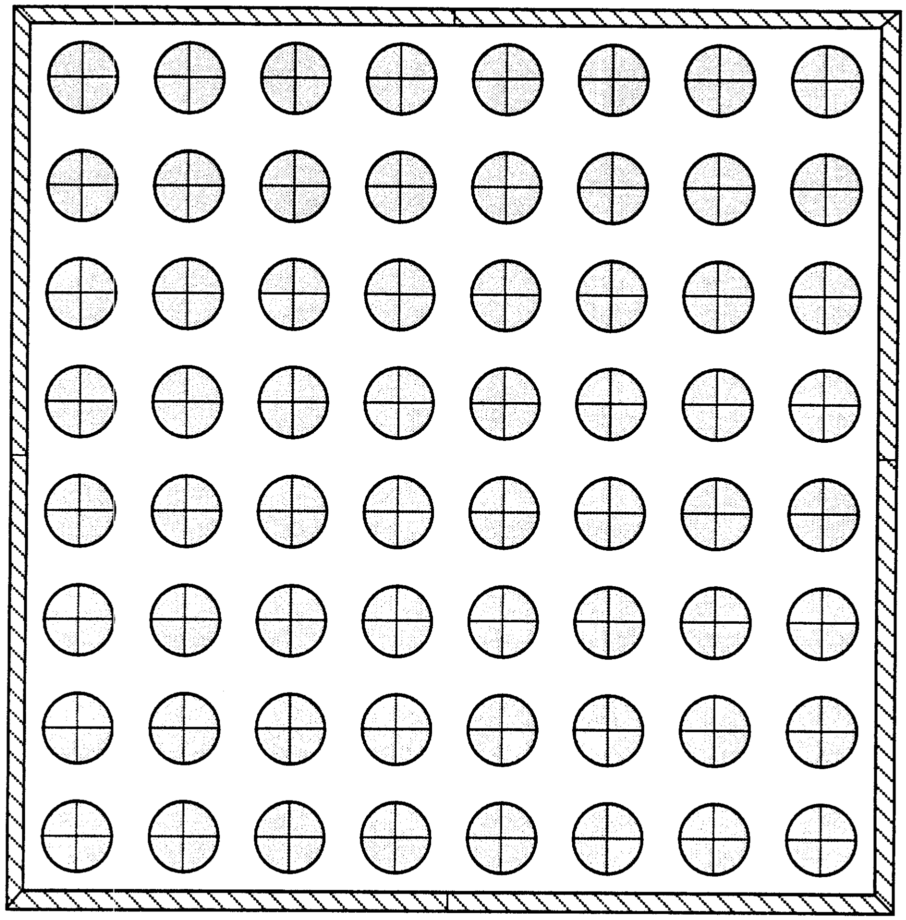

Figure 7-4 RADGEN Radiation Exchange Factor Model (90°-Segment)

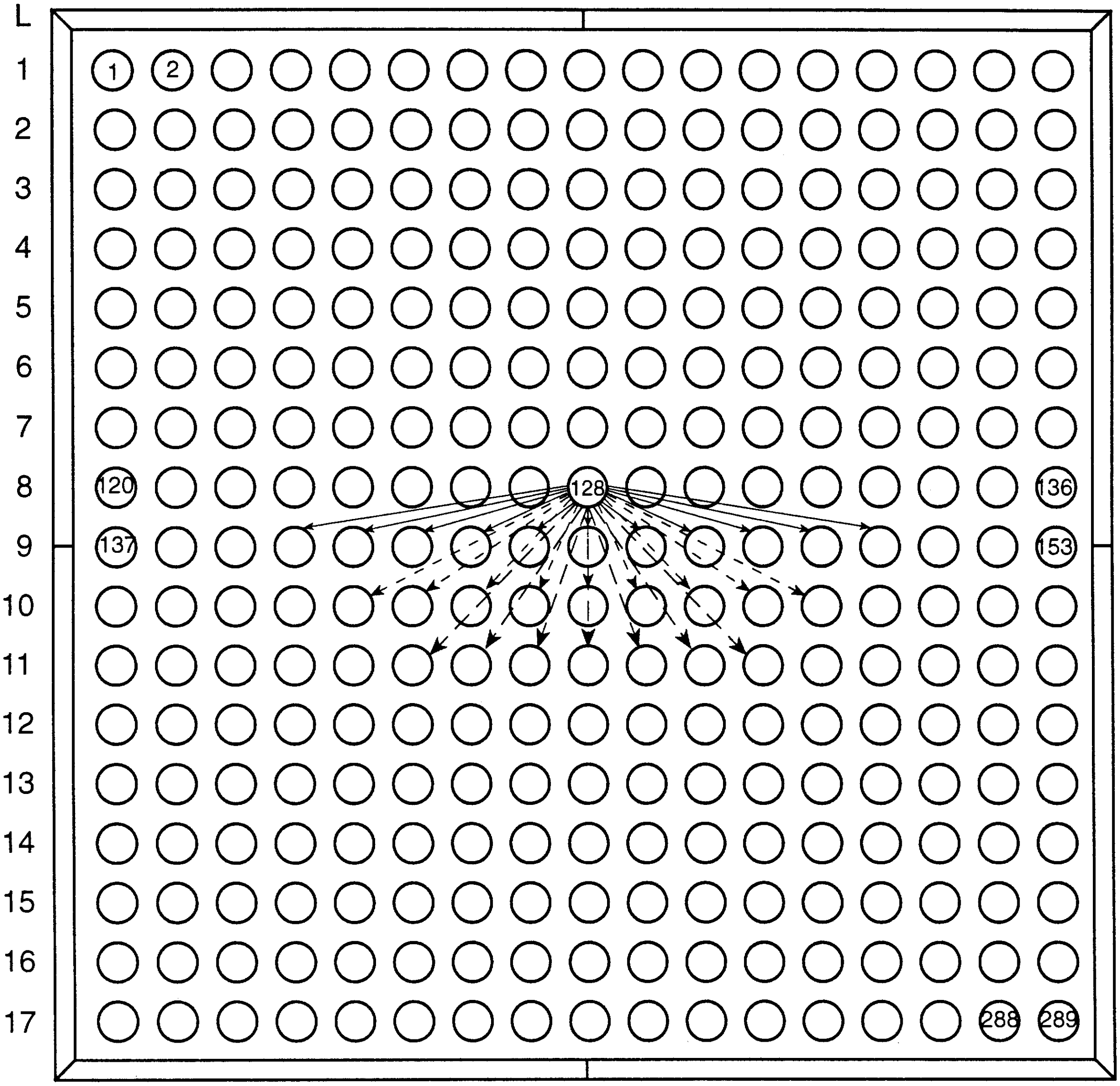

Figure 7-5 Exchange Factors, F_{ij}, in the 17x17 Array

stands for the sequential number of rows of rods, i.e., $F_{128\text{-}9}$ is the exchange factor of rod 128 to row 9, and it is expressed as

$$F_{128\text{-}9} = \sum_{j=137}^{153} F_{ij} \tag{7-29}$$

where

i = 128, rod number

j = 137 to 153, rod numbers.

Practically, if rod j is several rows away from rod i, F_{ij} in the right hand side of Equation 7-29 is negligible and its effect on $F_{k\text{-}L}$ can be ignored.

From Table 7-3, it is obvious that the edge effect disappears four columns from the wall and that the interior can be taken as infinite rows of rods since, for the same value of L, $F_{k\text{-}L}$ is not a function of position, i.e., $F_{k\text{-}L}$ does not change for the same L when k = 124, 125, ..., 132. From Appendix 6:

$$G_{i\text{-}j} = F_{ij} / \varepsilon_i \tag{A6-5}$$

where

i = rod number

j = rod number

If all rod emissivities are equal (i.e., $\varepsilon_i = \varepsilon_r$),, summing over all i, j from Equation A6-5 yields

$$G_{I\text{-}J} = F_{IJ} / \varepsilon_r \tag{7-30}$$

where

$$G_{I\text{-}J} = \sum_i \sum_j G_{i\text{-}j} \tag{7-31}$$

$$F_{IJ} = \sum_i \sum_j F_{ij} \tag{7-32}$$

I = sequential number of row

J = sequential number of row

The Radiative Coefficient, C_{rad}, is (Page 168 [2])

$$C_{rad} = \varepsilon_r \left(G_{I\text{-}(I+1)} + 2^2 G_{I\text{-}(I+2)} + \ldots\ n^2 G_{I\text{-}(I+n)} \right) \frac{\Delta x}{\Delta y} \tag{7-33}$$

Table 7-3. Exchange Factors from RADGEN Based on TAPE10 file

k (L = 8)	$F_{k\text{-}L}$ (L = 9)	$F_{k\text{-}L}$ (L = 10)	$F_{k\text{-}L}$ (L = 11)	$F_{k\text{-}L}$ (L = 12)
120	0.2062	0.03707	0.01254	3.667×10^{-3}
121	0.2411	0.02982	4.4319×10^{-3}	1.513×10^{-4}
122	0.2491	0.02775	4.2114×10^{-3}	8.632×10^{-5}
123	0.2503	0.02743	4.1789×10^{-3}	7.913×10^{-5}
124	0.2503	0.02743	4.1789×10^{-3}	7.893×10^{-5}
125	0.2503	0.02743	4.1789×10^{-3}	7.893×10^{-5}
126	0.2503	0.02743	4.1789×10^{-3}	7.893×10^{-5}
127	0.2503	0.02743	4.1789×10^{-3}	7.893×10^{-5}
128	0.2503	0.02743	4.1789×10^{-3}	7.893×10^{-5}
129	0.2503	0.02743	4.1789×10^{-3}	7.893×10^{-5}
130	0.2503	0.02743	4.1789×10^{-3}	7.893×10^{-5}
131	0.2503	0.02743	4.1789×10^{-3}	7.893×10^{-5}
132	0.2503	0.02743	4.1789×10^{-3}	7.893×10^{-5}
133	0.2503	0.02743	4.1789×10^{-3}	7.913×10^{-5}
134	0.2491	0.02775	4.2114×10^{-3}	8.632×10^{-5}
135	0.2411	0.02982	4.4319×10^{-3}	1.513×10^{-4}
136	0.2062	0.03707	0.01254	3.667×10^{-3}
Rods 120 to 136 lie in the 8-th row from left to right of Figure 7-5				

For Square Array, $\Delta x = \Delta y$ (Figure 7-3). Hence,

$$C_{rad} = \varepsilon_r \left(\sum_{K=1}^{n} K^2 \cdot G_{I-(I+K)} \right) \tag{7-34}$$

Since the effect of rods more than 4 rows (or columns) away can be neglected, Equation 7-34 can be rewritten as

$$C_{rad} \approx \varepsilon_r \left(\sum_{K=1}^{4} K^2 \cdot G_{I-(I+K)} \right) \tag{7-35}$$

Using Equation 7-30, Equation 7-35 can be reduced to

$$C_{rad} \approx \sum_{K=1}^{4} K^2 \cdot F_{I,I+K} \tag{7-36}$$

Using RADGEN data from Table 7-3, we get radiative coefficient for 90°-segment, $C_{rad}(90°)$.

$$\begin{aligned} C_{rad}(90^\circ) &= 0.2503 + 2^2(0.02743) + 3^2(4.1789\text{x}10^{-3}) + 4^2(7.893\text{x}10^{-5}) \\ &= 0.3989 \end{aligned} \tag{7-37}$$

On the other hand, the radiation coefficient C_{rad} of 15° segment with $\varepsilon_r = 0.8$ and p/d = 1.326 can be obtained from Appendix H [2].

$$C_{rad}(15^\circ) \approx 0.3920 \pm \text{error from reading Figure H-1.} \tag{7-38}$$

The error is 0.5% which was determined by Mr. Yoon of KAERI and Prof. Todreas upon independent examination of Figure H-1 [2].

The relative error between COBRA-SFS/RADGEN (90° or 360°) and the MIT Method (15°) is

$$\left| \frac{C_{rad}(15^\circ) - C_{rad}(90^\circ)}{C_{rad}(15^\circ)} \right| \times 100\% = \left| \frac{0.3920 - 0.3989}{0.3920} \right| \times 100\% = 1.8\%$$

The total error between the two methods lies within the range 1.8% ± 0.5%. Hence, the maximum error is 2.3%.

The importance of the 2.3% error is next evaluated by using the MIT Method since the corresponding errors of rod and wall emissivities are not clear. It is assumed in the evaluation that both wall radiative coefficients, $C_{rad,w,1}$ and $C_{rad,w,2}$ have the same error as C_{rad}. Results of the eight error combinations of C_{rad}, $C_{rad,w,1}$, and $C_{rad,w,2}$ are shown in Table 7-4.

Table 7-4. Maximum Effect on Peak Clad Temperatures (°C) of 90° vs. 15° Rod Segments —$\dot{Q}$ = 4684 W, N_2, 17x17, Conduction and Radiation, the MIT Method

$C_{rad,w,1}$ (= 0.148, *base*)		+ 2.3%	+ 2.3%	- 2.3%	- 2.3%
$C_{rad,w,2}$ (= 0.117, *base*)		+ 2.3%	- 2.3%	+ 2.3%	- 2.3%
C_{rad} (= 0.3754, *base*)	+ 2.3% (0.3840)	409.97	411.60	410.33	411.97
	- 2.3% (0.3668)	414.22	415.80	414.58	416.18

For the 15° segments in 17x17 fuel bundle whose p/d = 1.326, $\varepsilon_r = 0.8$, $\varepsilon_w = 0.3$, the radiative coefficients, C_{rad}, $C_{rad,w,1}$ and $C_{rad,w,2}$ are 0.3754, 0.148, 0.117, respectively, as obtained from Appendix H [2].

As shown in Table 7-5, this combination of C_{rad}, $C_{rad,w,1}$ and $C_{rad,w,2}$ will produce a peak clad temperature of 413.03°C using the MIT Method, while other conditions are identical to those cases in Table 7-4. Hence, even under the worst combination, the deviation in peak clad temperature of 90° rod segment from that of the 15° segment is within 3.2°C, i.e., upon rounding, 413°C compared to 410°C and 416.2°C.

7.1.3 Conduction and Radiation

In the preceding sections we examined the conduction and radiation mechanisms separately. We deduced the value of GK necessary for conduction and determined that the COBRA-SFS radiation result was accurate compared to the MIT Method within 3.2°C.

It is desirable now to assess the COBRA-SFS results under conduction plus radiation heat transfer by comparison with the MIT Method. The value of GK from Table 7-2 are used to eliminate differences due to conduction. Four cases considered are fill gases of nitrogen and helium as well as bundle powers of 4684 W and 1750 W.

Results are presented in Table 7-5. We find that:

(1) COBRA-SFS predicts lower peak clad temperatures (increasingly so at higher power) which indicates that COBRA-SFS is less conservative.

(2) Under the same conditions, the difference between the two methods is larger for N_2 than for He. This is due to the fact that helium has a higher thermal conductivity than nitrogen so that radiation is not as important for helium as it is for nitrogen. ($k_{He} \approx 5\ k_{N2}$) Hence, this comparison, which illustrates differences in the radiation models (since GK's are established to equalize conduction contributions), will show the most difference in the nitrogen cases.

(3) Except for the high power nitrogen case, the temperatures differ by 2 to 6°C, which is consistent with the error in clad temperature due to differences in radiation modeling as demonstrated in Table 7-4.

(4) In the combined Conduction and Radiation calculation, Cycle 2 code of COBRA-SFS has, in general, smaller temperature differences than Cycle 1 code. The improvement is especially eminent for high power nitrogen case (Compare columns 5 and 7.).

(5) Comparing Tables 7-2 and 7-5, it is concluded that, in dry spent fuel storage cask, heat conduction is dominated by radiation in nitrogen cases. (Refer also to Figure 7-6 and Appendix 8.)

7.1.4 Sensitivity Study on Emissivities

As to be mentioned in Section 7.4, measured data for rod and wall emissivities ought to be used in the analysis. Since, however, a conclusive data set does not exist, the commonly

Table 7-5. Comparison in the Peak Clad Temperature between COBRA-SFS and the MIT Method—Conduction and Radiation, 17x17 Bundle, GK Corresponding to Cases in Table 7-2

Fill Gases	Power (W)	MIT Method (°C)	COBRA-SFS			
			Cycle 1 (°C)	Differences* (°C)	Cycle 2 (°C)	Difference* (°C)
N_2	4684	413.0	398.9#	- 14.1	404.7#	-8.3
	1750	269.6	264.2	- 5.4	264.3	-5.3
He	4684	287.2	281.5	- 5.7	281.4	-5.8
	1750	181.0	178.2	- 2.8	178.3	-2.7

* Differences (°C) = $T_{COBRA\text{-}SFS}$ (°C) - T_{MIT} (°C)

\# Input decks for Cycle 1 codes are provided in Appendices 3 and 4.
Input decks for Cycle 2 codes are provided in Appendices 9 and 10.

recommended emissivities, i.e., 0.8 for rod, 0.2 ~ 0.3 for wall, can be used and the sensitivity of peak clad temperature to variations in these emissivities assessed.

1). Rod Emissivity

The results of the sensitivity study on rod emissivity (ε_r) are shown in Table 7-6. From Table 7-6, we find:

(1) The uncertainty in peak clad temperature is about 10°C/0.1 change in ε_r.

(2) The larger the rod emissivity, the smaller the peak clad temperature, since larger rod emissivity indicates more radiative heat transfer.

2). Wall Emissivity

The results of the sensitivity study on wall emissivity (ε_w) are listed in Table 7-7. This Table indicates that:

(1) The uncertainty in peak clad temperature is about 10°C/0.05 change in ε_w, which is about twice as much as that for rod emissivity. Hence, the accuracy of the wall emissivity is more important to determine.

(2) The larger the wall emissivity, the smaller the peak clad temperature since larger wall emissivity indicates more radiative heat transfer.

7.1.5 Summary

Theoretical expressions (Equations 7-21 and 7-27) for the length conduction factor, GK, have been developed. From Equation 7-21, the theoretical value for GK can be obtained and is given in Table 7-2 for the 17x17 fuel bundle. From COBRA-SFS conduction calculations which produce the same peak clad temperatures as the MIT Method (Table 7-2), GK values of 14 to 18 resulted using Cycle 1 code and 12 to 18 from the pre-released Cycle 2 code. The difference stems from the fact that the theoretical expressions consider only 1D heat transfer, whereas the COBRA-SFS calculations are for the 3D bundle with a non-uniform axial heat flux distribution as prescribed by KAERI (see Appendix 5 for sample input). In fact, we believe that 2D heat transfer in the COBRA-SFS calculation is responsible for the difference since the peak clad temperature occurs within the mesh containing the peak axial heat flux position for 19 axial nodes. The 3D effect is very small, i.e., axial heat conduction is negligible. Hence, GK values in Table 7-2 from the COBRA-SFS calculations should be used in successive calculations.

Next, the effect of non-uniform emissivity for the rod surface is studied using 15° and 90° segments. COBRA-SFS (90°-segment) may predict a peak clad temperature that deviates from the MIT Method (15°-segment) by about 3°C (Table 7-4). Table 7-4 also shows this deviation is probably such that the COBRA-SFS result is less than the MIT result, taking into account the fact that C_{rad} (90°) is slightly larger than C_{rad} (15°). (See Equations 7-37 and 7-38.)

Table 7-6. Sensitivity Study on Rod Emissivity—Conduction and Radiation, 17x17 Bundle, $\dot{Q}$ = 4684 W, N_2, GK = 17.1, ε_w = 0.3

ε_r	Peak Clad Temperatures (˚C)
0.70	409.4
0.80	**398.9**
0.85	394.0
0.90	389.3

Table 7-7. Sensitivity Study on Wall Emissivity—Conduction and Radiation, 17x17 Bundle, $\dot{Q}$ = 4684 W, N_2, GK = 17.1, ε_r = 0.8

ε_w	Peak Clad Temperatures (°C)
0.25	409.5
0.30	**398.9**
0.35	390.6

The combined conduction and radiation calculation does show that COBRA-SFS predicts lower peak clad temperatures than the MIT Method. This discrepancy is about 2 to 6°C, except for the higher power nitrogen case which is 14°C (Table 7-5). This tendency is consistent with the prediction in Table 7-4.

Sensitivity studies of the emissivities show that the peak clad temperature decreases about 10°C by increasing the rod emissivity by 0.1, or by increasing the wall emissivity by 0.05. Hence, the selection of emissivities is important to achieve a more accurate peak clad temperature (See Section 7.4.2.) and reduce the uncertainty on clad temperatures.

7.1.6 Recommendations

Currently KAERI uses a GK factor of 1.0, a 90° segment, and rod and wall emissivities of 0.8 and 0.3, respectively. The resulting peak clad temperatures are identified as the base case and are given in Table 6-1.

We recommend that KAERI uses GK factors of Table 7-2. We have no recommended change in the COBRA-SFS radiation model (RADGEN). With combined conduction and radiation, the change of GK factor will yield peak clad temperatures of Table 7-5. Table 7-8 summaries the change in peak clad temperature resulting from this recommendation. The benefit of this recommendation is a reduction in peak clad temperature of 30°C (~7%) for nitrogen and 87°C (~24%) for helium. The change for helium is larger because of its larger susceptibility to change in the conduction model stemming from its high thermal conductivity. Finally, it would be desirable to measure the wall and clad emissivities of typical materials.

7.2 Lumped Effective Conductivity

The spent fuel cask analyzed (KSC-7) contains seven fuel bundles, each of which is a 17x17 array as described in Figure 5-1. Hence, the analysis would require a very long computation time and can only be undertaken on computers with a vast amount of memory as well as disc space to store output files unless the bundles are homogenized into smaller ones.

Homogenization is a process which lumps larger fuel bundles, i.e., 17x17 bundles in typical PWR fuel design nowadays, into smaller bundles, i.e., 8x8 bundles, without changing their physical characteristics. By homogenization, we can increase computation speed substantially as well as reduce requirements on computer memory and space.

The process for performing this homogenization is presented next.

Table 7-8. Reduction in Peak Clad Temperature under Conduction and Radiation from the Recommended Change in GK Factor (17x17, 4684 W, $\varepsilon_r = 0.8$, $\varepsilon_w = 0.3$)

	Nitrogen	Helium
Base Case, Table 6-1	428.0°C	368.4°C
Recommended GK, Table 7-5	398.9°C	281.5°C
Reduction in $T_{max,clad}$	-29.1°C	-86.9°C
Percentage Reduction in $T_{max,clad}$	-6.8%	-23.6%

7.2.1 Principle of Homogenization

The following parameters are to be maintained the same in the lumped bundle as in the 17x17 array.

1) Volumetric energy generation rate, q''',
2) Total clad and fuel cross-sectional areas,
3) Axial fuel length,
4) The pitch-to-diameter ratio, and
5) Inner and outer side lengths of bundle wall ($L_{ci}/4$, $L_{co}/4$) (see Figures 5-1 and 5-2).

Assumptions 1, 2 and 3 combined will keep the total decay power constant. Following assumption 5, the lumped fuel bundles can be fitted into spent fuel cask as if they were the original unlumped bundles since the lumped bundles have the same outer dimension as their original counterparts. As a consequence of homogenization, an emissivity modification factor must be introduced to compensate for excessive radiation heat transfer in the lumped bundle resulting from fewer rods and hence greater view factor for the peak-clad-temperature rod. This modification is quantified in Section 7.2.4.

7.2.2 Implementation of Homogenization

Based on the five assumptions, the geometric parameters, i.e., clad outside and inside diameters, fuel pellet diameter, and pitch, can be calculated for the lumped array. In the following derivation, the capital letters represent the original array, i.e. 17x17, while the small letters stand for the lumped array.

1) Find the clad outside diameter, d_{co}, for the lumped bundle using Assumption 2.

$$N \times N \times \frac{\pi}{4} D_{co}^2 = n \times n \times \frac{\pi}{4} d_{co}^2 \tag{7-39}$$

To solve for d_{co}, we have

$$d_{co} = \frac{N}{n} D_{co} \tag{7-40}$$

where

N = number of rods each row in the original array, i.e. 17

n = number of rods each row in lumped array, i.e., 8

D_{co} = clad outside diameter for the original array

d_{co} = clad outside diameter for lumped array

For KSC-7 fuel bundles, N = 17, D_{co} = 0.3740", assuming n = 8, we obtain

$$d_{co} = 17/8 \times 0.3740" = 0.7948"$$

2) Find the lumped pitch, p, using Assumption 4.

$$\frac{P}{D_{co}} = \frac{p}{d_{co}} \quad \text{or} \quad p = \frac{d_{co}}{D_{co}} P \tag{7-41}$$

where

P = pitch for the original array

p = pitch for the lumped array

For KSC-7 fuel bundles, $P/D_{co} = 1.326$

$$p = \left(\frac{P}{D_{co}}\right) d_{co} = 1.326 \times 0.7984" = 1.054"$$

3) Find the lumped clad inside diameter, d_{ci}, using Assumption 2.

$$N \times N \times \frac{\pi}{4}\left(D_{co}^2 - D_{ci}^2\right) = n \times n \times \frac{\pi}{4}\left(d_{co}^2 - d_{ci}^2\right) \tag{7-42}$$

where

D_{ci} = clad inside diameters for the original array

d_{ci} = clad inside diameters for the lumped array

So,

$$d_{ci} = \sqrt{d_{co}^2 - \frac{N^2}{n^2}\left(D_{co}^2 - D_{ci}^2\right)}$$

$$= \sqrt{d_{co}^2 - \left(\frac{N}{n} D_{co}\right)^2 + \frac{N^2}{n^2} D_{ci}^2} \tag{7-43}$$

Substituting Equation 7-40 into Equation 7-43 yields

$$d_{ci} = \sqrt{d_{co}^2 - d_{co}^2 + \frac{N^2}{n^2} D_{ci}^2}$$

Hence, we get

$$d_{ci} = \frac{N}{n} D_{ci} \tag{7-44}$$

For KSC-7 spent fuel, N = 17, D_{ci} = 0.3290", assuming n = 8, we have d_{ci} = 0.6991".

4) Find the lumped clad thickness, δ_c.

$$\delta_c = \frac{1}{2}\left(d_{co} - d_{ci}\right) \tag{7-45}$$

Substituting Equations 7-40, 7-44 into Equation 7-45 yields,

$$\delta_c = \frac{1}{2} \cdot \left(\frac{N}{n} \cdot D_{co} - \frac{N}{n} \cdot D_{ci}\right)$$

$$= \frac{N}{n} \cdot \left(\frac{D_{co} - D_{ci}}{2}\right)$$

Hence $$\delta_c = \frac{N}{n} \Delta c \tag{7-46}$$

where

Δc = clad thickness for the original array

δ_c = clad thickness for the lumped array

Since d_{co} = 0.7948" and d_{ci} = 0.6991" have been determined, we use Equation 7-45 to evaluate δ_c = 0.04785".

5) Find the lumped fuel pellet diameter, d_f, using Assumption 2.

$$N \times N \times \frac{\pi}{4} D_f^2 = n \times n \times \frac{\pi}{4} d_f^2 \tag{7-47}$$

or $$d_f = \frac{N}{n} D_f \tag{7-48}$$

where

D_f = fuel pellet diameter diameters for the original array

d_f = fuel pellet diameter diameters for the lumped array

For KSC-7 spent fuel, N = 17, D_f = 0.3224", assuming n = 8, we get d_f = 0.6851".

6) Find the lumped gap thickness, δ_g.

$$\delta_g = \frac{d_{ci} - d_f}{2} \tag{7-49}$$

Substituting Equations 7-44 and 7-48 into Equation 7-49 yields

$$\delta_g = \frac{1}{2}\left(\frac{N}{n} D_{ci} - \frac{N}{n} D_f\right)$$

$$= \frac{N}{n}\left(\frac{D_{ci} - D_f}{2}\right)$$

Hence $$\delta_g = \frac{N}{n} \Delta g \tag{7-50}$$

where

Δg = gap thickness for the original array

δ_g = gap thickness for the lumped array

Since d_{ci} = 0.6991" and d_f = 0.6851" have been determined, we use Equation 7-49 to get δ_g = 0.0070".

7) Find the edge-rod-center-to-wall distance, w, (see Figure 7-1) using Assumption 5.

$$\frac{\ell_{ci}}{4} = \frac{L_{ci}}{4} \tag{7-51}$$

where

ℓ_{ci} = inner circumferential length for the original array

L_{ci} = inner circumferential length for the lumped array

From Figures 5-1, 5-2 and 7-1, the following relationship holds

$$(n - 1)p + 2w = \frac{L_{ci}}{4} \qquad (7\text{-}52)$$

or

$$w = \frac{\frac{L_{ci}}{4} - (n - 1)p}{2} \qquad (7\text{-}53)$$

where

w = distance from inside wall to the center of the nearest rod in the lumped array

Since $L_{ci}/4 = 9.055"$, $p = 1.054"$, assuming $n = 8$, we get $w = 0.8385"$.

7.2.3 Lumped Fuel Bundle Analysis

A spectrum of lumped $n \times n$ arrays are obtained using the above method. The MIT Method is then employed to compute the peak clad temperature in cases of conduction-only (C-only), and conduction and radiation (C+R). The results are shown in Table 7-9 and Figure 7-6.

From these results, it is observed that:

(1) For conduction-only, the peak clad temperature does not change with lumped array sizes. This is what we expected since homogenization should yield the same peak clad temperature as the original bundle. Hence, the homogenization process is adequate for the conduction-only case.

(2) For conduction and radiation, however, the peak clad temperature is a function of the lumped array size, n. The smaller the lumped bundle size, n, the lower the peak clad temperature and, hence, the higher the radiative heat transfer.

(3) In dry spent fuel cask thermal calculation, i.e., filled with nitrogen, radiation heat transfer is the dominant factor. For 17x17 bundle, radiation reduces the peak clad temperature from 1088.6°C (Conduction-only) to 413.0°C (Conduction and Radiation). This result is consistent with that of a simple hand calculation as illustrated in Appendix 8.

This phenomenon is also observed in COBRA-SFS. Qualitatively, it can be explained by studying Figures 5-1 and 5-2. For the lumped bundle, i.e., 8x8, fuel rods are less densely spaced so that radiation from one rod is less shielded by its surrounding neighbors. This decreased shielding by surrounding fuel rods increases radiative heat transfer from the center hot rod to its neighboring rods and subsequently to the bundle wall. Hence, the peak clad temperature is lower than it should be if the lumped bundle is to represent the full size array. Hence, measures must be taken to compensate for the abnormal temperature decrement in the lumped fuel bundle.

Table 7-9. Major Geometric Parameters and Peak Clad Temperature for the Lumped and the Original Arrays—$\dot{Q}$ = 4684 W, N_2, the MIT Method, $\varepsilon_w = 0.3$, $\varepsilon_r = 0.8$

n × n	d_{co} (in.)	p (in.)	w (in.)	$T_{max,clad}$ (°C)	
				C-only	C+R
3 x 3	2.1193	2.8102	1.1173	1089.2	309.2
5 x 5	1.2716	1.6861	1.1553	1089.3	325.5
7 x 7	0.9083	1.2044	0.9143	1089.1	342.4
8 x 8	0.7948	1.0539	0.8385	1089.0	350.6
10 x 10	0.6358	0.8431	0.7336	1089.1	366.3
12 x 12	0.5298	0.7025	0.6638	1089.4	380.9
14 x 14	0.4541	0.6021	0.6139	1089.5	394.5
16 x 16	0.3974	0.5270	0.5750	1088.8	407.1
17 x 17	0.3740	0.4961	0.5587	1088.6	413.0

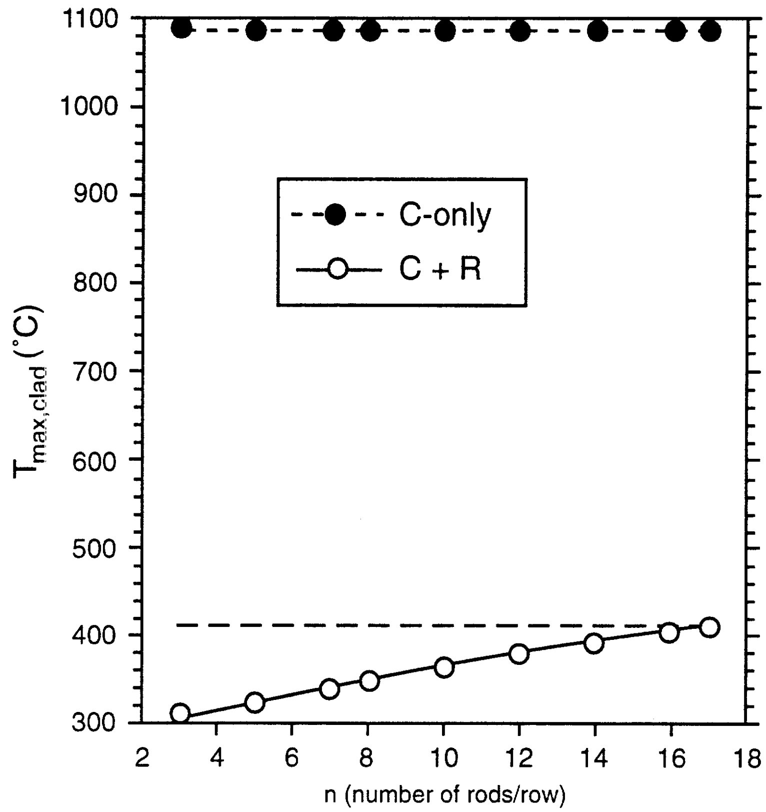

Figure 7-6. $T_{max,clad}$ versus Number of Rods Lumped per Row.

7.2.4 Means to Compensate for the Excess Radiative Heat Transfer

The reduced shielding in the lumped model tends to decrease the peak clad temperature. This decrement is not conservative. Hence, ways must be found to compensate for the excess radiation heat exchange, i.e., by reducing effective emissivity in Equation 7-90. One approach to achieve this goal is to introduce a radiation modification factor to adjust the rod emissivity, ε_r, the other is to introduce a radiation modification factor to adjust the wall emissivity, ε_w. The former approach is chosen in this study since the rod emissivity affects only the wall while the wall emissivity affects both its enclosed rods and its outer surrounding (i.e., inner shell) in a cask calculation (see Figures 5-3 and 5-4). In COBRA-SFS, we take the peak clad temperature of the 17x17 array as the standard value under conduction and radiation. Then we calculate the peak clad temperature for the lumped array under the same physical condition, except with a modified rod emissivity. If this temperature is different from the standard value, we adjust the rod emissivity and iterate until the two temperatures are equal. Finally, the rod emissivity modification factor, $F_{\varepsilon r}$, is obtained for this lumped array using the following definition:

$$F_{\varepsilon r} = \frac{\varepsilon_r^L}{\varepsilon_r^T} \qquad (7\text{-}54)$$

where

$F_{\varepsilon r}$ = rod emissivity modification factor
ε_r^L = modified rod emissivity in the lumped array
ε_r^T = true value of rod emissivity in the original array, i.e., 17x17

The rod emissivity modification factor, $F_{\varepsilon r}$, is a function of several factors, i.e., ε_r, ε_w, but most significantly it is a function of lumped array size. A study focused on determining the modification factor was performed and the result is illustrated in Figure 7-7 using COBRA-SFS / RADGEN. We do not know exactly why there is a small dip when the 4x4 lumped array is chosen. Note that this study was based on conduction represented by GK = 10.8 since it was performed before the GK study in Table 7-2 was finished (for a change in GK factor, the methodology is provide in Section 7.2.7). Even though for the combined conduction and radiation case, small changes in GK do not perturb the results significantly, we still must develop the true GK values for the homogenized bundles. Using COBRA-SFS (Cycle 2) and with input deck and method provided here, Kao[11] improved the GK factors for the lumped 8x8 bundle which are shown in Table 7-10.

In summary, the homogenization procedure thus not only modifies geometry, but introduces a rod emissivity modification factor.

7.2.5 Verification of the Homogenization Procedure for Varying Wall Temperatures

The exact value of the bundle wall temperature in the KSC-7 cask are not known and will vary from bundle to bundle (Figure 5-3). In this study we demonstrate that the homogenization

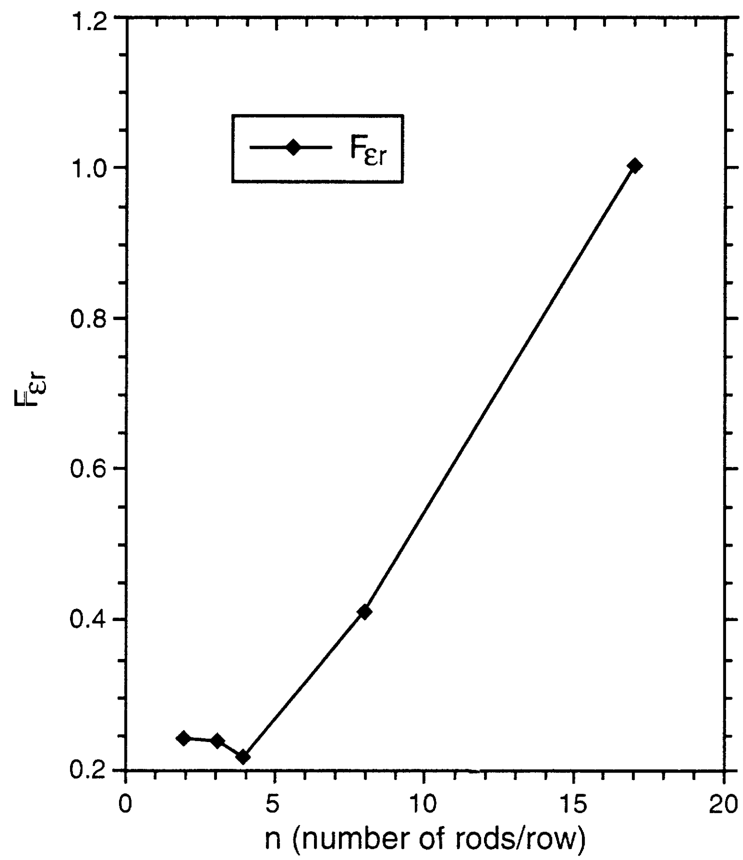

Figure 7-7 Radiation Factor and Its Corresponding Array Size.

Table 7-10 GK Factors for Lumped 8x8 bundle (COBRA-SFS)

Fill Gases	Powers (W)	Actual GK (Cycle1 / Cycle2)	Theoretical GK (Eq. 7-27)
N_2	4684	>100 / 23.1	13.4
	1750	31.6 / 30.8	14.0
He	4684	59.0 / 57.0	15.6
	1750	65.0 / 63.0	14.9

procedure is applicable independent of the wall temperature. To do so we will examine results at wall temperatures of 40°C, 96°C, 150°C, 200°C, and 250°C using COBRA-SFS.

Figure 7-8 shows the peak clad temperature as a function of the bundle wall temperature. For bundle wall temperatures ranging from 40°C to 250°C, the peak clad temperature deviates by no more than 4°C for arrays lumped to as small as 3x3. Hence, the homogenization procedure (geometry adjustment and the radiation modification factor) is adequate in representing the 17x17 arrays of the KSC-7 cask by lumped smaller arrays.

7.2.6 Summary

The principle of homogenization is outlined in Section 7.2.1, followed by the derivation of the specific homogenization expressions.

Lumped fuel bundle analysis shows an excessive radiative heat transfer due to the diminished shielding by the rods in the lumped fuel array. This effect is compensated for by introducing the emissivity modification factor ($F_{\varepsilon r}$). The factor is numerically shown in Figure 7-7. The value of the factor decreases as the number of rods in the homogenized array decreases. For the lumped 8x8 square array, $F_{\varepsilon r}$ is recommended to be 0.40.

Finally, the homogenization procedure is validated by varying wall temperatures for several different bundle sizes (Figure 7-8).

7.2.7 Recommendations

Currently KAERI uses a GK factor of 1.0, a 90° clad circumference segment, and rod and wall emissivities of 0.8 and 0.5 (see Appendix 4), respectively, in the lumped 8x8 bundle analysis. We recommend the following parameters for the homogenized bundle:

1) The same total decay power as in the original 17x17 bundle.
2) Geometries as described from Equations 7-39 to 7-53.
3) Wall emissivity of $\varepsilon_w = 0.3$.
4) Rod emissivity modification factor, $F_{\varepsilon r} \approx 0.4$ for the lumped 8x8 bundle. This yields an input rod emissivity of $\varepsilon_r = 0.8\ (0.4) = 0.32$.
5) Conduction length factor, GK = 10.8 for Cycle 1 code or values in Table 7-10 for Cycle 2 code for the lumped 8x8 bundle.

Table 7-11 illustrates that the introduction of rod emissivity modification factor will result in a 55°C correction in peak clad temperature in the lumped bundle.

The effect of the recommended correction in rod emissivity which keeps peak clad temperature as 413.0°C is shown in Table 7-11. Note GK = 10.8 is assumed in this calculation. If, for consistency with the GK factor recommended for the standard bundle, KAERI wants to use GK values in Table 7-10 for the 8x8 bundle, then the rod emissivity factor, $F_{\varepsilon r}$, may need slight modification. The computation steps should be accomplished as follows:

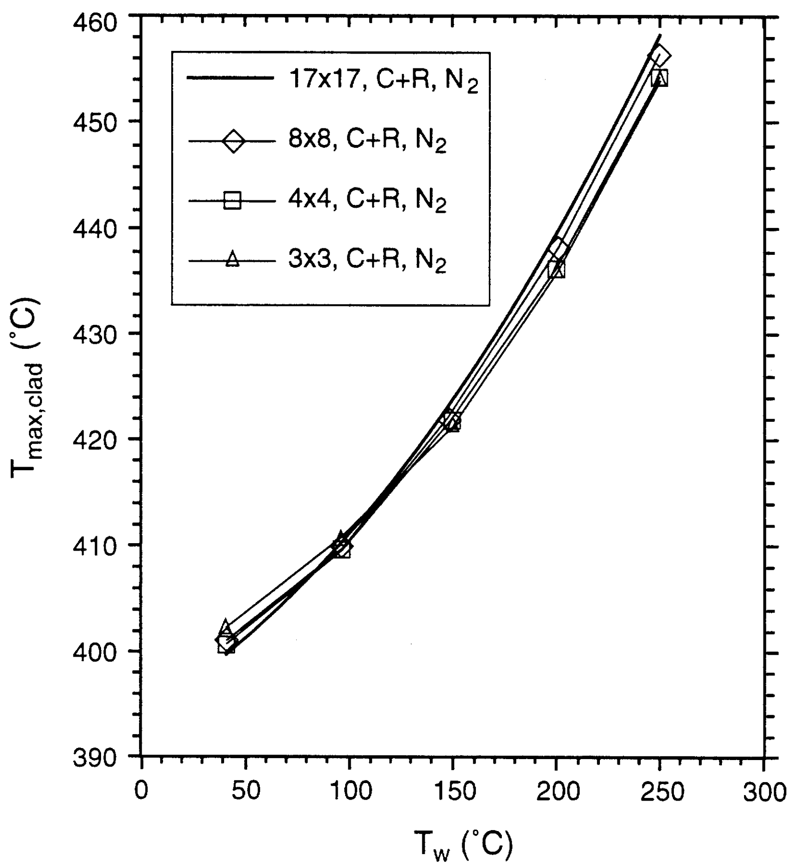

Figure 7-8. $T_{max,clad}$ versus T_w (17x17, 8x8, 4x4 and 3x3) at 4684 W.

Table 7-11. Peak Clad Temperatures vs. Rod Emissivity—8x8 Bundle, Conduction and Radiation, N_2, GK = 10.8, $\varepsilon_w = 0.3$

ε_r	$F_{\varepsilon r}$	$T_{clad,max}$ (°C)
0.8	1.0	358.2
0.32	0.40	413.0

Step 1: Change GK from 10.8 to respective values in Table 7-10 in COBRA-SFS input file.

Step 2: Change rod emissivity to a new value in the input file of RADGEN.

Step 3: Run RADGEN.

Step 4: Run COBRA-SFS.

Step 5: Compare the peak clad temperature obtained from COBRA-SFS with corresponding MIT result provided in Table 7-5.

Step 6: If the two temperatures do not match, repeat Steps 2 to 5. Otherwise, the modified rod emissivity is the one used in Step 2.

7.3 Lumped Effective Conductivity Thermal Analysis of the KSC-7 Cask

An analytical heat transfer model has been developed for the KSC-7 cask. This work is comprised of four parts:

1) A set of generic equations for conductive heat transfer is developed,
2) A set of generic equations for radiative heat transfer is developed,
3) A set of analytic solution equations is developed specifically for the KSC-7 geometry, and
4) Solution procedures to find the maximum temperature is provided for coding of the method.

The four parts are elaborated in the following sections.

7.3.1 Conductive Heat Transfer

From *Nuclear Systems I* (Page 297,[9]), a generic equation for the heat conduction is obtained

$$\rho C_p(\vec{r},t)\frac{\partial T(\vec{r},t)}{\partial t} = \nabla \cdot k(\vec{r},T)\nabla T(\vec{r},t) + q'''(\vec{r},t) \tag{7-55}$$

where

ρ	= density of heat conduction medium, kg/m^3
C_p	= specific heat capacity at constant pressure, J/(kg °C)
k	= thermal conductivity of the medium, W/(m °C)
q'''	= volumetric power density, W/m^3
t	= transient time, sec
T	= temperature, °C
r	= geometric location, m

In steady state, physical parameters are no longer functions of time, Equation 7-55 can be rewritten as

$$\nabla \cdot k(\vec{r},T)\nabla T(\vec{r}) + q'''(\vec{r}) = 0 \tag{7-56}$$

Let us consider two cases of cylindrical geometry where $q''' \neq 0$ and $q''' = 0$, as illustrated in Figure 7-9.

1) Pellet

For homogeneous symmetric solid cylinder ($r_i = 0$) with volumetric energy generation rate, $q''' \neq 0$, i.e., reactor fuel pellet thermal conductivity, k, and volumetric power density, q''', are no longer functions of location, $\vec{r}$, Equation 7-56 can be simplified to:

$$\nabla \cdot k(T)\nabla T(\vec{r}) + q''' = 0 \tag{7-57}$$

or

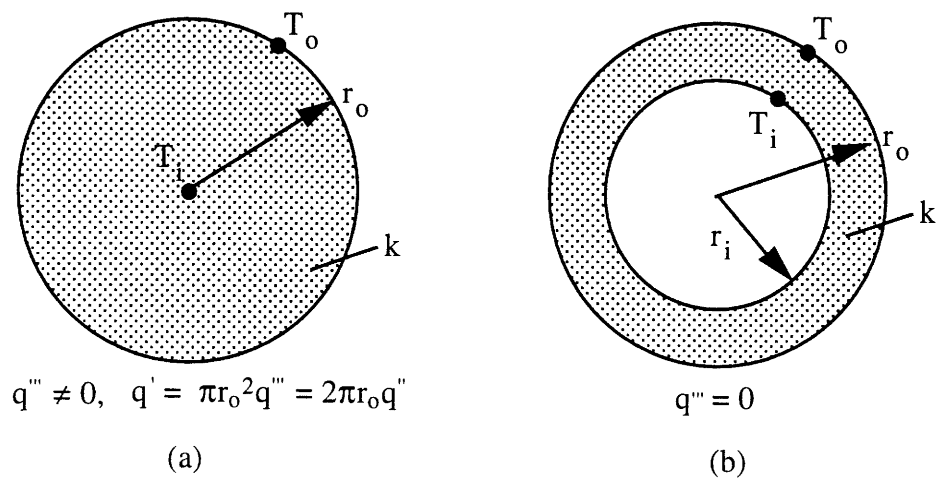

Figure 7-9. Conductive Heat Transfer Model.

$$\frac{1}{r}\left[\frac{d}{dr}\left(kr\frac{dT}{dr}\right)\right] + q''' = 0 \tag{7-58}$$

or equivalently,

$$\frac{d}{dr}\left(kr\frac{dT}{dr}\right) + q'''r = 0 \tag{7-59}$$

Integrating once, we get

$$k\frac{dT}{dr} + \frac{1}{2}q'''r = \frac{C_1}{r} \tag{7-60}$$

where

C_1 = integration constant

Applying boundary condition at the pellet centerline, $\left.\frac{dT}{dr}\right|_{r=r_i=0}$, we deduce $C_1 = 0$ and Equation 7-60 becomes

$$k\frac{dT}{dr} = -\frac{1}{2}q'''r \tag{7-61}$$

With another integration, Equation 7-61 becomes

$$\int_{T_i}^{T_o} kdT = -\frac{1}{2}\int_{r_i}^{r_o} q'''rdr = -\frac{1}{2}\int_{0}^{r_o} q'''rdr = -\frac{q'''}{4}r_o^2 \tag{7-62}$$

where

T_i = temperature at the pellet centerline, K

To = temperature at pellet outer surface, K

r_o = pellet radius, m

If the thermal conductivity, k, is independent of temperature, Equation 7-62 can be rewritten as

$$k(T_i - T_o) = \frac{r_o^2}{4}q'''$$

or

$$T_i = T_o + \frac{r_o^2}{4k}q''' \tag{7-63}$$

For solid fuel pellet, $q' = \pi r_o^2 q'''$, Equation 7-63 is equivalent to

$$T_i = T_o + \frac{q'}{4\pi k} \tag{7-64}$$

2) Cladding

For homogeneous, symmetric cylindrical shell with volumetric energy generation rate $q''' = 0$, i.e., fuel clad with $q''' = 0$, Equation 7-58 becomes:

$$\frac{1}{r}\frac{d}{dr}\left(kr\frac{dT}{dr}\right) = 0 \qquad (7\text{-}65)$$

Integrate Equation 7-65 once, we have

$$k\frac{dT}{dr} = \frac{C_2}{r} \qquad (7\text{-}66)$$

where

C_2 = integration constant

Applying boundary condition at cladding outer surface

$$q'' = -k\frac{dT}{dr}\bigg|_{r=r_o} \qquad (7\text{-}67)$$

to solve for constant C_2

$$C_2 = -q''r_o = -\frac{q'}{2\pi} \qquad (7\text{-}68)$$

Substituting Equations 7-68 into 7-66 yields

$$k\frac{dT}{dr} = -\frac{q'}{2\pi}\cdot\frac{1}{r} \qquad (7\text{-}69)$$

Integrate Equation 7-69 again, we have

$$\int_{T_i}^{T_o} kdT = -\frac{q'}{2\pi}\int_{r_i}^{r_o}\frac{dr}{r} \qquad (7\text{-}70)$$

where

T_i = temperature at the pellet centerline, K

T_o = temperature at pellet outer surface, K

r_i = inside clad radius, m

r_o = outside clad radius, m

If the thermal conductivity, k, is independent of temperature, Equation 7-70 can be rewritten as

$$k(T_o - T_i) = -\frac{q'}{2\pi}\ln\frac{r_o}{r_i}$$

or

$$T_i = T_o + \frac{q'}{2\pi k} \ln \frac{r_o}{r_i} \qquad (7\text{-}71)$$

The thin shell approximation can be used to simplify Equation 7-71 if $r_o/r_i \approx 1.0$ or $(r_o - r_i)/r_i << 1$

$$\ln\left(\frac{r_o}{r_i}\right) = \ln\left(1 + \frac{r_o - r_i}{r_i}\right) = \frac{r_o - r_i}{r_i} + o\left(\frac{r_o - r_i}{r_i}\right) \approx \frac{\delta}{r_i} \qquad (7\text{-}72)$$

where

δ = the shell thickness, $r_o - r_i$

$o\left(\frac{r_o - r_i}{r_i}\right)$ = higher than first order of $\left(\frac{r_o - r_i}{r_i}\right)$

With Equation 7-72, Equation 7-71 is approximated as

$$T_i = T_o + \frac{q'}{2\pi k \frac{r_i}{\delta}} \qquad (7\text{-}73)$$

As an approximate method, Equation 7-73 will simplify mathematical manipulation. However, the exact solution, Equation 7-71, will be used in our derivation for KSC-7 cask.

7.3.2 Radiative Heat Transfer

1) Energy Balance on a Grey Body Surface

Figure 7-10a illustrates the energies emitted, reflected and absorbed on a grey body surface (solid line). Dashed lines 1 – 1 and 2 – 2 represent two imaginary planes very close to the grey body surface.

The energy, i.e., power, balance per unit area on the plane 1 – 1 can be expressed as

$$q'' = E - \alpha G \qquad (7\text{-}74)$$

where

q'' = net energy flux from plane 1 – 1 per unit surface area, W/m^2

E = radiation energy flux directly from the grey body to the surroundings per unit surface area, W/m^2

G = incoming energy flux from the surroundings to the grey body per unit surface area, W/m^2

α = grey body absorption coefficient.

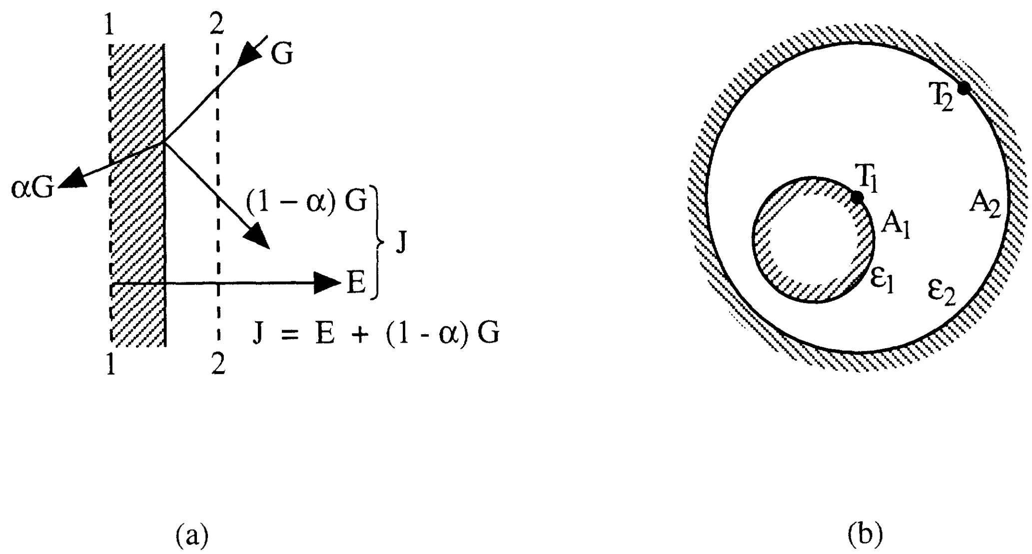

Figure 7-10. Radiative Heat Transfer Model: (a) Energy Balance on a Grey Body Surface; (b) Radiative Heat Transfer Between Surface and Its Enclosed Surface.

The energy balance per unit area on the plane 2 – 2 can be written as

$$q'' = J - G \tag{7-75}$$

where

J = effective radiation of the grey body per unit area, W/m^2.

Eliminating G in Equations 7-74 and 7-75 yields

$$J = \frac{E}{\alpha} - \left(\frac{1}{\alpha} - 1\right) q'' \tag{7-76}$$

Now at thermal equilibrium, $\alpha = \varepsilon$, so

$$E_b = E / \varepsilon = E / \alpha \tag{7-77}$$

Substituting Equations 7-77 into 7-76 yields

$$J = E_b - \left(\frac{1}{\varepsilon} - 1\right) q'' \tag{7-78}$$

where

E_b = black body radiation per unit area , W/m^2
and from Stefan-Boltzmann Radiation Law, $E_b = \sigma T^4$ (7-79)

ε = grey body emissivity

T = absolute temperature, K.

2) Radiative Heat Transfer between a Surface and Its Enclosed Surface

Figure 7-10b describes the radiative heat transfer between one surface (A_2) and the enclosed surface (A_1). The heat transferred radiatively, $Q_{1,2}$, from grey body surface A_1 to surface A_2 is

$$Q_{1,2} = J_1 A_1 F_{1,2} - J_2 A_2 F_{2,1} \tag{7-80}$$

where

$Q_{1,2}$ = radiative heat transfer from grey surface A_1 to A_2, W/m^2

A_1, A_2 = grey body surface areas, m^2

$F_{1,2}$ = view factors from surface 1 to surface 2

$F_{2,1}$ = view factors from surface 2 to surface 1

Since convex surface A_1 is completely enclosed by surface A_2, the effective radiation of surface A_1, J_1, can fully reach surface A_2. Hence, $F_{1,2} = 1.0$. Thus, Equation 7-80 is reduced to

$$Q_{1,2} = J_1 A_1 - J_2 A_2 F_{2,1} \tag{7-81}$$

Apply Equation 7-77 to surfaces A_1 and A_2 by multiplying their surface areas, respectively, we get

$$J_1A_1 = A_1E_{b1} - \left(\frac{1}{\varepsilon_1} - 1\right)q''_{1,2}A_1$$

or

$$J_1A_1 = A_1E_{b1} - \left(\frac{1}{\varepsilon_1} - 1\right)Q_{1,2} \tag{7-82}$$

and similarly

$$J_2A_2 = A_2E_{b2} - \left(\frac{1}{\varepsilon_2} - 1\right)Q_{2,1} \tag{7-83}$$

Substituting Equations 7-82 and 7-83 into Equation 7-81, and using $Q_{1,2} = -Q_{2,1}$ in steady state, to obtain the radiative heat transfer from surface A_1 to surface A_2, $Q_{1,2}$

$$Q_{1,2} = \frac{E_{b1}A_1 - F_{2,1}E_{b2}A_2}{\frac{1}{\varepsilon_1} + F_{2,1}\left(\frac{1}{\varepsilon_2} - 1\right)} \tag{7-84}$$

Since

$$A_1F_{1,2} = A_2F_{2,1} \tag{7-85a}$$

Solve for $F_{2,1}$, we get

$$F_{2,1} = \frac{A_1}{A_2}F_{1,2} \tag{7-85b}$$

When $F_{1,2} = 1.0$, Equation 7-85b will be reduced to

$$F_{2,1} = \frac{A_1}{A_2} \tag{7-86}$$

Substituting Equation 7-86 into Equation 7-84 yields

$$Q_{1,2} = \frac{A_1(E_{b1} - E_{b2})}{\frac{1}{\varepsilon_1} + \frac{A_1}{A_2}\left(\frac{1}{\varepsilon_2} - 1\right)} \tag{7-87}$$

Using Equation 7-79, Equation 7-87 can be reduced as

$$Q_{1,2} = \frac{A_1\sigma\left(T_1^4 - T_2^4\right)}{\frac{1}{\varepsilon_1} + \frac{A_1}{A_2}\left(\frac{1}{\varepsilon_2} - 1\right)} \tag{7-88}$$

or

$$Q_{1,2} = A_1 \varepsilon_{1,2} \sigma \left(T_1^4 - T_2^4\right) \tag{7-89}$$

where

$\varepsilon_{1,2}$ = effective emissivity between Surface A_1 and Surface A_2, and

$$\varepsilon_{1,2} \equiv \left[\frac{1}{\varepsilon_1} + \frac{A_1}{A_2}\left(\frac{1}{\varepsilon_2} - 1\right)\right]^{-1} \tag{7-90}$$

7.3.3 Application to the KSC-7 Cask

In this section the foregoing models for conduction and radiation heat transfer will be used to develop an analytic solution for the maximum clad temperature in steady state in the KSC-7 cask. Figure 7-11 illustrates the simplified, symmetric representation of the quarter cask geometry which is analyzed to yield the desired peak clad temperature, T_6.

The KSC-7 cask is modeled using cylindrical shells (Figure 7-11) to represent their counterparts in Figure 5-3. Please note that the model provided here accounts for heat transfer from the fuel region to the leaded gamma-ray shield. However, equations can be added similarly if more outer shells are to be modeled.

1) $T_0 \rightarrow T_1$: Heat is transferred convectively on the outer surface of the lead shield if it is the outmost surface. Heat convection equation on the outer surface is

$$q'' = h\,(T_1 - T_o) \tag{7-91}$$

or

$$T_1 - T_o = \frac{q''}{h} \tag{7-92}$$

or equivalently

$$T_1 - T_o = \frac{q'}{2\pi R_1 h} \tag{7-93}$$

where

T_0 = outer fluid temperature, K

T_1 = temperature at lead shield outer surface, K

h = heat transfer coefficient between outer fluid and surface, $W/(m^2 {}^\circ C)$

R_1 = outer radius of lead shield, m

q'' = surface heat flux, W/m^2

q' = linear heat flux ($=2\pi R_1 q''$), W/m

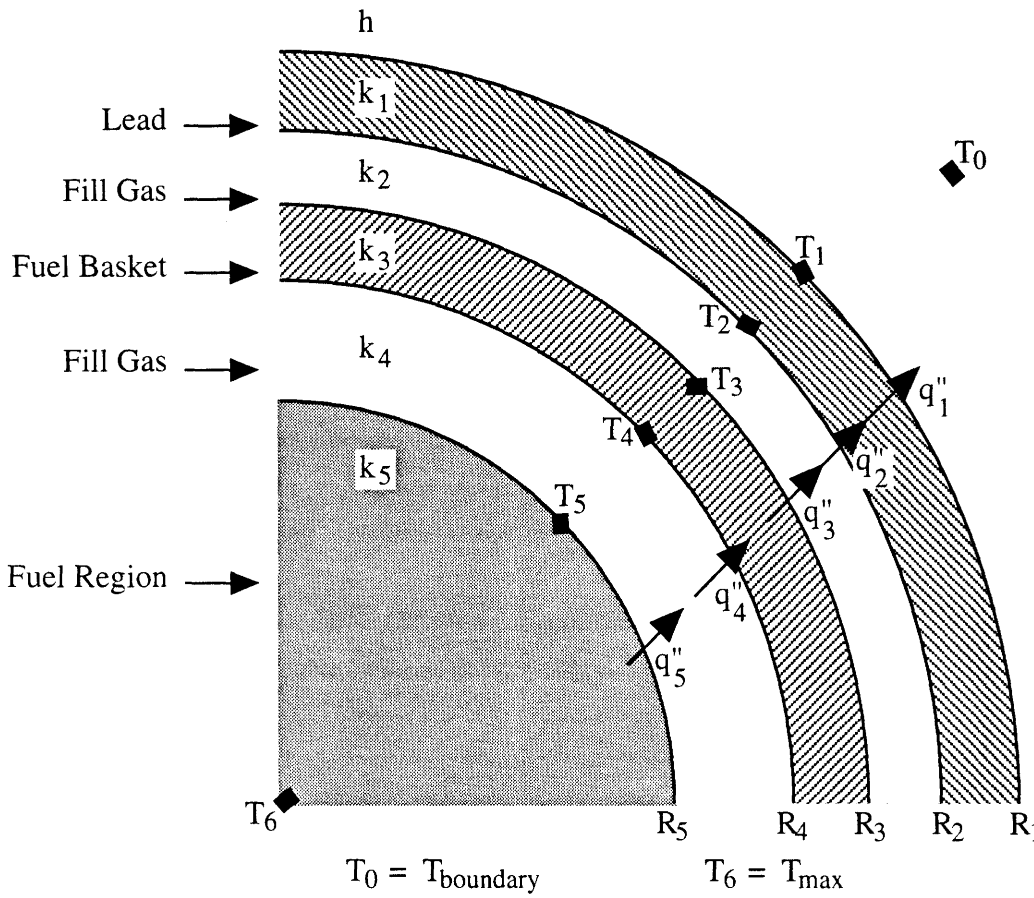

Figure 7-11. Analytical Model for KSC-7 Cask

2) $T_1 \rightarrow T_2$: Heat is transferred conductively through the lead shield

From Equation 7-71

$$T_2 - T_1 = \frac{q'}{2\pi k_1} \ln \frac{R_1}{R_2} \tag{7-94}$$

where

T_2 = temperature at outer surface of lead shield, K

k_1 = thermal conductivity of lead shield, W/(m °C)

R_2 = inner radius of lead shield, m

3) $T_2 \rightarrow T_3$: Conduction and Radiation (ignore convection):

Assume heat convection can be ignored in the fill gas, then heat conduction and radiation exist in the fill gas. Total linear heat flux is the sum of that of conduction and that of radiation, or

$$q' = q'_{3,2\ cond} + q'_{3,2\ rad} \tag{7-95}$$

where

$q'_{3,2rad}$ = radiative linear heat flux

$$q'_{3,2\ cond} = \frac{2\pi k_2}{\ln \frac{R_2}{R_3}} (T_3 - T_2) \tag{7-96}$$

= conductive linear heat flux

From Equations 7-87 and 7-90

$$Q_{3,2\ rad} = A_3 \varepsilon_{3,2} (E_{b3} - E_{b2}) \tag{7-97}$$

where

T_3 = temperature at outer surface of fuel basket, K

A_3 = outer surface area of fuel basket (= $2\pi D_3$), m^2

D_3 = effective diameter of fuel basket, m

R_3 = effective radius of fuel basket, m

L_a = axial length of fuel basket, m

$Q_{3,2rad} = q'_{3,2rad} \cdot L_a$ (7-98)

Using Equation 7-79 and equating Equations 7-97 and 7-98 yields

$$q'_{3,2\ rad} = 2\pi R_3 \varepsilon_{3,2} \sigma (T_3^4 - T_2^4) \tag{7-99}$$

where

$$\varepsilon_{3,2} = \frac{1}{\frac{1}{\varepsilon_3} + \frac{A_3}{A_2}\left(\frac{1}{\varepsilon_2} - 1\right)}$$

$$= \frac{1}{\frac{1}{\varepsilon_3} + \frac{R_3}{R_2}\left(\frac{1}{\varepsilon_2} - 1\right)} \quad (7\text{-}100)$$

Substituting Equations 7-96 and 7-99 into Equation 7-95 yields

$$q' = \frac{2\pi k_2}{\ln \frac{R_2}{R_3}}(T_3 - T_2) + 2\pi R_3 \varepsilon_{3,2} \sigma (T_3^4 - T_2^4) \quad (7\text{-}101)$$

Since mathematically

$$T_3^4 - T_2^4 = (T_3^2 + T_2^2)(T_3 + T_2)(T_3 - T_2) \quad (7\text{-}102)$$

Equation 7-101 can be re-formulated as

$$q' = \left[\frac{2\pi k_2}{\ln \frac{R_2}{R_3}} + 2\pi R_3 \varepsilon_{3,2} \sigma (T_3^2 + T_2^2)(T_3 + T_2)\right] \cdot (T_3 - T_2) \quad (7\text{-}103)$$

or

$$T_3 - T_2 = \frac{q'}{2\pi\left[\frac{k_2}{ln\left(\frac{R_2}{R_3}\right)} + R_3 \cdot \varepsilon_{3,2} \cdot \sigma (T_3^2 + T_2^2)(T_3 + T_2)\right]} \quad (7\text{-}104)$$

Note if the temperature gradient in fill gas is not significant, that is, $\frac{|T_2 - T_3|}{T_2} << 1$ and $\frac{|T_2 - T_3|}{T_3} << 1$, then

$$(T_3^2 + T_2^2) \cdot (T_3 + T_2) \approx 4T_2^3 \quad (7\text{-}105)$$

Equation 7-103 can be simplified as

$$q' = 2\pi \cdot \left[\frac{k_2}{\ln \frac{R_2}{R_3}} + 4R_3 \varepsilon_{3,2} \sigma T_2^3\right] \cdot (T_3 - T_2) \quad (7\text{-}106)$$

or

$$q' = 2\pi k_{eff,2}(T_3 - T_2) \quad (7\text{-}107)$$

where

$$k_{eff,2} = \frac{k_2}{\ln\left(\frac{R_2}{R_3}\right)} + 4R_3\varepsilon_{3,2}\sigma T_2^3 \qquad (7\text{-}108)$$

= effective thermal conductivity, W/(m °C)

and Equation 7-107 becomes equivalently

$$T_3 - T_2 = \frac{q'}{2\pi k_{eff,2}} \qquad (7\text{-}109)$$

4) $T_3 \rightarrow T_4$: Heat is transferred conductively in fuel basket

From generic Equation 7-71

$$T_4 - T_3 = \frac{q'}{2\pi k_3} \ln\frac{R_3}{R_4} \qquad (7\text{-}110)$$

where

R_4 = effective inner radius of fuel basket, m

k_3 = thermal conductivity of fuel basket, W/(m °C)

T_4 = temperature at inner surface of fuel basket, K

5) $T_4 \rightarrow T_5$ Conduction and Radiation (ignore convection):

If heat convection can be ignored through fill gas, then total heat transfer is the sum of conductive and radiative heat transfer.

Similarly, following the steps to derive Equation 7-104,, we get

$$T_5 - T_4 = \frac{q'}{\frac{2\pi k_4}{\ln\frac{R_4}{R_5}} + 2\pi R_5\varepsilon_{5,4}\sigma(T_5^2 + T_4^2)(T_5 + T_4)} \qquad (7\text{-}111)$$

where

R_5 = effective fuel radius, m

k_4 = thermal conductivity of fill gas in fuel basket, W/(m °C)

T_5 = fuel outside surface temperature, K

If the temperature gradient is not significant across gas between pellet and clad, $|T_4 - T_5| << T_4$ or T_5, then

Hence Equation 7-111 can be simplified as

$$T_5 - T_4 = \frac{q'}{2\pi k_{eff,4}} \tag{7-113}$$

where

$$k_{eff,4} = \frac{k_4}{\ln\left(\frac{R_4}{R_5}\right)} + 4R_5\varepsilon_{5,4}\sigma T_4^3 \tag{7-114}$$

and

$$\varepsilon_{5,4} = \frac{1}{\frac{1}{\varepsilon_5} + \frac{R_5}{R_4}\left(\frac{1}{\varepsilon_4} - 1\right)} \tag{7-115}$$

6) $T_5 \rightarrow T_6$: Heat is transferred conductively through fuel region
From generic Equation 7-71

$$T_6 - T_5 = \frac{q'}{4\pi k_5} \tag{7-116}$$

where

k_5 = thermal conductivity of cladding, W/(m °C)
T_6 = peak cladding temperature, K

7.3.4 Procedure to Find T_6

T_0, q', properties of materials, i.e., thermal conductivity, k, surface emissivities, geometry, are the knowns, while T_6 is the unknown. Follow the procedure described below to find the unknown.

1) T_1 can be determined using Equation 7-93;

2) T_2 can be determined using Equation 7-94;

3) T_3 can be determined using Equation 7-104. This step requires iteration since T_3, the unknown, appears in the right hand side of the equation.

4) T_4 can be determined using Equation 7-110;

5) T_5 can be determined using Equation 7-111. Similar to Step 3, this step also requires iteration since T_5, the unknown, appears in the right hand side of the equation.

6) T_6 can be determined using Equation 7-116.

The above steps are illustrated in Figure 7-12. Note that:

(1) Since Equations 7-104 and 7-111 are used in Steps 3 and 5 in proposed KSC-7 analytical calculation, no approximation for $T_i^4 - T_j^4 = \left(T_i^2 + T_j^2\right)(T_i + T_j)(T_i - T_j)$ is not made, i.e., Equations 7-105 and 7-112 are not used;

(2) If axial power peaking factor, $F_{peak} \neq 1.0$, q' should be replaced by $(q' \cdot F_{peak})$.

7.3.5 Summary

The maximum clad temperature, T_6, for KSC-7 has been determined by a best estimate analytic procedure described in Parts A through D above. This analytic result can be used to test the COBRA-SFS calculated result for reasonableness and thereby confirm the input data. If an analytic bounding calculation is desired, this analytic procedure can be adjusted step by step to insure a bounding result.

7.4 Comments on KAERI's COBRA-SFS Thermal Analysis of the KSC-7 Cask

7.4.1 Examination of KSC-7 Input Files from KAERI

Upon receiving the KSC-7 input files from KAERI through electronic-mail, we checked the 8x8 lumped fuel bundle and found that some of the inputs are not consistent with our calculation using 17x17 bundle data provided by KAERI and our homogenization method. A partial summary of the input discrepancies are presented in Table 7-12. A complete input file of our work from which KAERI can identify all discrepancies is appended to this report.

7.4.2 Emissivity

Emissivities are properties of the material of the rods and the wall. They are important in determining radiation heat transfer which dominates heat transfer in the dry spent fuel cask. Hence, they should be chosen carefully so as to predict peak clad temperature correctly.

The measured values for the emissivities are recommended because these are the relevant values under the specific cask conditions. If they have to be estimated, then the uncertainty in the estimation, i.e., sensitivity study, must be taken into account in determining the uncertainty in the peak clad temperature. We have not surveyed the literature for measured values. Commonly used emissivity values in COBRA-SFS calculations are 0.8 for the rod emissivity, 0.25 for the stainless steel, and 0.2 for the aluminum wall emissivities in the spent fuel cask calculations [1, 12].

After reviewing KAERI's thermal analysis of KSC-7 cask, we found that rod emissivity, ε_r, is taken as 0.8, while wall emissivity, ε_w, is 0.5. The value of ε_w appears too large even if the stainless steel wall is borated, and this, according to our sensitivity study in Chapter 7, led to underprediction of the peak clad temperature.

$$
\begin{array}{ccccccc}
T_0 & \xrightarrow[\text{Eq. 93}]{1)} & T_1 & \xrightarrow[\text{Eq. 94}]{2)} & T_2 & \underset{\text{Eq. 104}}{\overset{3)}{\rightleftarrows}} & T_3 \\
 & & & & & \text{Eq. 110} & \downarrow \; 4) \\
 & & T_6 & \xleftarrow[\text{Eq. 116}]{6)} & T_5 & \underset{\text{Eq. 111}}{\overset{5)}{\rightleftarrows}} & T_4
\end{array}
$$

(Numbers above the arrow are step numbers.)

Figure 7-12 Analytical Steps to Find Peak Clad Temperature, T_6

Table 7-12. Data Discrepancy between MIT and KAERI 8x8 Fuel Bundles (for COBRA-SFS)

		MIT	KAERI
Rod outside diameter (in.)		0.7948	0.8051
Pellet diameter (in.)		0.6851	0.6996
Cladding thickness (in.)		0.0476	0.0423
Flow area (in^2)	Channels 1 and 9	0.5797	0.5016
	Channels 2 to 8	0.6361	0.5916
	Channels 11 to 17	0.6148	0.6294
Wetted perimeter (in)	Channels 1 and 9	2.302	2.218
	Channels 2 to 8	2.303	2.332
	Channels 11 to 17	2.497	2.529
Heated perimeter (in)	Channels 1 and 9	0.6242	0.6323
	Channels 2 to 8	1.248	1.265
	Channels 11 to 17	2.497	2.529

The emissivity for the boundary wall is taken to be 1.0 (BDRY.2), which means the boundary wall is, instead of a gray body, a black body. Hence, this assumption is not conservative. A sensitivity study on the boundary wall emissivity is recommended.

Furthermore, other parameters in BDRY.2 can be referenced in Section 3.4.1.1 [1]. Note that the characteristic length, L, is the height of the surface for vertical orientation and the diameter of the cylinder for horizontal orientation.

We suggest that the measured value be used in KAERI's analysis and the radiation factor described in Section 7.2 be utilized.

7.4.3 Power Density

Since the total decay power for the seven 17x17 fuel assemblies contained in the KSC-7 cask is 32.3 kW, each assembly has one-seventh the total power (≈ 4614 W). This power determines the nominal power density of the fuel pellet (OPER.2). The value of the power density, 0.0069367 (PDN in OPER.2), as provided by KAERI, seems to be a little small. KAERI needs to find an appropriate value by checking the total power printed in the output file of COBRA-SFS against the true value of about 4614 W.

7.4.4 Examination of KSC-7 Results from KAERI (Quarter Model)

The peak clad temperature, 480°C for helium and 516°C for air cavity, should not be in the location that is indicated by KAERI. We think it should occur at the central region of the cask. We recommend KAERI check input files, especially the portion concerning the implementation of the adequate adiabatic boundary conditions.

7.4.5 Examination of KSC-7 Results from KAERI (Full Model)

The peak clad temperature, 518°C for helium and 545°C for air cavity, appears at the reasonable location. However, the boundary temperature, 135°C, as illustrated in the figures is not only different from the quarter cask model but cannot be derived from the boundary condition Group BDRY.3 of the input file, which indicates a boundary axial temperature profile of 140°C (284°F) for the top and bottom, and 150°C (302°F) for the middle of the cask. We think the boundary temperature profile should be the same in the quarter model as in the full model.

CHAPTER 8

RECOMMENDATIONS FOR FUTURE WORK

8.1 Conduction

The theoretically derived GK values are in satisfactory agreement with the practical ones from COBRA-SFS for the 17x17 bundle. However, it is not the case for the lumped 8x8 bundle. Theoretical GK's are listed in Table 7-10. In practice they are several times larger (see Table 7-10). We have not found the exact reasons yet, but one speculation is that it is due to the fact that, in lumped fuel model, the gaps between fuel rods are larger which decreases the enhancement effect of cladding in heat transfer, reduces heat conduction and therefore, increases GK's (Compare gaps between Figures 5-1 and 5-2.). Fortunately, this is not a significant factor when radiation is taken into account since, in practice, radiation is dominant in dry storage spent fuel cask, especially with low thermal conductivity fill gas such as N_2. For conservatism, a value of 10.8 for GK is acceptable for the lumped 8x8 bundle.

8.2 Radiation

As mentioned in Section 7.4, the radiative heat transfer mechanism is dominant in the heat transfer of dry spent fuel storage cask. Hence, the adequate representation of the radiative heat transfer, i.e., by rod and wall emissivities, is quite necessary and future work should be focused on the determination of these emissivities and their uncertainties. This work will enable the effect of the uncertainty in the peak clad temperature to be reduced.

8.3 Convection

The code developer's recommendation for the convective heat transfer Nusselt number (Nu = 3.66) is based on the assumption of fully developed fluid velocity and temperature profiles (forced flow) in laminar flow inside a circular tube with constant wall temperature profile [12, 13].

The adoption of this value for the KSC-7 cask analysis is questionable with regard to the following points:

(1) The fuel in the cask is in a bundle array geometry, not a circular tube.

(2) The bundle wall temperature is not constant axially.

(3) The fluid (N_2 or He) within the cask is in natural convection, not forced convection.

(4) The flow pattern may not be laminar flow. It should be determined first whether it is laminar flow or turbulent flow.

Nusselt numbers for other geometries are given in [13] and are cited here in Table 8-1. The Nusselt number for a fuel bundle is not immediately available.

Future work in the convective heat transfer mechanism should develop an appropriate Nusselt number specific to the situation of the KSC-7 for longitudinal flow. Also, the presence of transverse flow needs to be accommodated by more fundamental adjustment in the momentum equation set of COBRA-SFS.

Table 8-1 Nusselt Numbers for Fully Developed Velocity and Temperature Profiles in Tubes of Various Cross Sections (from [13])

Cross-Section Shape	b / a	$Nu_{(H)}$ *	$Nu_{(T)}$
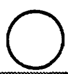		4.364	3.66
a 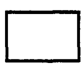 b	1.0	3.61	2.98
	1.43	3.73	3.08
	2.0	4.12	3.39
	3.0	4.79	3.96
	4.0	5.33	4.44
	8.0	6.49	5.60
	∞	8.235	7.54
		5.385	4.86
		3.00	2.35

* The constant-heat-rate solutions are based on constant axial heat rate, but with constant temperature around the tube periphery.

REFERENCES

[1] D.R. Rector, et al., "*COBRA-SFS: A Thermal-Hydraulic Analysis Computer Code*", PNL-6049 Vol. II: User's Manual, November 1986.

[2] R.D. Manteufel, "*Heat Transfer in an Enclosed Rod Array*", Ph.D. thesis, Dept. of Mech. Engr., Massachusetts Institute of Technology, May 1991.

[3] R.D. Manteufel and N.E. Todreas, "*Effective Thermal Conductivity and Edge Conductance Model for a Spent Fuel Assembly*", *Nuclear Technology*, V.105, March 1994.

[4] D.R. Rector, et al., "*COBRA-SFS: A Thermal-Hydraulic Analysis Computer Code*", PNL-6049 Vol. I: *Mathematical Models and Solution Method*, November 1986.

[5] D.R. Rector, et al., "*RADGEN: A Radiation Exchange Factor Generator for Rod Bundles*", PNL-6342, October 1987.

[6] P.M. Lovett, "*An Experiment to Simulate the Heat Transfer Properties of A Dry, Horizontal Spent Nuclear Fuel Assembly*", Vols. I and II, Dept. of Nucl. Engr., Massachusetts Institute of Technology, MITNE-294, September 1991.

[7] S. Wolfram, "*Mathematia: A System for Doing Mathematics by Computer*", Wolfram Research Inc., second edition, 1991.

[8] "*Mathematia: A System for Doing Mathematics by Computer – User's Guide for the Macintosh*", Wolfram Research Inc., 1991.

[9] N. Todreas and M. Kazimi, "*Nuclear Systems I: Thermal Hydraulic Fundamentals*", Hemisphere Publishing Corp., 1990.

[10] N.E. Todreas, personal communication with KAERI, June 1993 ~ January 1995.

[11] T.M. Kao, "*22.902 Special Problem Term Paper*" and its "*Amendments*", Dept. of Nucl. Engr., Massachusetts Institute of Technology, August, 1995.

[12] Personal communications with Judith M. Cuta, PNL, March 1994 ~ January 1995.

[13] W.M. Kays and M.E. Crawford, "*Convective Heat and Mass Transfer*", 2nd edition, McGraw-Hill, 1980.

[14] R.L. Cox, "*Radiation Heat Transfer in Arrays of Parallel Cylinders*", ORNL-5239, Oak Ridge National Laboratory, Oak Ridge, Tennessee, 1977.

[15] E.H. Kwack, "*COBRA-SFS Sample Problem: Thermal Analysis of KSC-4 Cask*", communication with N. Todreas, June 10, 1993.

[16] X. Chen and N.E. Todreas, "*Thermal Analysis of Dry Spent Fuel Transportation and Storage Casks - Draft for Final Review*", MIT-ANP-TR-029, January 10, 1995.

[17] N.E. Todreas, "*Proposal: Thermal Analysis of Dry Spent Fuel Transportation and Storage Casks*", Dept. of Nucl. Engr., Massachusetts Institute of Technology, 1993.

APPENDICES

APPENDIX 1

LUMPED 8X8 FUEL BUNDLE ANALYSIS —INPUT FILE FOR COBRA-SFS(Cycle 1)

```
+2000
    1              KSC-7 CASK ( 8X8 FUEL, NITROG, 10/94)
PROP        12       1
            0.        100.     133.9     .0154     .240     14.08     .0463
            0.        200.     157.9     .0174     .241     16.67     .0518
            0.        300.     182.1     .0193     .243     19.23     .0580
            0.        400.     206.5     .0212     .245     21.74     .0630
            0.        500.     231.1     .0231     .247     24.27     .0680
            0.        600.     256.0     .0250     .250     26.81     .0720
            0.        700.     281.1     .0268     .253     29.33     .0770
            0.        800.     306.7     .0286     .256     31.85     .0810
            0.        900.     332.5     .0303     .259     34.36     .0850
            0.       1000.     358.6     .0319     .262     36.90     .0889
            0.       2000.     617.2     .0471     .286     62.11     .1242
            0.       5000.     868.9     .0587     .302     83.40     .1449
        1STEEL                         1.E8
CHAN         1     19
         160.0          90.0
      1      1     81      0
      1      1      0      1
   1.57972.302.6242     2.4415.9465     10.4415.9465
   2.63612.3031.248     3.44151.054     11.2592.9465
   3.63612.3031.248     4.44151.054     12.2592.9465
   4.63612.3031.248     5.44151.054     13.2592.9465
   5.63612.3031.248     6.44151.054     14.2592.9465
   6.63612.3031.248     7.44151.054     15.2592.9465
   7.63612.3031.248     8.44151.054     16.2592.9465
   8.63612.3031.248     9.4415.9465     17.2592.9465
   9.57972.302.6242    18.4415.9465
  10.63612.3031.248    11.2592.9465     19.44151.054
  11.61482.4972.497    12.25921.054     20.25921.054
  12.61482.4972.497    13.25921.054     21.25921.054
  13.61482.4972.497    14.25921.054     22.25921.054
  14.61482.4972.497    15.25921.054     23.25921.054
  15.61482.4972.497    16.25921.054     24.25921.054
  16.61482.4972.497    17.25921.054     25.25921.054
  17.61482.4972.497    18.2592.9465     26.25921.054
  18.63612.3031.248    27.44151.054
  19.63612.3031.248    20.2592.9465     28.44151.054
  20.61482.4972.497    21.25921.054     29.25921.054
  21.61482.4972.497    22.25921.054     30.25921.054
  22.61482.4972.497    23.25921.054     31.25921.054
  23.61482.4972.497    24.25921.054     32.25921.054
  24.61482.4972.497    25.25921.054     33.25921.054
  25.61482.4972.497    26.25921.054     34.25921.054
  26.61482.4972.497    27.2592.9465     35.25921.054
  27.63612.3031.248    36.44151.054
```

28.63612.3031.248	29.2592.9465	37.44151.054
29.61482.4972.497	30.25921.054	38.25921.054
30.61482.4972.497	31.25921.054	39.25921.054
31.61482.4972.497	32.25921.054	40.25921.054
32.61482.4972.497	33.25921.054	41.25921.054
33.61482.4972.497	34.25921.054	42.25921.054
34.61482.4972.497	35.25921.054	43.25921.054
35.61482.4972.497	36.2592.9465	44.25921.054
36.63612.3031.248	45.44151.054	
37.63612.3031.248	38.2592.9465	46.44151.054
38.61482.4972.497	39.25921.054	47.25921.054
39.61482.4972.497	40.25921.054	48.25921.054
40.61482.4972.497	41.25921.054	49.25921.054
41.61482.4972.497	42.25921.054	50.25921.054
42.61482.4972.497	43.25921.054	51.25921.054
43.61482.4972.497	44.25921.054	52.25921.054
44.61482.4972.497	45.2592.9465	53.25921.054
45.63612.3031.248	54.44151.054	
46.63612.3031.248	47.2592.9465	55.44151.054
47.61482.4972.497	48.25921.054	56.25921.054
48.61482.4972.497	49.25921.054	57.25921.054
49.61482.4972.497	50.25921.054	58.25921.054
50.61482.4972.497	51.25921.054	59.25921.054
51.61482.4972.497	52.25921.054	60.25921.054
52.61482.4972.497	53.25921.054	61.25921.054
53.61482.4972.497	54.2592.9465	62.25921.054
54.63612.3031.248	63.44151.054	
55.63612.3031.248	56.2592.9465	64.44151.054
56.61482.4972.497	57.25921.054	65.25921.054
57.61482.4972.497	58.25921.054	66.25921.054
58.61482.4972.497	59.25921.054	67.25921.054
59.61482.4972.497	60.25921.054	68.25921.054
60.61482.4972.497	61.25921.054	69.25921.054
61.61482.4972.497	62.25921.054	70.25921.054
62.61482.4972.497	63.2592.9465	71.25921.054
63.63612.3031.248	72.44151.054	
64.63612.3031.248	65.2592.9465	73.4415.9465
65.61482.4972.497	66.25921.054	74.2592.9465
66.61482.4972.497	67.25921.054	75.2592.9465
67.61482.4972.497	68.25921.054	76.2592.9465
68.61482.4972.497	69.25921.054	77.2592.9465
69.61482.4972.497	70.25921.054	78.2592.9465
70.61482.4972.497	71.25921.054	79.2592.9465
71.61482.4972.497	72.2592.9465	80.2592.9465
72.63612.3031.248	81.4415.9465	
73.57972.302.6242	74.4415.9465	
74.63612.3031.248	75.44151.054	
75.63612.3031.248	76.44151.054	
76.63612.3031.248	77.44151.054	
77.63612.3031.248	78.44151.054	
78.63612.3031.248	79.44151.054	
79.63612.3031.248	80.44151.054	
80.63612.3031.248	81.4415.9465	
81.57972.302.6242		

RODS 1	1	0	0	0					
1 1	64								
1.7948	1.	1	.25	2	.25	10	.25	11	.25
2.7948	1.	2	.25	3	.25	11	.25	12	.25
3.7948	1.	3	.25	4	.25	12	.25	13	.25
4.7948	1.	4	.25	5	.25	13	.25	14	.25
5.7948	1.	5	.25	6	.25	14	.25	15	.25
6.7948	1.	6	.25	7	.25	15	.25	16	.25
7.7948	1.	7	.25	8	.25	16	.25	17	.25
8.7948	1.	8	.25	9	.25	17	.25	18	.25
9.7948	1.	10	.25	11	.25	19	.25	20	.25
10.7948	1.	11	.25	12	.25	20	.25	21	.25
11.7948	1.	12	.25	13	.25	21	.25	22	.25
12.7948	1.	13	.25	14	.25	22	.25	23	.25
13.7948	1.	14	.25	15	.25	23	.25	24	.25
14.7948	1.	15	.25	16	.25	24	.25	25	.25
15.7948	1.	16	.25	17	.25	25	.25	26	.25
16.7948	1.	17	.25	18	.25	26	.25	27	.25
17.7948	1.	19	.25	20	.25	28	.25	29	.25
18.7948	1.	20	.25	21	.25	29	.25	30	.25
19.7948	1.	21	.25	22	.25	30	.25	31	.25
20.7948	1.	22	.25	23	.25	31	.25	32	.25
21.7948	1.	23	.25	24	.25	32	.25	33	.25
22.7948	1.	24	.25	25	.25	33	.25	34	.25
23.7948	1.	25	.25	26	.25	34	.25	35	.25
24.7948	1.	26	.25	27	.25	35	.25	36	.25
25.7948	1.	28	.25	29	.25	37	.25	38	.25
26.7948	1.	29	.25	30	.25	38	.25	39	.25
27.7948	1.	30	.25	31	.25	39	.25	40	.25
28.7948	1.	31	.25	32	.25	40	.25	41	.25
29.7948	1.	32	.25	33	.25	41	.25	42	.25
30.7948	1.	33	.25	34	.25	42	.25	43	.25
31.7948	1.	34	.25	35	.25	43	.25	44	.25
32.7948	1.	35	.25	36	.25	44	.25	45	.25
33.7948	1.	37	.25	38	.25	46	.25	47	.25
34.7948	1.	38	.25	39	.25	47	.25	48	.25
35.7948	1.	39	.25	40	.25	48	.25	49	.25
36.7948	1.	40	.25	41	.25	49	.25	50	.25
37.7948	1.	41	.25	42	.25	50	.25	51	.25
38.7948	1.	42	.25	43	.25	51	.25	52	.25
39.7948	1.	43	.25	44	.25	52	.25	53	.25
40.7948	1.	44	.25	45	.25	53	.25	54	.25
41.7948	1.	46	.25	47	.25	55	.25	56	.25
42.7948	1.	47	.25	48	.25	56	.25	57	.25
43.7948	1.	48	.25	49	.25	57	.25	58	.25
44.7948	1.	49	.25	50	.25	58	.25	59	.25
45.7948	1.	50	.25	51	.25	59	.25	60	.25
46.7948	1.	51	.25	52	.25	60	.25	61	.25
47.7948	1.	52	.25	53	.25	61	.25	62	.25
48.7948	1.	53	.25	54	.25	62	.25	63	.25
49.7948	1.	55	.25	56	.25	64	.25	65	.25
50.7948	1.	56	.25	57	.25	65	.25	66	.25
51.7948	1.	57	.25	58	.25	66	.25	67	.25
52.7948	1.	58	.25	59	.25	67	.25	68	.25
53.7948	1.	59	.25	60	.25	68	.25	69	.25

```
   54.7948     1.    60    .25    61    .25    69    .25    70    .25
   55.7948     1.    61    .25    62    .25    70    .25    71    .25
   56.7948     1.    62    .25    63    .25    71    .25    72    .25
   57.7948     1.    64    .25    65    .25    73    .25    74    .25
   58.7948     1.    65    .25    66    .25    74    .25    75    .25
   59.7948     1.    66    .25    67    .25    75    .25    76    .25
   60.7948     1.    67    .25    68    .25    76    .25    77    .25
   61.7948     1.    68    .25    69    .25    77    .25    78    .25
   62.7948     1.    69    .25    70    .25    78    .25    79    .25
   63.7948     1.    70    .25    71    .25    79    .25    80    .25
   64.7948     1.    71    .25    72    .25    80    .25    81    .25
  3.0.  .059   655.  .6851 10.    0.1    409.  .04761000.  .7948
SLAB     1     3       8
   1                          5000.
   1      11.860               2     2      1      8      1
   2      11.860               1     3      1
   3      11.860               1     4      1
   4      11.860               1     5      1
   5      11.860               1     6      1
   6      11.860               1     7      1
   7      11.860               1     8      1
   8      11.860
   1        99.4       .8389
   2        74.8       1.054
   3       149.6       .5270
   1      5     1     1    1     1    2    2    1    3    2    1    4    2
                1     5    3
   2      5     1     5    3     1    6    2    1    7    2    1    8    2
                1     9    1
   3      5     1     9    1     1   18    2    1   27    2    1   36    2
                1    45    3
   4      5     1    45    3     1   54    2    1   63    2    1   72    2
                1    81    1
   5      5     1    81    1     1   80    2    1   79    2    1   78    2
                1    77    3
   6      5     1    77    3     1   76    2    1   75    2    1   74    2
                1    73    1
   7      5     1    73    1     1   64    2    1   55    2    1    4    2
                1    37    3
   8      5     1    37    3     1   28    2    1   19    2    1   10    2
                1     1    1

RADG      1     1
   1      1     8     1    2     3    4    5    6    7    8
HEAT      1     0     1
            1.00                        1.00
10.8
DRAG      1
100.    -1.0                  100. -1.0  .05
BDRY      1     1     8    0
   1      1.00E+8
   1      2   0.0 204.8  1.0    204.8
   1      14.921      1
   1      1.0   1   1.0      1
   2      14.921      1
```

```
    1         1.0   1     1.0       1
    3         14.921        1
    1         1.0   1     1.0       1
    4         14.921        1
    1         1.0   1     1.0       1
    5         14.921        1
    1         1.0   1     1.0       1
    6         14.921        1
    1         1.0   1     1.0       1
    7         14.921        1
    1         1.0   1     1.0       1
    8         14.921        1
    1         1.0   1     1.0       1
CALC          1
    0.                                                                  0.15
              20
OPER          1   0             3                                                          1
  0.0                        400.     0.0        .0073437      400.
    10
    0.          0.0.0499     0.0   .05     .706    .151.029  .251.206   .751.206
    .851.029.9499          .706   .95      0.0    1.0           0.0
OUTP 1101
ENDD
```

APPENDIX 2

LUMPED 8X8 BUNDLE ANALYSIS—INPUT FILE FOR RADGEN (Cycle 1)

```
    0
Korean Spent Fuel Cask (8X8, lumped)
    01.326    8    8
.7948.4411.4411.4411.4411
  .32  0.3
    0
    0
```

APPENDIX 3

17X17 BUNDLE ANALYSIS—INPUT FILE FOR COBRA-SFS (Cycle 1)

```
 3000
   1          THERMAL ANALYSYS OF KSC-7 CASK (17X17 ARRAY 1 ASS'Y)
PROP     11     1
         1.       100.      133.9      .0154       .240      14.08      .0463
         2.       200.      157.9      .0174       .241      16.67      .0518
         3.       300.      182.1      .0193       .243      19.23      .0580
         4.       400.      206.5      .0212       .245      21.74      .0630
         5.       500.      231.1      .0231       .247      24.27      .0680
         6.       600.      256.0      .0250       .250      26.81      .0720
         7.       700.      281.1      .0268       .253      29.33      .0770
         8.       800.      306.7      .0286       .256      31.85      .0810
        10.       900.      332.5      .0303       .259      34.36      .0850
        15.      1000.      358.6      .0319       .262      36.90      .0889
        20.      2000.      617.2      .0471       .286      62.11      .1242
    1STEEL                             1.E8
CHAN      1    19
     160.0       90.0
   1     1   324     0
   1     1     0     0     1
   1.28511.412.2938     2.3720.5276    19.3720.5276
   2.22241.084.5875     3.3720.4961    20.1220.5276
   3.22241.084.5875     4.3720.4961    21.1220.5276
   4.22241.084.5875     5.3720.4961    22.1220.5276
   5.22241.084.5875     6.3720.4961    23.1220.5276
   6.22241.084.5875     7.3720.4961    24.1220.5276
   7.22241.084.5875     8.3720.4961    25.1220.5276
   8.22241.084.5875     9.3720.4961    26.1220.5276
   9.22241.084.5875    10.3720.4961    27.1220.5276
  10.22241.084.5875    11.3720.4961    28.1220.5276
  11.22241.084.5875    12.3720.4961    29.1220.5276
  12.22241.084.5875    13.3720.4961    30.1220.5276
  13.22241.084.5875    14.3720.4961    31.1220.5276
  14.22241.084.5875    15.3720.4961    32.1220.5276
  15.22241.084.5875    16.3720.4961    33.1220.5276
  16.22241.084.5875    17.3720.4961    34.1220.5276
  17.22241.084.5875    18.3720.5276    35.1220.5276
  18.28511.412.2938    36.3720.5276
  19.22241.084.5875    20.1220.5276    37.3720.4961
  20.13621.1751.175    21.1220.4961    38.1220.4961
  21.13621.1751.175    22.1220.4961    39.1220.4961
  22.13621.1751.175    23.1220.4961    40.1220.4961
  23.13621.1751.175    24.1220.4961    41.1220.4961
  24.13621.1751.175    25.1220.4961    42.1220.4961
  25.13621.1751.175    26.1220.4961    43.1220.4961
  26.13621.1751.175    27.1220.4961    44.1220.4961
  27.13621.1751.175    28.1220.4961    45.1220.4961
  28.13621.1751.175    29.1220.4961    46.1220.4961
  29.13621.1751.175    30.1220.4961    47.1220.4961
  30.13621.1751.175    31.1220.4961    48.1220.4961
  31.13621.1751.175    32.1220.4961    49.1220.4961
  32.13621.1751.175    33.1220.4961    50.1220.4961
  33.13621.1751.175    34.1220.4961    51.1220.4961
```

34.13621.1751.175	35.1220.4961	52.1220.4961
35.13621.1751.175	36.1220.5276	53.1220.4961
36.22241.084.5875	54.3720.4961	
37.22241.084.5875	38.1220.5276	55.3720.4961
38.13621.1751.175	39.1220.4961	56.1220.4961
39.13621.1751.175	40.1220.4961	57.1220.4961
40.13621.1751.175	41.1220.4961	58.1220.4961
41.13621.1751.175	42.1220.4961	59.1220.4961
42.13621.1751.175	43.1220.4961	60.1220.4961
43.13621.1751.175	44.1220.4961	61.1220.4961
44.13621.1751.175	45.1220.4961	62.1220.4961
45.13621.1751.175	46.1220.4961	63.1220.4961
46.13621.1751.175	47.1220.4961	64.1220.4961
47.13621.1751.175	48.1220.4961	65.1220.4961
48.13621.1751.175	49.1220.4961	66.1220.4961
49.13621.1751.175	50.1220.4961	67.1220.4961
50.13621.1751.175	51.1220.4961	68.1220.4961
51.13621.1751.175	52.1220.4961	69.1220.4961
52.13621.1751.175	53.1220.4961	70.1220.4961
53.13621.1751.175	54.1220.5276	71.1220.4961
54.22241.084.5875	72.3720.4961	
55.22241.084.5875	56.1220.5276	73.3720.4961
56.13621.1751.175	57.1220.4961	74.1220.4961
57.13621.1751.175	58.1220.4961	75.1220.4961
58.13621.1751.175	59.1220.4961	76.1220.4961
59.13621.1751.175	60.1220.4961	77.1220.4961
60.13621.1751.175	61.1220.4961	78.1220.4961
61.13621.1751.175	62.1220.4961	79.1220.4961
62.13621.1751.175	63.1220.4961	80.1220.4961
63.13621.1751.175	64.1220.4961	81.1220.4961
64.13621.1751.175	65.1220.4961	82.1220.4961
65.13621.1751.175	66.1220.4961	83.1220.4961
66.13621.1751.175	67.1220.4961	84.1220.4961
67.13621.1751.175	68.1220.4961	85.1220.4961
68.13621.1751.175	69.1220.4961	86.1220.4961
69.13621.1751.175	70.1220.4961	87.1220.4961
70.13621.1751.175	71.1220.4961	88.1220.4961
71.13621.1751.175	72.1220.5276	89.1220.4961
72.22241.084.5875	90.3720.4961	
73.22241.084.5875	74.1220.5276	91.3720.4961
74.13621.1751.175	75.1220.4961	92.1220.4961
75.13621.1751.175	76.1220.4961	93.1220.4961
76.13621.1751.175	77.1220.4961	94.1220.4961
77.13621.1751.175	78.1220.4961	95.1220.4961
78.13621.1751.175	79.1220.4961	96.1220.4961
79.13621.1751.175	80.1220.4961	97.1220.4961
80.13621.1751.175	81.1220.4961	98.1220.4961
81.13621.1751.175	82.1220.4961	99.1220.4961
82.13621.1751.175	83.1220.4961	100.1220.4961
83.13621.1751.175	84.1220.4961	101.1220.4961
84.13621.1751.175	85.1220.4961	102.1220.4961
85.13621.1751.175	86.1220.4961	103.1220.4961

86.13621.1751.175	87.1220.4961	104.1220.4961
87.13621.1751.175	88.1220.4961	105.1220.4961
88.13621.1751.175	89.1220.4961	106.1220.4961
89.13621.1751.175	90.1220.5276	107.1220.4961
90.22241.084.5875	108.3720.4961	
91.22241.084.5875	92.1220.5276	109.3720.4961
92.13621.1751.175	93.1220.4961	110.1220.4961
93.13621.1751.175	94.1220.4961	111.1220.4961
94.13621.1751.175	95.1220.4961	112.1220.4961
95.13621.1751.175	96.1220.4961	113.1220.4961
96.13621.1751.175	97.1220.4961	114.1220.4961
97.13621.1751.175	98.1220.4961	115.1220.4961
98.13621.1751.175	99.1220.4961	116.1220.4961
99.13621.1751.175	100.1220.4961	117.1220.4961
100.13621.1751.175	101.1220.4961	118.1220.4961
101.13621.1751.175	102.1220.4961	119.1220.4961
102.13621.1751.175	103.1220.4961	120.1220.4961
103.13621.1751.175	104.1220.4961	121.1220.4961
104.13621.1751.175	105.1220.4961	122.1220.4961
105.13621.1751.175	106.1220.4961	123.1220.4961
106.13621.1751.175	107.1220.4961	124.1220.4961
107.13621.1751.175	108.1220.5276	125.1220.4961
108.22241.084.5875	126.3720.4961	
109.22241.084.5875	110.1220.5276	127.3720.4961
110.13621.1751.175	111.1220.4961	128.1220.4961
111.13621.1751.175	112.1220.4961	129.1220.4961
112.13621.1751.175	113.1220.4961	130.1220.4961
113.13621.1751.175	114.1220.4961	131.1220.4961
114.13621.1751.175	115.1220.4961	132.1220.4961
115.13621.1751.175	116.1220.4961	133.1220.4961
116.13621.1751.175	117.1220.4961	134.1220.4961
117.13621.1751.175	118.1220.4961	135.1220.4961
118.13621.1751.175	119.1220.4961	136.1220.4961
119.13621.1751.175	120.1220.4961	137.1220.4961
120.13621.1751.175	121.1220.4961	138.1220.4961
121.13621.1751.175	122.1220.4961	139.1220.4961
122.13621.1751.175	123.1220.4961	140.1220.4961
123.13621.1751.175	124.1220.4961	141.1220.4961
124.13621.1751.175	125.1220.4961	142.1220.4961
125.13621.1751.175	126.1220.5276	143.1220.4961
126.22241.084.5875	144.3720.4961	
127.22241.084.5875	128.1220.5276	145.3720.4961
128.13621.1751.175	129.1220.4961	146.1220.4961
129.13621.1751.175	130.1220.4961	147.1220.4961
130.13621.1751.175	131.1220.4961	148.1220.4961
131.13621.1751.175	132.1220.4961	149.1220.4961
132.13621.1751.175	133.1220.4961	150.1220.4961
133.13621.1751.175	134.1220.4961	151.1220.4961
134.13621.1751.175	135.1220.4961	152.1220.4961
135.13621.1751.175	136.1220.4961	153.1220.4961
136.13621.1751.175	137.1220.4961	154.1220.4961
137.13621.1751.175	138.1220.4961	155.1220.4961

138.13621.1751.175	139.1220.4961	156.1220.4961
139.13621.1751.175	140.1220.4961	157.1220.4961
140.13621.1751.175	141.1220.4961	158.1220.4961
141.13621.1751.175	142.1220.4961	159.1220.4961
142.13621.1751.175	143.1220.4961	160.1220.4961
143.13621.1751.175	144.1220.5276	161.1220.4961
144.22241.084.5875	162.3720.4961	
145.22241.084.5875	146.1220.5276	163.3720.4961
146.13621.1751.175	147.1220.4961	164.1220.4961
147.13621.1751.175	148.1220.4961	165.1220.4961
148.13621.1751.175	149.1220.4961	166.1220.4961
149.13621.1751.175	150.1220.4961	167.1220.4961
150.13621.1751.175	151.1220.4961	168.1220.4961
151.13621.1751.175	152.1220.4961	169.1220.4961
152.13621.1751.175	153.1220.4961	170.1220.4961
153.13621.1751.175	154.1220.4961	171.1220.4961
154.13621.1751.175	155.1220.4961	172.1220.4961
155.13621.1751.175	156.1220.4961	173.1220.4961
156.13621.1751.175	157.1220.4961	174.1220.4961
157.13621.1751.175	158.1220.4961	175.1220.4961
158.13621.1751.175	159.1220.4961	176.1220.4961
159.13621.1751.175	160.1220.4961	177.1220.4961
160.13621.1751.175	161.1220.4961	178.1220.4961
161.13621.1751.175	162.1220.5276	179.1220.4961
162.22241.084.5875	180.3720.4961	
163.22241.084.5875	164.1220.5276	181.3720.4961
164.13621.1751.175	165.1220.4961	182.1220.4961
165.13621.1751.175	166.1220.4961	183.1220.4961
166.13621.1751.175	167.1220.4961	184.1220.4961
167.13621.1751.175	168.1220.4961	185.1220.4961
168.13621.1751.175	169.1220.4961	186.1220.4961
169.13621.1751.175	170.1220.4961	187.1220.4961
170.13621.1751.175	171.1220.4961	188.1220.4961
171.13621.1751.175	172.1220.4961	189.1220.4961
172.13621.1751.175	173.1220.4961	190.1220.4961
173.13621.1751.175	174.1220.4961	191.1220.4961
174.13621.1751.175	175.1220.4961	192.1220.4961
175.13621.1751.175	176.1220.4961	193.1220.4961
176.13621.1751.175	177.1220.4961	194.1220.4961
177.13621.1751.175	178.1220.4961	195.1220.4961
178.13621.1751.175	179.1220.4961	196.1220.4961
179.13621.1751.175	180.1220.5276	197.1220.4961
180.22241.084.5875	198.3720.4961	
181.22241.084.5875	182.1220.5276	199.3720.4961
182.13621.1751.175	183.1220.4961	200.1220.4961
183.13621.1751.175	184.1220.4961	201.1220.4961
184.13621.1751.175	185.1220.4961	202.1220.4961
185.13621.1751.175	186.1220.4961	203.1220.4961
186.13621.1751.175	187.1220.4961	204.1220.4961
187.13621.1751.175	188.1220.4961	205.1220.4961
188.13621.1751.175	189.1220.4961	206.1220.4961
189.13621.1751.175	190.1220.4961	207.1220.4961

190.13621.1751.175	191.1220.4961	208.1220.4961
191.13621.1751.175	192.1220.4961	209.1220.4961
192.13621.1751.175	193.1220.4961	210.1220.4961
193.13621.1751.175	194.1220.4961	211.1220.4961
194.13621.1751.175	195.1220.4961	212.1220.4961
195.13621.1751.175	196.1220.4961	213.1220.4961
196.13621.1751.175	197.1220.4961	214.1220.4961
197.13621.1751.175	198.1220.5276	215.1220.4961
198.22241.084.5875	216.3720.4961	
199.22241.084.5875	200.1220.5276	217.3720.4961
200.13621.1751.175	201.1220.4961	218.1220.4961
201.13621.1751.175	202.1220.4961	219.1220.4961
202.13621.1751.175	203.1220.4961	220.1220.4961
203.13621.1751.175	204.1220.4961	221.1220.4961
204.13621.1751.175	205.1220.4961	222.1220.4961
205.13621.1751.175	206.1220.4961	223.1220.4961
206.13621.1751.175	207.1220.4961	224.1220.4961
207.13621.1751.175	208.1220.4961	225.1220.4961
208.13621.1751.175	209.1220.4961	226.1220.4961
209.13621.1751.175	210.1220.4961	227.1220.4961
210.13621.1751.175	211.1220.4961	228.1220.4961
211.13621.1751.175	212.1220.4961	229.1220.4961
212.13621.1751.175	213.1220.4961	230.1220.4961
213.13621.1751.175	214.1220.4961	231.1220.4961
214.13621.1751.175	215.1220.4961	232.1220.4961
215.13621.1751.175	216.1220.5276	233.1220.4961
216.22241.084.5875	234.3720.4961	
217.22241.084.5875	218.1220.5276	235.3720.4961
218.13621.1751.175	219.1220.4961	236.1220.4961
219.13621.1751.175	220.1220.4961	237.1220.4961
220.13621.1751.175	221.1220.4961	238.1220.4961
221.13621.1751.175	222.1220.4961	239.1220.4961
222.13621.1751.175	223.1220.4961	240.1220.4961
223.13621.1751.175	224.1220.4961	241.1220.4961
224.13621.1751.175	225.1220.4961	242.1220.4961
225.13621.1751.175	226.1220.4961	243.1220.4961
226.13621.1751.175	227.1220.4961	244.1220.4961
227.13621.1751.175	228.1220.4961	245.1220.4961
228.13621.1751.175	229.1220.4961	246.1220.4961
229.13621.1751.175	230.1220.4961	247.1220.4961
230.13621.1751.175	231.1220.4961	248.1220.4961
231.13621.1751.175	232.1220.4961	249.1220.4961
232.13621.1751.175	233.1220.4961	250.1220.4961
233.13621.1751.175	234.1220.5276	251.1220.4961
234.22241.084.5875	252.3720.4961	
235.22241.084.5875	236.1220.5276	253.3720.4961
236.13621.1751.175	237.1220.4961	254.1220.4961
237.13621.1751.175	238.1220.4961	255.1220.4961
238.13621.1751.175	239.1220.4961	256.1220.4961
239.13621.1751.175	240.1220.4961	257.1220.4961
240.13621.1751.175	241.1220.4961	258.1220.4961
241.13621.1751.175	242.1220.4961	259.1220.4961

242.13621.1751.175	243.1220.4961	260.1220.4961
243.13621.1751.175	244.1220.4961	261.1220.4961
244.13621.1751.175	245.1220.4961	262.1220.4961
245.13621.1751.175	246.1220.4961	263.1220.4961
246.13621.1751.175	247.1220.4961	264.1220.4961
247.13621.1751.175	248.1220.4961	265.1220.4961
248.13621.1751.175	249.1220.4961	266.1220.4961
249.13621.1751.175	250.1220.4961	267.1220.4961
250.13621.1751.175	251.1220.4961	268.1220.4961
251.13621.1751.175	252.1220.5276	269.1220.4961
252.22241.084.5875	270.3720.4961	
253.22241.084.5875	254.1220.5276	271.3720.4961
254.13621.1751.175	255.1220.4961	272.1220.4961
255.13621.1751.175	256.1220.4961	273.1220.4961
256.13621.1751.175	257.1220.4961	274.1220.4961
257.13621.1751.175	258.1220.4961	275.1220.4961
258.13621.1751.175	259.1220.4961	276.1220.4961
259.13621.1751.175	260.1220.4961	277.1220.4961
260.13621.1751.175	261.1220.4961	278.1220.4961
261.13621.1751.175	262.1220.4961	279.1220.4961
262.13621.1751.175	263.1220.4961	280.1220.4961
263.13621.1751.175	264.1220.4961	281.1220.4961
264.13621.1751.175	265.1220.4961	282.1220.4961
265.13621.1751.175	266.1220.4961	283.1220.4961
266.13621.1751.175	267.1220.4961	284.1220.4961
267.13621.1751.175	268.1220.4961	285.1220.4961
268.13621.1751.175	269.1220.4961	286.1220.4961
269.13621.1751.175	270.1220.5276	287.1220.4961
270.22241.084.5875	288.3720.4961	
271.22241.084.5875	272.1220.5276	289.3720.4961
272.13621.1751.175	273.1220.4961	290.1220.4961
273.13621.1751.175	274.1220.4961	291.1220.4961
274.13621.1751.175	275.1220.4961	292.1220.4961
275.13621.1751.175	276.1220.4961	293.1220.4961
276.13621.1751.175	277.1220.4961	294.1220.4961
277.13621.1751.175	278.1220.4961	295.1220.4961
278.13621.1751.175	279.1220.4961	296.1220.4961
279.13621.1751.175	280.1220.4961	297.1220.4961
280.13621.1751.175	281.1220.4961	298.1220.4961
281.13621.1751.175	282.1220.4961	299.1220.4961
282.13621.1751.175	283.1220.4961	300.1220.4961
283.13621.1751.175	284.1220.4961	301.1220.4961
284.13621.1751.175	285.1220.4961	302.1220.4961
285.13621.1751.175	286.1220.4961	303.1220.4961
286.13621.1751.175	287.1220.4961	304.1220.4961
287.13621.1751.175	288.1220.5276	305.1220.4961
288.22241.084.5875	306.3720.4961	
289.22241.084.5875	290.1220.5276	307.3720.5276
290.13621.1751.175	291.1220.4961	308.1220.5276
291.13621.1751.175	292.1220.4961	309.1220.5276
292.13621.1751.175	293.1220.4961	310.1220.5276
293.13621.1751.175	294.1220.4961	311.1220.5276

```
  294.13621.1751.175  295.1220.4961  312.1220.5276
  295.13621.1751.175  296.1220.4961  313.1220.5276
  296.13621.1751.175  297.1220.4961  314.1220.5276
  297.13621.1751.175  298.1220.4961  315.1220.5276
  298.13621.1751.175  299.1220.4961  316.1220.5276
  299.13621.1751.175  300.1220.4961  317.1220.5276
  300.13621.1751.175  301.1220.4961  318.1220.5276
  301.13621.1751.175  302.1220.4961  319.1220.5276
  302.13621.1751.175  303.1220.4961  320.1220.5276
  303.13621.1751.175  304.1220.4961  321.1220.5276
  304.13621.1751.175  305.1220.4961  322.1220.5276
  305.13621.1751.175  306.1220.5276  323.1220.5276
  306.22241.084.5875  324.3720.5276
  307.28511.412.2938  308.3720.5276
  308.22241.084.5875  309.3720.4961
  309.22241.084.5875  310.3720.4961
  310.22241.084.5875  311.3720.4961
  311.22241.084.5875  312.3720.4961
  312.22241.084.5875  313.3720.4961
  313.22241.084.5875  314.3720.4961
  314.22241.084.5875  315.3720.4961
  315.22241.084.5875  316.3720.4961
  316.22241.084.5875  317.3720.4961
  317.22241.084.5875  318.3720.4961
  318.22241.084.5875  319.3720.4961
  319.22241.084.5875  320.3720.4961
  320.22241.084.5875  321.3720.4961
  321.22241.084.5875  322.3720.4961
  322.22241.084.5875  323.3720.4961
  323.22241.084.5875  324.3720.5276
  324.28511.412.2938

RODS     1    1    0    0    0
   1     1  289
    1.3740    1.    1  .25    2  .25   19  .25   20  .25
    2.3740    1.    2  .25    3  .25   20  .25   21  .25
    3.3740    1.    3  .25    4  .25   21  .25   22  .25
    4.3740    1.    4  .25    5  .25   22  .25   23  .25
    5.3740    1.    5  .25    6  .25   23  .25   24  .25
    6.3740    1.    6  .25    7  .25   24  .25   25  .25
    7.3740    1.    7  .25    8  .25   25  .25   26  .25
    8.3740    1.    8  .25    9  .25   26  .25   27  .25
    9.3740    1.    9  .25   10  .25   27  .25   28  .25
   10.3740    1.   10  .25   11  .25   28  .25   29  .25
   11.3740    1.   11  .25   12  .25   29  .25   30  .25
   12.3740    1.   12  .25   13  .25   30  .25   31  .25
   13.3740    1.   13  .25   14  .25   31  .25   32  .25
   14.3740    1.   14  .25   15  .25   32  .25   33  .25
   15.3740    1.   15  .25   16  .25   33  .25   34  .25
   16.3740    1.   16  .25   17  .25   34  .25   35  .25
   17.3740    1.   17  .25   18  .25   35  .25   36  .25
   18.3740    1.   19  .25   20  .25   37  .25   38  .25
```

19.3740	1.	20	.25	21	.25	38	.25	39	.25
20.3740	1.	21	.25	22	.25	39	.25	40	.25
21.3740	1.	22	.25	23	.25	40	.25	41	.25
22.3740	1.	23	.25	24	.25	41	.25	42	.25
23.3740	1.	24	.25	25	.25	42	.25	43	.25
24.3740	1.	25	.25	26	.25	43	.25	44	.25
25.3740	1.	26	.25	27	.25	44	.25	45	.25
26.3740	1.	27	.25	28	.25	45	.25	46	.25
27.3740	1.	28	.25	29	.25	46	.25	47	.25
28.3740	1.	29	.25	30	.25	47	.25	48	.25
29.3740	1.	30	.25	31	.25	48	.25	49	.25
30.3740	1.	31	.25	32	.25	49	.25	50	.25
31.3740	1.	32	.25	33	.25	50	.25	51	.25
32.3740	1.	33	.25	34	.25	51	.25	52	.25
33.3740	1.	34	.25	35	.25	52	.25	53	.25
34.3740	1.	35	.25	36	.25	53	.25	54	.25
35.3740	1.	37	.25	38	.25	55	.25	56	.25
36.3740	1.	38	.25	39	.25	56	.25	57	.25
37.3740	1.	39	.25	40	.25	57	.25	58	.25
38.3740	1.	40	.25	41	.25	58	.25	59	.25
39.3740	1.	41	.25	42	.25	59	.25	60	.25
40.3740	1.	42	.25	43	.25	60	.25	61	.25
41.3740	1.	43	.25	44	.25	61	.25	62	.25
42.3740	1.	44	.25	45	.25	62	.25	63	.25
43.3740	1.	45	.25	46	.25	63	.25	64	.25
44.3740	1.	46	.25	47	.25	64	.25	65	.25
45.3740	1.	47	.25	48	.25	65	.25	66	.25
46.3740	1.	48	.25	49	.25	66	.25	67	.25
47.3740	1.	49	.25	50	.25	67	.25	68	.25
48.3740	1.	50	.25	51	.25	68	.25	69	.25
49.3740	1.	51	.25	52	.25	69	.25	70	.25
50.3740	1.	52	.25	53	.25	70	.25	71	.25
51.3740	1.	53	.25	54	.25	71	.25	72	.25
52.3740	1.	55	.25	56	.25	73	.25	74	.25
53.3740	1.	56	.25	57	.25	74	.25	75	.25
54.3740	1.	57	.25	58	.25	75	.25	76	.25
55.3740	1.	58	.25	59	.25	76	.25	77	.25
56.3740	1.	59	.25	60	.25	77	.25	78	.25
57.3740	1.	60	.25	61	.25	78	.25	79	.25
58.3740	1.	61	.25	62	.25	79	.25	80	.25
59.3740	1.	62	.25	63	.25	80	.25	81	.25
60.3740	1.	63	.25	64	.25	81	.25	82	.25
61.3740	1.	64	.25	65	.25	82	.25	83	.25
62.3740	1.	65	.25	66	.25	83	.25	84	.25
63.3740	1.	66	.25	67	.25	84	.25	85	.25
64.3740	1.	67	.25	68	.25	85	.25	86	.25
65.3740	1.	68	.25	69	.25	86	.25	87	.25
66.3740	1.	69	.25	70	.25	87	.25	88	.25
67.3740	1.	70	.25	71	.25	88	.25	89	.25
68.3740	1.	71	.25	72	.25	89	.25	90	.25
69.3740	1.	73	.25	74	.25	91	.25	92	.25
70.3740	1.	74	.25	75	.25	92	.25	93	.25

71.3740	1.	75	.25	76	.25	93	.25	94	.25
72.3740	1.	76	.25	77	.25	94	.25	95	.25
73.3740	1.	77	.25	78	.25	95	.25	96	.25
74.3740	1.	78	.25	79	.25	96	.25	97	.25
75.3740	1.	79	.25	80	.25	97	.25	98	.25
76.3740	1.	80	.25	81	.25	98	.25	99	.25
77.3740	1.	81	.25	82	.25	99	.25	100	.25
78.3740	1.	82	.25	83	.25	100	.25	101	.25
79.3740	1.	83	.25	84	.25	101	.25	102	.25
80.3740	1.	84	.25	85	.25	102	.25	103	.25
81.3740	1.	85	.25	86	.25	103	.25	104	.25
82.3740	1.	86	.25	87	.25	104	.25	105	.25
83.3740	1.	87	.25	88	.25	105	.25	106	.25
84.3740	1.	88	.25	89	.25	106	.25	107	.25
85.3740	1.	89	.25	90	.25	107	.25	108	.25
86.3740	1.	91	.25	92	.25	109	.25	110	.25
87.3740	1.	92	.25	93	.25	110	.25	111	.25
88.3740	1.	93	.25	94	.25	111	.25	112	.25
89.3740	1.	94	.25	95	.25	112	.25	113	.25
90.3740	1.	95	.25	96	.25	113	.25	114	.25
91.3740	1.	96	.25	97	.25	114	.25	115	.25
92.3740	1.	97	.25	98	.25	115	.25	116	.25
93.3740	1.	98	.25	99	.25	116	.25	117	.25
94.3740	1.	99	.25	100	.25	117	.25	118	.25
95.3740	1.	100	.25	101	.25	118	.25	119	.25
96.3740	1.	101	.25	102	.25	119	.25	120	.25
97.3740	1.	102	.25	103	.25	120	.25	121	.25
98.3740	1.	103	.25	104	.25	121	.25	122	.25
99.3740	1.	104	.25	105	.25	122	.25	123	.25
100.3740	1.	105	.25	106	.25	123	.25	124	.25
101.3740	1.	106	.25	107	.25	124	.25	125	.25
102.3740	1.	107	.25	108	.25	125	.25	126	.25
103.3740	1.	109	.25	110	.25	127	.25	128	.25
104.3740	1.	110	.25	111	.25	128	.25	129	.25
105.3740	1.	111	.25	112	.25	129	.25	130	.25
106.3740	1.	112	.25	113	.25	130	.25	131	.25
107.3740	1.	113	.25	114	.25	131	.25	132	.25
108.3740	1.	114	.25	115	.25	132	.25	133	.25
109.3740	1.	115	.25	116	.25	133	.25	134	.25
110.3740	1.	116	.25	117	.25	134	.25	135	.25
111.3740	1.	117	.25	118	.25	135	.25	136	.25
112.3740	1.	118	.25	119	.25	136	.25	137	.25
113.3740	1.	119	.25	120	.25	137	.25	138	.25
114.3740	1.	120	.25	121	.25	138	.25	139	.25
115.3740	1.	121	.25	122	.25	139	.25	140	.25
116.3740	1.	122	.25	123	.25	140	.25	141	.25
117.3740	1.	123	.25	124	.25	141	.25	142	.25
118.3740	1.	124	.25	125	.25	142	.25	143	.25
119.3740	1.	125	.25	126	.25	143	.25	144	.25
120.3740	1.	127	.25	128	.25	145	.25	146	.25
121.3740	1.	128	.25	129	.25	146	.25	147	.25
122.3740	1.	129	.25	130	.25	147	.25	148	.25

123.3740	1.	130	.25	131	.25	148	.25	149	.25
124.3740	1.	131	.25	132	.25	149	.25	150	.25
125.3740	1.	132	.25	133	.25	150	.25	151	.25
126.3740	1.	133	.25	134	.25	151	.25	152	.25
127.3740	1.	134	.25	135	.25	152	.25	153	.25
128.3740	1.	135	.25	136	.25	153	.25	154	.25
129.3740	1.	136	.25	137	.25	154	.25	155	.25
130.3740	1.	137	.25	138	.25	155	.25	156	.25
131.3740	1.	138	.25	139	.25	156	.25	157	.25
132.3740	1.	139	.25	140	.25	157	.25	158	.25
133.3740	1.	140	.25	141	.25	158	.25	159	.25
134.3740	1.	141	.25	142	.25	159	.25	160	.25
135.3740	1.	142	.25	143	.25	160	.25	161	.25
136.3740	1.	143	.25	144	.25	161	.25	162	.25
137.3740	1.	145	.25	146	.25	163	.25	164	.25
138.3740	1.	146	.25	147	.25	164	.25	165	.25
139.3740	1.	147	.25	148	.25	165	.25	166	.25
140.3740	1.	148	.25	149	.25	166	.25	167	.25
141.3740	1.	149	.25	150	.25	167	.25	168	.25
142.3740	1.	150	.25	151	.25	168	.25	169	.25
143.3740	1.	151	.25	152	.25	169	.25	170	.25
144.3740	1.	152	.25	153	.25	170	.25	171	.25
145.3740	1.	153	.25	154	.25	171	.25	172	.25
146.3740	1.	154	.25	155	.25	172	.25	173	.25
147.3740	1.	155	.25	156	.25	173	.25	174	.25
148.3740	1.	156	.25	157	.25	174	.25	175	.25
149.3740	1.	157	.25	158	.25	175	.25	176	.25
150.3740	1.	158	.25	159	.25	176	.25	177	.25
151.3740	1.	159	.25	160	.25	177	.25	178	.25
152.3740	1.	160	.25	161	.25	178	.25	179	.25
153.3740	1.	161	.25	162	.25	179	.25	180	.25
154.3740	1.	163	.25	164	.25	181	.25	182	.25
155.3740	1.	164	.25	165	.25	182	.25	183	.25
156.3740	1.	165	.25	166	.25	183	.25	184	.25
157.3740	1.	166	.25	167	.25	184	.25	185	.25
158.3740	1.	167	.25	168	.25	185	.25	186	.25
159.3740	1.	168	.25	169	.25	186	.25	187	.25
160.3740	1.	169	.25	170	.25	187	.25	188	.25
161.3740	1.	170	.25	171	.25	188	.25	189	.25
162.3740	1.	171	.25	172	.25	189	.25	190	.25
163.3740	1.	172	.25	173	.25	190	.25	191	.25
164.3740	1.	173	.25	174	.25	191	.25	192	.25
165.3740	1.	174	.25	175	.25	192	.25	193	.25
166.3740	1.	175	.25	176	.25	193	.25	194	.25
167.3740	1.	176	.25	177	.25	194	.25	195	.25
168.3740	1.	177	.25	178	.25	195	.25	196	.25
169.3740	1.	178	.25	179	.25	196	.25	197	.25
170.3740	1.	179	.25	180	.25	197	.25	198	.25
171.3740	1.	181	.25	182	.25	199	.25	200	.25
172.3740	1.	182	.25	183	.25	200	.25	201	.25
173.3740	1.	183	.25	184	.25	201	.25	202	.25
174.3740	1.	184	.25	185	.25	202	.25	203	.25

175.3740	1.	185	.25	186	.25	203	.25	204	.25
176.3740	1.	186	.25	187	.25	204	.25	205	.25
177.3740	1.	187	.25	188	.25	205	.25	206	.25
178.3740	1.	188	.25	189	.25	206	.25	207	.25
179.3740	1.	189	.25	190	.25	207	.25	208	.25
180.3740	1.	190	.25	191	.25	208	.25	209	.25
181.3740	1.	191	.25	192	.25	209	.25	210	.25
182.3740	1.	192	.25	193	.25	210	.25	211	.25
183.3740	1.	193	.25	194	.25	211	.25	212	.25
184.3740	1.	194	.25	195	.25	212	.25	213	.25
185.3740	1.	195	.25	196	.25	213	.25	214	.25
186.3740	1.	196	.25	197	.25	214	.25	215	.25
187.3740	1.	197	.25	198	.25	215	.25	216	.25
188.3740	1.	199	.25	200	.25	217	.25	218	.25
189.3740	1.	200	.25	201	.25	218	.25	219	.25
190.3740	1.	201	.25	202	.25	219	.25	220	.25
191.3740	1.	202	.25	203	.25	220	.25	221	.25
192.3740	1.	203	.25	204	.25	221	.25	222	.25
193.3740	1.	204	.25	205	.25	222	.25	223	.25
194.3740	1.	205	.25	206	.25	223	.25	224	.25
195.3740	1.	206	.25	207	.25	224	.25	225	.25
196.3740	1.	207	.25	208	.25	225	.25	226	.25
197.3740	1.	208	.25	209	.25	226	.25	227	.25
198.3740	1.	209	.25	210	.25	227	.25	228	.25
199.3740	1.	210	.25	211	.25	228	.25	229	.25
200.3740	1.	211	.25	212	.25	229	.25	230	.25
201.3740	1.	212	.25	213	.25	230	.25	231	.25
202.3740	1.	213	.25	214	.25	231	.25	232	.25
203.3740	1.	214	.25	215	.25	232	.25	233	.25
204.3740	1.	215	.25	216	.25	233	.25	234	.25
205.3740	1.	217	.25	218	.25	235	.25	236	.25
206.3740	1.	218	.25	219	.25	236	.25	237	.25
207.3740	1.	219	.25	220	.25	237	.25	238	.25
208.3740	1.	220	.25	221	.25	238	.25	239	.25
209.3740	1.	221	.25	222	.25	239	.25	240	.25
210.3740	1.	222	.25	223	.25	240	.25	241	.25
211.3740	1.	223	.25	224	.25	241	.25	242	.25
212.3740	1.	224	.25	225	.25	242	.25	243	.25
213.3740	1.	225	.25	226	.25	243	.25	244	.25
214.3740	1.	226	.25	227	.25	244	.25	245	.25
215.3740	1.	227	.25	228	.25	245	.25	246	.25
216.3740	1.	228	.25	229	.25	246	.25	247	.25
217.3740	1.	229	.25	230	.25	247	.25	248	.25
218.3740	1.	230	.25	231	.25	248	.25	249	.25
219.3740	1.	231	.25	232	.25	249	.25	250	.25
220.3740	1.	232	.25	233	.25	250	.25	251	.25
221.3740	1.	233	.25	234	.25	251	.25	252	.25
222.3740	1.	235	.25	236	.25	253	.25	254	.25
223.3740	1.	236	.25	237	.25	254	.25	255	.25
224.3740	1.	237	.25	238	.25	255	.25	256	.25
225.3740	1.	238	.25	239	.25	256	.25	257	.25
226.3740	1.	239	.25	240	.25	257	.25	258	.25

227.3740	1.	240	.25	241	.25	258	.25	259	.25
228.3740	1.	241	.25	242	.25	259	.25	260	.25
229.3740	1.	242	.25	243	.25	260	.25	261	.25
230.3740	1.	243	.25	244	.25	261	.25	262	.25
231.3740	1.	244	.25	245	.25	262	.25	263	.25
232.3740	1.	245	.25	246	.25	263	.25	264	.25
233.3740	1.	246	.25	247	.25	264	.25	265	.25
234.3740	1.	247	.25	248	.25	265	.25	266	.25
235.3740	1.	248	.25	249	.25	266	.25	267	.25
236.3740	1.	249	.25	250	.25	267	.25	268	.25
237.3740	1.	250	.25	251	.25	268	.25	269	.25
238.3740	1.	251	.25	252	.25	269	.25	270	.25
239.3740	1.	253	.25	254	.25	271	.25	272	.25
240.3740	1.	254	.25	255	.25	272	.25	273	.25
241.3740	1.	255	.25	256	.25	273	.25	274	.25
242.3740	1.	256	.25	257	.25	274	.25	275	.25
243.3740	1.	257	.25	258	.25	275	.25	276	.25
244.3740	1.	258	.25	259	.25	276	.25	277	.25
245.3740	1.	259	.25	260	.25	277	.25	278	.25
246.3740	1.	260	.25	261	.25	278	.25	279	.25
247.3740	1.	261	.25	262	.25	279	.25	280	.25
248.3740	1.	262	.25	263	.25	280	.25	281	.25
249.3740	1.	263	.25	264	.25	281	.25	282	.25
250.3740	1.	264	.25	265	.25	282	.25	283	.25
251.3740	1.	265	.25	266	.25	283	.25	284	.25
252.3740	1.	266	.25	267	.25	284	.25	285	.25
253.3740	1.	267	.25	268	.25	285	.25	286	.25
254.3740	1.	268	.25	269	.25	286	.25	287	.25
255.3740	1.	269	.25	270	.25	287	.25	288	.25
256.3740	1.	271	.25	272	.25	289	.25	290	.25
257.3740	1.	272	.25	273	.25	290	.25	291	.25
258.3740	1.	273	.25	274	.25	291	.25	292	.25
259.3740	1.	274	.25	275	.25	292	.25	293	.25
260.3740	1.	275	.25	276	.25	293	.25	294	.25
261.3740	1.	276	.25	277	.25	294	.25	295	.25
262.3740	1.	277	.25	278	.25	295	.25	296	.25
263.3740	1.	278	.25	279	.25	296	.25	297	.25
264.3740	1.	279	.25	280	.25	297	.25	298	.25
265.3740	1.	280	.25	281	.25	298	.25	299	.25
266.3740	1.	281	.25	282	.25	299	.25	300	.25
267.3740	1.	282	.25	283	.25	300	.25	301	.25
268.3740	1.	283	.25	284	.25	301	.25	302	.25
269.3740	1.	284	.25	285	.25	302	.25	303	.25
270.3740	1.	285	.25	286	.25	303	.25	304	.25
271.3740	1.	286	.25	287	.25	304	.25	305	.25
272.3740	1.	287	.25	288	.25	305	.25	306	.25
273.3740	1.	289	.25	290	.25	307	.25	308	.25
274.3740	1.	290	.25	291	.25	308	.25	309	.25
275.3740	1.	291	.25	292	.25	309	.25	310	.25
276.3740	1.	292	.25	293	.25	310	.25	311	.25
277.3740	1.	293	.25	294	.25	311	.25	312	.25
278.3740	1.	294	.25	295	.25	312	.25	313	.25

```
  279.3740   1.  295  .25  296  .25  313  .25  314  .25
  280.3740   1.  296  .25  297  .25  314  .25  315  .25
  281.3740   1.  297  .25  298  .25  315  .25  316  .25
  282.3740   1.  298  .25  299  .25  316  .25  317  .25
  283.3740   1.  299  .25  300  .25  317  .25  318  .25
  284.3740   1.  300  .25  301  .25  318  .25  319  .25
  285.3740   1.  301  .25  302  .25  319  .25  320  .25
  286.3740   1.  302  .25  303  .25  320  .25  321  .25
  287.3740   1.  303  .25  304  .25  321  .25  322  .25
  288.3740   1.  304  .25  305  .25  322  .25  323  .25
  289.3740   1.  305  .25  306  .25  323  .25  324  .25
 3.0 .059 655. .3224  10.  0.1 409..02241000. .374
SLAB     1    2    8
    1                        5000.
    1    11.860               2    2    1    8    1
    2    11.860               1    3    1
    3    11.860               1    4    1
    4    11.860               1    5    1
    5    11.860               1    6    1
    6    11.860               1    7    1
    7    11.860               1    8    1
    8    11.860
    1      141.      .5591
    2      158.      .4961
    1    9    1    1    1    1    2    2    1    3    2    1    4    2
              1    5    2    1    6    2    1    7    2    1    8    2
              1    9    2
    2    9    1   10    2    1   11    2    1   12    2    1   13    2
              1   14    2    1   15    2    1   16    2    1   17    2
              1   18    1
    3    9    1   18    1    1   36    2    1   54    2    1   72    2
              1   90    2    1  108    2    1  126    2    1  144    2
              1  162    2
    4    9    1  180    2    1  198    2    1  216    2    1  234    2
              1  252    2    1  270    2    1  288    2    1  306    2
              1  324    1
    5    9    1  316    2    1  317    2    1  318    2    1  319    2
              1  320    2    1  321    2    1  322    2    1  323    2
              1  324    1
    6    9    1  307    1    1  308    2    1  309    2    1  310    2
              1  311    2    1  312    2    1  313    2    1  314    2
              1  315    2
    7    9    1  163    2    1  181    2    1  199    2    1  217    2
              1  235    2    1  253    2    1  271    2    1  289    2
              1  307    1
    8    9    1    1    1    1   19    2    1   37    2    1   55    2
              1   73    2    1   91    2    1  109    2    1  127    2
              1  145    2

RADG     1    1
    1    1    8    1    2    3    4    5    6    7    8
HEAT     1    0    1
```

```
                1.00                    1.00
 17.1
DRAG      1
 100. -1.0                   100. -1.0  .05
BDRY      1    1    8    0
    1  1.00E+8
    1    2 0.0 204.8 1.0 204.8
    1    14.921    1
    1  1.0    1  1.0    1
    2    14.921    1
    1  1.0    1  1.0    1
    3    14.921    1
    1  1.0    1  1.0    1
    4    14.921    1
    1  1.0    1  1.0    1
    5    14.921    1
    1  1.0    1  1.0    1
    6    14.921    1
    1  1.0    1  1.0    1
    7    14.921    1
    1  1.0    1  1.0    1
    8    14.921    1
    1  1.0    1  1.0    1
CALC      1
   0.                                          0.25
       10
OPER      1    0    3                                            1
 0.0            400.    .0     .0073437     400.
   10
   0.  0.0.0499  0.0  .05 .706  .151.029  .251.206  .751:206
  .851.029.9499 .706  .95  0.0  1.0  0.0
OUTP 1101
ENDD
```

APPENDIX 4

17X17 BUNDLE ANALYSIS—INPUT FILE FOR RADGEN (Cycle 1)

```
    0
Korean Spent Fuel Cask -- KSC-7 (17*17)
    01.326   17   17
 .374 .372 .372 .372 .372
   0.8  0.3
    0
    0
```

APPENDIX 5

QUARTER SECTION MODEL OF KAERI
(Received via E-mail on 10/07/94)

```
+2000
   1           KSC-7 CASK (1/4 SECTION MODEL, 8X8 FUEL, NITROG, '94.9)
PROP     11     3
         0.       100.      133.9      .0154       .240      14.08      .0463
         0.       200.      157.9      .0174       .241      16.67      .0518
         0.       300.      182.1      .0193       .243      19.23      .0580
         0.       400.      206.5      .0212       .245      21.74      .0630
         0.       500.      231.1      .0231       .247      24.27      .0680
         0.       600.      256.0      .0250       .250      26.81      .0720
         0.       700.      281.1      .0268       .253      29.33      .0770
         0.       800.      306.7      .0286       .256      31.85      .0810
         0.       900.      332.5      .0303       .259      34.36      .0850
         0.      1000.      358.6      .0319       .262      36.90      .0889
         0.      2000.      617.2      .0471       .286      62.11      .1242
    1STEEL                             8.99
    2LEAD                             19.16
    3SILIC                             3.500
CHAN      6    24
     160.0         0.0
    1    1    25    0
    1    1     0    0     1
    1.29581.166.6323     2.39051.067     6.1310.9645
    2.59162.3321.265     3.39051.067     7.2619.9645
    3.59162.3321.265     4.39051.067     8.2619.9645
    4.59162.3321.265     5.3905.9645     9.2619.9645
    5.50162.218.6323    10.3905.9645
    6.31471.2651.265     7.26191.067    11.13101.067
    7.62942.5292.529     8.26191.067    12.26191.067
    8.62942.5292.529     9.26191.067    13.26191.067
    9.62942.5292.529    10.2619.9645    14.26191.067
   10.59162.3321.265    15.39051.067
   11.31471.2651.265    12.26191.067    16.13101.067
   12.62942.5292.529    13.26191.067    17.26191.067
   13.62942.5292.529    14.26191.067    18.26191.067
   14.62942.5292.529    15.2619.9645    19.26191.067
   15.59162.3321.265    20.39051.067
   16.31471.2651.265    17.26191.067    21.13101.067
   17.62942.5292.529    18.26191.067    22.26191.067
   18.62942.5292.529    19.26191.067    23.26191.067
   19.62942.5292.529    20.2619.9645    24.26191.067
   20.59162.3321.265    25.39051.067
   21.1574.6323.6323    22.13101.067
   22.31471.2651.265    23.13101.067
   23.31471.2651.265    24.13101.067
   24.31471.2651.265    25.1310.9645
   25.29581.166.6323
    2    2    45    0
    1    1     0    0     1
    1.50162.218.6323     2.3905.9645    10.3905.9645
    2.59162.3321.265     3.39051.067    11.2619.9645
    3.59162.3321.265     4.39051.067    12.2619.9645
    4.59162.3321.265     5.39051.067    13.2619.9645
```

```
 5.59162.3321.265    6.39051.067    14.2619.9645
 6.59162.3321.265    7.39051.067    15.2619.9645
 7.59162.3321.265    8.39051.067    16.2619.9645
 8.59162.3321.265    9.3905.9645    17.2619.9645
 9.50162.218.6323   18.3905.9645
10.59162.3321.265   11.2619.9645    19.39051.067
11.62942.5292.529   12.26191.067    20.26191.067
12.62942.5292.529   13.26191.067    21.26191.067
13.62942.5292.529   14.26191.067    22.26191.067
14.62942.5292.529   15.26191.067    23.26191.067
15.62942.5292.529   16.26191.067    24.26191.067
16.62942.5292.529   17.26191.067    25.26191.067
17.62942.5292.529   18.2619.9645    26.26191.067
18.59162.3321.265   27.39051.067
19.59162.3321.265   20.2619.9645    28.39051.067
20.62942.5292.529   21.26191.067    29.26191.067
21.62942.5292.529   22.26191.067    30.26191.067
22.62942.5292.529   23.26191.067    31.26191.067
23.62942.5292.529   24.26191.067    32.26191.067
24.62942.5292.529   25.26191.067    33.26191.067
25.62942.5292.529   26.26191.067    34.26191.067
26.62942.5292.529   27.2619.9645    35.26191.067
27.59162.3321.265   36.39051.067
28.59162.3321.265   29.2619.9645    37.39051.067
29.62942.5292.529   30.26191.067    38.26191.067
30.62942.5292.529   31.26191.067    39.26191.067
31.62942.5292.529   32.26191.067    40.26191.067
32.62942.5292.529   33.26191.067    41.26191.067
33.62942.5292.529   34.26191.067    42.26191.067
34.62942.5292.529   35.26191.067    43.26191.067
35.62942.5292.529   36.2619.9645    44.26191.067
36.59162.3321.265   45.39051.067
37.29581.166.6323   38.1310.9645
38.31471.2651.265   39.13101.067
39.31471.2651.265   40.13101.067
40.31471.2651.265   41.13101.067
41.31471.2651.265   42.13101.067
42.31471.2651.265   43.13101.067
43.31471.2651.265   44.13101.067
44.31471.2651.265   45.1310.9645
45.29581.166.6323
 3    3   81    0
 1    1    0    0    1
 1.50162.218.6323    2.3905.9645    10.3905.9645
 2.59162.3321.265    3.39051.067    11.2619.9645
 3.59162.3321.265    4.39051.067    12.2619.9645
 4.59162.3321.265    5.39051.067    13.2619.9645
 5.59162.3321.265    6.39051.067    14.2619.9645
 6.59162.3321.265    7.39051.067    15.2619.9645
 7.59162.3321.265    8.39051.067    16.2619.9645
 8.59162.3321.265    9.3905.9645    17.2619.9645
 9.50162.218.6323   18.3905.9645
```

10.59162.3321.265	11.2619.9645	19.39051.067
11.62942.5292.529	12.26191.067	20.26191.067
12.62942.5292.529	13.26191.067	21.26191.067
13.62942.5292.529	14.26191.067	22.26191.067
14.62942.5292.529	15.26191.067	23.26191.067
15.62942.5292.529	16.26191.067	24.26191.067
16.62942.5292.529	17.26191.067	25.26191.067
17.62942.5292.529	18.2619.9645	26.26191.067
18.59162.3321.265	27.39051.067	
19.59162.3321.265	20.2619.9645	28.39051.067
20.62942.5292.529	21.26191.067	29.26191.067
21.62942.5292.529	22.26191.067	30.26191.067
22.62942.5292.529	23.26191.067	31.26191.067
23.62942.5292.529	24.26191.067	32.26191.067
24.62942.5292.529	25.26191.067	33.26191.067
25.62942.5292.529	26.26191.067	34.26191.067
26.62942.5292.529	27.2619.9645	35.26191.067
27.59162.3321.265	36.39051.067	
28.59162.3321.265	29.2619.9645	37.39051.067
29.62942.5292.529	30.26191.067	38.26191.067
30.62942.5292.529	31.26191.067	39.26191.067
31.62942.5292.529	32.26191.067	40.26191.067
32.62942.5292.529	33.26191.067	41.26191.067
33.62942.5292.529	34.26191.067	42.26191.067
34.62942.5292.529	35.26191.067	43.26191.067
35.62942.5292.529	36.2619.9645	44.26191.067
36.59162.3321.265	45.39051.067	
37.59162.3321.265	38.2619.9645	46.39051.067
38.62942.5292.529	39.26191.067	47.26191.067
39.62942.5292.529	40.26191.067	48.26191.067
40.62942.5292.529	41.26191.067	49.26191.067
41.62942.5292.529	42.26191.067	50.26191.067
42.62942.5292.529	43.26191.067	51.26191.067
43.62942.5292.529	44.26191.067	52.26191.067
44.62942.5292.529	45.2619.9645	53.26191.067
45.59162.3321.265	54.39051.067	
46.59162.3321.265	47.2619.9645	55.39051.067
47.62942.5292.529	48.26191.067	56.26191.067
48.62942.5292.529	49.26191.067	57.26191.067
49.62942.5292.529	50.26191.067	58.26191.067
50.62942.5292.529	51.26191.067	59.26191.067
51.62942.5292.529	52.26191.067	60.26191.067
52.62942.5292.529	53.26191.067	61.26191.067
53.62942.5292.529	54.2619.9645	62.26191.067
54.59162.3321.265	63.39051.067	
55.59162.3321.265	56.2619.9645	64.39051.067
56.62942.5292.529	57.26191.067	65.26191.067
57.62942.5292.529	58.26191.067	66.26191.067
58.62942.5292.529	59.26191.067	67.26191.067
59.62942.5292.529	60.26191.067	68.26191.067
60.62942.5292.529	61.26191.067	69.26191.067
61.62942.5292.529	62.26191.067	70.26191.067

```
62.62942.5292.529   63.2619.9645   71.26191.067
63.59162.3321.265   72.39051.067
64.59162.3321.265   65.2619.9645   73.3905.9645
65.62942.5292.529   66.26191.067   74.2619.9645
66.62942.5292.529   67.26191.067   75.2619.9645
67.62942.5292.529   68.26191.067   76.2619.9645
68.62942.5292.529   69.26191.067   77.2619.9645
69.62942.5292.529   70.26191.067   78.2619.9645
70.62942.5292.529   71.26191.067   79.2619.9645
71.62942.5292.529   72.2619.9645   80.2619.9645
72.59162.3321.265   81.3905.9645
73.50162.218.6323   74.3905.9645
74.59162.3321.265   75.39051.067
75.59162.3321.265   76.39051.067
76.59162.3321.265   77.39051.067
77.59162.3321.265   78.39051.067
78.59162.3321.265   79.39051.067
79.59162.3321.265   80.39051.067
80.59162.3321.265   81.3905.9645
81.50162.218.6323
  4    4    1    0
  1    1    0    0    2
  1 19.0 24.8
  5    5    1    0
  1    1    0    0    2
  1 41.0 31.3
  6    6    1    0
  1    1    0    0    2
  1 16.5 16.6

RODS    1    1    1    0    0
  1    1   16
  1.8051   1.    1  .25    2  .25    6  .25    7  .25
  2.8051   1.    2  .25    3  .25    7  .25    8  .25
  3.8051   1.    3  .25    4  .25    8  .25    9  .25
  4.8051   1.    4  .25    5  .25    9  .25   10  .25
  5.8051   1.    6  .25    7  .25   11  .25   12  .25
  6.8051   1.    7  .25    8  .25   12  .25   13  .25
  7.8051   1.    8  .25    9  .25   13  .25   14  .25
  8.8051   1.    9  .25   10  .25   14  .25   15  .25
  9.8051   1.   11  .25   12  .25   16  .25   17  .25
 10.8051   1.   12  .25   13  .25   17  .25   18  .25
 11.8051   1.   13  .25   14  .25   18  .25   19  .25
 12.8051   1.   14  .25   15  .25   19  .25   20  .25
 13.8051   1.   16  .25   17  .25   21  .25   22  .25
 14.8051   1.   17  .25   18  .25   22  .25   23  .25
 15.8051   1.   18  .25   19  .25   23  .25   24  .25
 16.8051   1.   19  .25   20  .25   24  .25   25  .25
  2    2   32
  1.8051   1.    1  .25    2  .25   10  .25   11  .25
  2.8051   1.    2  .25    3  .25   11  .25   12  .25
  3.8051   1.    3  .25    4  .25   12  .25   13  .25
```

4.8051	1.	4	.25	5	.25	13	.25	14	.25
5.8051	1.	5	.25	6	.25	14	.25	15	.25
6.8051	1.	6	.25	7	.25	15	.25	16	.25
7.8051	1.	7	.25	8	.25	16	.25	17	.25
8.8051	1.	8	.25	9	.25	17	.25	18	.25
9.8051	1.	10	.25	11	.25	19	.25	20	.25
10.8051	1.	11	.25	12	.25	20	.25	21	.25
11.8051	1.	12	.25	13	.25	21	.25	22	.25
12.8051	1.	13	.25	14	.25	22	.25	23	.25
13.8051	1.	14	.25	15	.25	23	.25	24	.25
14.8051	1.	15	.25	16	.25	24	.25	25	.25
15.8051	1.	16	.25	17	.25	25	.25	26	.25
16.8051	1.	17	.25	18	.25	26	.25	27	.25
17.8051	1.	19	.25	20	.25	28	.25	29	.25
18.8051	1.	20	.25	21	.25	29	.25	30	.25
19.8051	1.	21	.25	22	.25	30	.25	31	.25
20.8051	1.	22	.25	23	.25	31	.25	32	.25
21.8051	1.	23	.25	24	.25	32	.25	33	.25
22.8051	1.	24	.25	25	.25	33	.25	34	.25
23.8051	1.	25	.25	26	.25	34	.25	35	.25
24.8051	1.	26	.25	27	.25	35	.25	36	.25
25.8051	1.	28	.25	29	.25	37	.25	38	.25
26.8051	1.	29	.25	30	.25	38	.25	39	.25
27.8051	1.	30	.25	31	.25	39	.25	40	.25
28.8051	1.	31	.25	32	.25	40	.25	41	.25
29.8051	1.	32	.25	33	.25	41	.25	42	.25
30.8051	1.	33	.25	34	.25	42	.25	43	.25
31.8051	1.	34	.25	35	.25	43	.25	44	.25
32.8051	1.	35	.25	36	.25	44	.25	45	.25
3 3	64								
1.8051	1.	1	.25	2	.25	10	.25	11	.25
2.8051	1.	2	.25	3	.25	11	.25	12	.25
3.8051	1.	3	.25	4	.25	12	.25	13	.25
4.8051	1.	4	.25	5	.25	13	.25	14	.25
5.8051	1.	5	.25	6	.25	14	.25	15	.25
6.8051	1.	6	.25	7	.25	15	.25	16	.25
7.8051	1.	7	.25	8	.25	16	.25	17	.25
8.8051	1.	8	.25	9	.25	17	.25	18	.25
9.8051	1.	10	.25	11	.25	19	.25	20	.25
10.8051	1.	11	.25	12	.25	20	.25	21	.25
11.8051	1.	12	.25	13	.25	21	.25	22	.25
12.8051	1.	13	.25	14	.25	22	.25	23	.25
13.8051	1.	14	.25	15	.25	23	.25	24	.25
14.8051	1.	15	.25	16	.25	24	.25	25	.25
15.8051	1.	16	.25	17	.25	25	.25	26	.25
16.8051	1.	17	.25	18	.25	26	.25	27	.25
17.8051	1.	19	.25	20	.25	28	.25	29	.25
18.8051	1.	20	.25	21	.25	29	.25	30	.25
19.8051	1.	21	.25	22	.25	30	.25	31	.25
20.8051	1.	22	.25	23	.25	31	.25	32	.25
21.8051	1.	23	.25	24	.25	32	.25	33	.25
22.8051	1.	24	.25	25	.25	33	.25	34	.25

```
  23.8051   1.   25  .25   26  .25   34  .25   35  .25
  24.8051   1.   26  .25   27  .25   35  .25   36  .25
  25.8051   1.   28  .25   29  .25   37  .25   38  .25
  26.8051   1.   29  .25   30  .25   38  .25   39  .25
  27.8051   1.   30  .25   31  .25   39  .25   40  .25
  28.8051   1.   31  .25   32  .25   40  .25   41  .25
  29.8051   1.   32  .25   33  .25   41  .25   42  .25
  30.8051   1.   33  .25   34  .25   42  .25   43  .25
  31.8051   1.   34  .25   35  .25   43  .25   44  .25
  32.8051   1.   35  .25   36  .25   44  .25   45  .25
  33.8051   1.   37  .25   38  .25   46  .25   47  .25
  34.8051   1.   38  .25   39  .25   47  .25   48  .25
  35.8051   1.   39  .25   40  .25   48  .25   49  .25
  36.8051   1.   40  .25   41  .25   49  .25   50  .25
  37.8051   1.   41  .25   42  .25   50  .25   51  .25
  38.8051   1.   42  .25   43  .25   51  .25   52  .25
  39.8051   1.   43  .25   44  .25   52  .25   53  .25
  40.8051   1.   44  .25   45  .25   53  .25   54  .25
  41.8051   1.   46  .25   47  .25   55  .25   56  .25
  42.8051   1.   47  .25   48  .25   56  .25   57  .25
  43.8051   1.   48  .25   49  .25   57  .25   58  .25
  44.8051   1.   49  .25   50  .25   58  .25   59  .25
  45.8051   1.   50  .25   51  .25   59  .25   60  .25
  46.8051   1.   51  .25   52  .25   60  .25   61  .25
  47.8051   1.   52  .25   53  .25   61  .25   62  .25
  48.8051   1.   53  .25   54  .25   62  .25   63  .25
  49.8051   1.   55  .25   56  .25   64  .25   65  .25
  50.8051   1.   56  .25   57  .25   65  .25   66  .25
  51.8051   1.   57  .25   58  .25   66  .25   67  .25
  52.8051   1.   58  .25   59  .25   67  .25   68  .25
  53.8051   1.   59  .25   60  .25   68  .25   69  .25
  54.8051   1.   60  .25   61  .25   69  .25   70  .25
  55.8051   1.   61  .25   62  .25   70  .25   71  .25
  56.8051   1.   62  .25   63  .25   71  .25   72  .25
  57.8051   1.   64  .25   65  .25   73  .25   74  .25
  58.8051   1.   65  .25   66  .25   74  .25   75  .25
  59.8051   1.   66  .25   67  .25   75  .25   76  .25
  60.8051   1.   67  .25   68  .25   76  .25   77  .25
  61.8051   1.   68  .25   69  .25   77  .25   78  .25
  62.8051   1.   69  .25   70  .25   78  .25   79  .25
  63.8051   1.   70  .25   71  .25   79  .25   80  .25
  64.8051   1.   71  .25   72  .25   80  .25   81  .25
    4    0    0
    5    0    0
    6    0    0
  3.0  .059 655..6996   10.   0.1 409..04231000..8051
SLAB      6   13   17
    1                     9598.
    2                     4998.
    3                     9998.
    4                     9999.
    5                     8491.
```

```
 6                       6139.
 1   1.9645               3    2    2    3    1    6    2
 2   11.860               1    3    2
 3   1.9645               2    4    1   11    3
 4   1.9645               2    5    2   11    3
 5   1.9645               2   16    4   17    4
 6   1.9645               1    7    1
 7   1.9645               1    8    2
 8   1.9645               2    9    1   12    4
 9   1.9645               1   10    2
10   1.9645               1   11    1
11   1.9645
12   1.1411               1   13    4
13   16.562               1   14    5
14   17.495               1   15    6
15   12.811               2   16    4   17    4
16   1.1395
17   1.1518
 1      50.     .7930
 2      37.     1.067
 3      74.     .5335
 4      99.     .7930
 5      74.     1.067
 6     148.     .5335
 7       4.      9.45
 8       2.     3.583
 9      11.     11.11
10       9.     12.69
11      25.      4.76
12       2.     3.543
13       2.     4.058
 1   10    1    1    3    1    2    2    1    3    2    1    4    2
           1    5    1    3   73    1    3   74    2    3   75    2
           3   76    2    3   77    3
 2   10    1    5    4    1   10    5    1   15    5    1   20    5
           1   25    6    2    1    4    2   10    5    2   19    5
           2   28    5    2   37    6
 3   10    2    1    1    2    2    2    2    3    2    2    4    2
           2    5    3    3   77    3    3   78    2    3   79    2
           3   80    2    3   81    1
 4    6    2    5    3    2    6    2    2    7    2    2    8    2
           2    9    1    5    1    7
 5    6    2    9    1    2   18    2    2   27    2    2   36    2
           2   45    3    6    1    7
 6    5    3   37    3    3   46    2    3   55    2    3   64    2
           3   73    1
 7    5    3    1    1    3   10    2    3   19    2    3   28    2
           3   37    3
 8    6    3    1    1    3    2    2    3    3    2    3    4    2
           3    5    3    4    1    7
 9    6    3    5    3    3    6    2    3    7    2    3    8    2
           3    9    1    4    1    7
```

```
   10     6     3     9     1     3    18     2     3    27     2     3    36     2
                3    45     3     5     1     7
   11     6     3    45     3     3    54     2     3    63     2     3    72     2
                3    81     1     5     1     7
   12     1     4     1     8
   13     1     4     1     9
   14     1     5     1    10
   15     1     6     1    11
   16     2     5     1    12     6     1    12
   17     1     6     1    13

RADG      6     6
    1     1     2     1     2
    2     2     4     3     4     5     2
    3     3     8     8     9    10    11     3     1     6     7
    4     4     4    12    13     9     8
    5     5     5    11    10    14    16     4
    6     6     4     5    16    15    17
HEAT      1     0     1
                  3.66                    3.66
  1.0   1.0
DRAG      2
 100. -1.0                   100. -1.0  .05
  64. -1.0                    64. -1.0  .05
BDRY      3     1     3     2
    1     1.0E-5    1.0E+9       .333  1.0
    2     1.2E-6
    3     .00040
    1     3   0.0 284.   0.5 302.   1.0 284.
   13     111.11     1
    1   1.0     1   1.0     1
   14     112.69     1
    1   1.0     1   1.0     1
   15     1 4.76     1
    1   1.0     1   1.0     1
    1228.5           3       275.
    1   1.0     2
    2   1.0     3     3    13     1      13.98    14     1      13.98    15     1      13.98
    3   1.0     1
    2228.5           3       275.
    1   1.0     2
    2   1.0     3     3    13     1      10.79    14     1      10.79    15     1      10.79
    3   1.0     1
CALC      1
   0.  0.01 0.01 0.01 0.01                  0.1  0.1  0.1  0.1
         50
OPER      1     0     3                                                           1
 0.0              600.    0.0    .0069367       600.                 0.0
   10
   0.   0.0.0499  0.0   .05 .706   .151.029  .251.206   .751.206
  .851.029.9499 .706   .95  0.0  1.0  0.0
OUTP 1101

ENDD
```

APPENDIX 6

SELECTED EQUATIONS FROM PROGRESS REPORT # 1 (Xinhui Chen and Neil.E. Todreas, 8/8/94)

COBRA-SFS uses exchange factors F_{ij} from the output file TAPE10 of RADGEN to perform the radiation calculation while the MIT method uses the absorption factors G_{i-j} from which C_{rad}, $C_{rad,w,1}$ and $C_{rad,w,2}$ are derived to analyze the net radiation heat transfer. Theoretically, the two methods are identical with $G_{i-j} = F_{ij}/\varepsilon_i$. This conclusion is shown below with several steps of matrix manipulations. Equation A6-1 is taken from Reference [5]. Please note there are a total of n^2 equations in the form of n sets of n simultaneous linear algebraic equations (where n is the total number of surfaces in an enclosure).

$$\begin{bmatrix} F_{11}\frac{1-\varepsilon_1}{\varepsilon_1}-\frac{1}{\varepsilon_1} & F_{12}\frac{1-\varepsilon_2}{\varepsilon_2} & \cdots & F_{1n}\frac{1-\varepsilon_n}{\varepsilon_n} \\ F_{21}\frac{1-\varepsilon_1}{\varepsilon_1} & F_{22}\frac{1-\varepsilon_2}{\varepsilon_2}-\frac{1}{\varepsilon_2} & \cdots & F_{2n}\frac{1-\varepsilon_n}{\varepsilon_n} \\ \cdots & \cdots & \cdots & \cdots \\ F_{n1}\frac{1-\varepsilon_1}{\varepsilon_1} & F_{n2}\frac{1-\varepsilon_2}{\varepsilon_2} & \cdots & F_{nn}\frac{1-\varepsilon_n}{\varepsilon_n}-\frac{1}{\varepsilon_n} \end{bmatrix} \cdot \begin{bmatrix} F_{1j} \\ F_{2j} \\ \cdots \\ F_{nj} \end{bmatrix} = \begin{bmatrix} -F_{1j}\varepsilon_j \\ -F_{2j}\varepsilon_j \\ \cdots \\ -F_{nj}\varepsilon_j \end{bmatrix} \qquad \text{(A6-1)}$$

$$(j = 1,2,\ldots n)$$

or

$$\begin{bmatrix} F_{11}(1-\varepsilon_1)-1 & F_{12}(1-\varepsilon_2) & \cdots & F_{1n}(1-\varepsilon_n) \\ F_{21}(1-\varepsilon_1) & F_{22}(1-\varepsilon_2)-1 & \cdots & F_{2n}(1-\varepsilon_n) \\ \cdots & \cdots & \cdots & \cdots \\ F_{n1}(1-\varepsilon_1) & F_{n2}(1-\varepsilon_2) & \cdots & F_{nn}(1-\varepsilon_n)-1 \end{bmatrix} \cdot \begin{bmatrix} F_{1j}/\varepsilon_1 \\ F_{2j}/\varepsilon_2 \\ \cdots \\ F_{nj}/\varepsilon_n \end{bmatrix} = -\begin{bmatrix} F_{1j}\varepsilon_j \\ F_{2j}\varepsilon_j \\ \cdots \\ F_{nj}\varepsilon_j \end{bmatrix} \qquad \text{(A6-2)}$$

or

$$\begin{bmatrix} 1-\rho_1F_{11} & -\rho_2F_{12} & \cdots & -\rho_nF_{1n} \\ -\rho_1F_{21} & 1-\rho_2F_{22} & \cdots & -\rho_nF_{2n} \\ \cdots & \cdots & \cdots & \cdots \\ -\rho_1F_{n1} & -\rho_2F_{n2} & \cdots & 1-\rho_nF_{nn} \end{bmatrix} \cdot \begin{bmatrix} G_{1-j} \\ G_{2-j} \\ \cdots \\ G_{nj} \end{bmatrix} = \begin{bmatrix} F_{1j}\varepsilon_j \\ F_{2j}\varepsilon_j \\ \cdots \\ F_{nj}\varepsilon_j \end{bmatrix} \qquad \text{(A6-3)}$$

where

$$\rho_i = 1-\varepsilon_i, \quad (i = 1,2,\ldots,n)$$

From Appendix K of Reference [2], we get the following absorption factor equations:

$$\begin{bmatrix} 1-\rho_1 F_{1-1} & -\rho_2 F_{1-2} & \cdots & -\rho_N F_{1-N} \\ -\rho_1 F_{2-1} & 1-\rho_2 F_{2-2} & \cdots & -\rho_N F_{2-N} \\ \cdots & \cdots & \cdots & \cdots \\ -\rho_1 F_{N-1} & -\rho_2 F_{N-2} & \cdots & 1-\rho_N F_{N-N} \end{bmatrix} \cdot \begin{bmatrix} G_{1-j} \\ G_{2-j} \\ \cdots \\ G_{N-j} \end{bmatrix} = \begin{bmatrix} F_{1-j}\varepsilon_j \\ F_{2-j}\varepsilon_j \\ \cdots \\ F_{N-j}\varepsilon_j \end{bmatrix} \qquad \text{(A6-4)}$$

By comparing Equations A6-3 and A6-4, we have

$$G_{1\text{-}j} = F_{1j} / \varepsilon_1,$$
$$G_{2\text{-}j} = F_{2j} / \varepsilon_2,$$
$$\ldots\ldots \quad \ldots\ldots$$

or

$$G_{i\text{-}j} = F_{ij} / \varepsilon_i \qquad \text{(A6-5)}$$

where

$i = 1, 2, \ldots, n$

$j = 1, 2, \ldots, n$

n = the total number of surfaces in an enclosure

It should be noted that a negative sign is missing in Equation 2.2 in Reference [5]. Then we referred to Cox's original thesis (Page 93, Equation 28) [14] to confirm that the negative sign should be present.

APPENDIX 7

OTHER WORK PERFORMED

Besides our work per the contract (i.e., the original contract, the no-cost extension and review meeting), we did some work beyond the contract scope which may be beneficial to KAERI. Hence, it is presented here for reference by KAERI.

A7.1 Transplantation of COBRA-SFS from CYBER Version to SUN Version

The current COBRA-SFS we obtained was the Cycle 1 code on the CDC CYBER 170 platform. Some non-executable statements in the source code are machine-dependent or machine-unique, so they were incompatible with the MIT computers. Many efforts were made to transplant the code to MIT's VAX, IBM and SUN Sparc stations simultaneously. After it had been installed on our SUN Sparc station, a benchmark problem was simulated to test the code at MIT (detailed description can be found in Section 7.1 [1]). A comparison between the SUN Sparc calculation and the CYBER 170 calculation is shown in Table A7-1. The selection of results for Rod 4 Assembly 1 is arbitrary. The results are identical to the PNL standard outputs within computer errors. Hence, it is concluded that the code transplanting is successful and the results are correct.

A7.2 Simulations of KAERI's KSC-4 Cask

Using COBRA-SFS, we simulated KAERI's KSC-4 cask for both nitrogen and helium as back fill gases under vertical and horizontal orientations. Table A7-2 summarizes the major temperature profiles between MIT and KAERI calculations [15] for vertical orientation. The input files are the same for both calculations except (a) the MIT calculation uses RADGEN and COBRA-SFS, while KAERI may use RADX-1 and COBRA-SFS, and (b) the fourth parameter in Group RODS.1 of the current MIT version of COBRA-SFS is NQAX[1], the flag for temperature dependent fuel properties.

NQAX = 0; constant fuel properties for all fuel types

= 1; temperature-dependent fuel properties for fuel type 1 only, input in Groups RODS.5 and RODS.6.

Table A7-1. Benchmark Problem: Validation of Code Transplantation—SUN SPARC vs. CYBER 170

Axial Zone (in.) (Rod 3, Assembly 1)	Clad Temperatures (°C)	
	SUN SPARC (MIT)	CYBER 170 (Standard)
0.0 – 2.5	205.1	205.1
2.5 – 5.0	210.6	210.6
5.0 – 7.5	215.4	215.4
7.5 – 10.0	219.7	219.7
10.0 – 12.5	223.3	223.3
12.5 – 15.0	226.6	226.6
15.0 – 17.5	229.4	229.4
17.5 – 20.0	231.8	231.8
20.0 – 22.5	234.0	234.0
22.5 – 25.0	235.9	235.9
25.0 – 27.5	237.5	237.5
27.5 – 30.0	238.9	238.9
Peak Clad Temperature (°C)	238.9	238.9

Table A7-2. Temperature Profile in KSC-4 Using COBRA-SFS—
Conduction, Convection and Radiation, Vertical Orientation

Locations	Temperatures (˚C)					
	N_2			He		
	MIT	KAERI	Difference	MIT	KAERI	Difference
Peak Clad	288.8	277	11.8	226.2	226	0.2
Fuel Basket	229.2	227	2.2	200.1	201	0.1
Lead Shield	117.9	120	-2.1	117.2	120	-2.8
Inner Shell	115.8	118	-2.2	115.1	118	-2.9
Resin Shield	97.9	99	-1.1	97.4	100	-2.6
Cask Surface	82.0	83	-1.0	81.7	83	-1.3
Ambient Temp.	38	38	0.0	38	38	0.0

In our case, NQAX should be zero. The data from KAERI indicates that their fourth parameter is 1, but they input neither Groups RODS.5 nor RODS.6. This leads us to guess that their parameter is defined differently in the Korean version of COBRA-SFS. The results show:

(1) As far as the peak clad temperature is concerned, the MIT calculation results are higher.

(2) Agreement between the two calculations is better in the helium case than in the nitrogen case, i.e., maximum temperature deviation of 3°C versus 12°C.

(3) Under the same conditions, the peak clad temperature for helium is lower than that for nitrogen indicating the dominant effects of radiation and conduction.

Table A7-3 summarizes the major temperature profiles for vertical and horizontal orientations using COBRA-SFS at MIT. From this table, we find

(1) Vertical orientation results deviate from horizontal orientation results much less for helium than for nitrogen, which indicates axial natural convection is less significant for helium than for nitrogen. This is reasonable since heat conduction is more significant in helium due to its higher thermal conductivity. Note that current version of COBRA-SFS (Cycle-1) cannot model natural convection transversely (page 2.9 [1]).

(2) For the KSC-4 case, axial natural convection is not a vital factor in the combined conductive, convective and radiative heat transfer.

(3) Under the same condition, the peak clad temperature for helium is lower than that for nitrogen.

Table A7-3. Temperature Profile in KSC-4 Using COBRA-SFS—Conduction, Convection and Radiation, Vertical and Horizontal Orientations

Locations	Temperatures (°C)					
	N_2			He		
	Vertical	Horizontal	Difference	Vertical	Horizontal	Difference
Peak Clad	288.8	289.9	-1.1	226.17	226.22	-0.05
Fuel Basket	229.2	230.6	-1.4	200.07	200.15	-0.08
Lead Shield	117.9	117.7	0.2	117.18	117.19	-0.01
Inner Shell	115.8	115.6	0.2	115.13	115.14	-0.01
Resin Shield	97.9	97.8	0.1	97.43	97.44	-0.01
Cask Surface	82.0	81.9	0.1	81.69	81.70	-0.01
Ambient Temp.	38	38	0.0	38	38	0.0

APPENDIX 8

Simple Hand Calculation with regard to Conduction-only and Conduction and Radiation Heat Transfer Mechanisms

It is shown in Table 7-9 and Figure 7-6 that radiation heat transfer dominates over conduction in the thermal calculation of dry spent fuel bundle, i.e., for 17x17 bundle at 4684 W with nitrogen as fill gas, the maximum clad temperature is 1088.4°C in Conduction-only case while it is about 400°C in the combined Conduction and Radiation case. Since power level and other conditions are the same in both cases, radiation alone will reduce the peak clad temperature by 675.6°C. This phenomenon is consistent with the following simple hand calculation.

For consistency, the same nomenclature is used as in Figure 7-1. Heat flux is designated as q"(x) which is a function of location, x, since from the center of the bundle to the wall, there are more and more rods whose decay heat needs to be transferred to the environment. Hence, q"(x) monotonically increases with x. For simplicity, the average heat flux from x=0 to x=L is designated as q" and is used in the calculation. Subscriptions 1 and 2 represent Conduction-only and Conduction and Radiation cases, respectively.

For Conduction-only, heat transfer equation is

$$\bar{q}_1'' = k_1 \cdot \frac{T_{m1} - T_w}{L} \qquad \text{(A8-1)}$$

For Conduction and Radiation, heat transfer equation can written as

$$\bar{q}_2'' = k_2 \cdot \frac{T_{m2} - T_w}{L} + \varepsilon \cdot \sigma \cdot (T_{m2}^4 - T_w^4) \qquad \text{(A8-2)}$$

where

k_1 = conductivity of N_2 at $(T_{m1} + T_w)/2$

k_2 = conductivity of N_2 at $(T_{m2} + T_w)/2$

ε = effective emissivity

Equating Equations A8-1 and A8-2 yields

$$k_1 \cdot \frac{T_{m1} - T_w}{L} = k_2 \cdot \frac{T_{m2} - T_w}{L} + \varepsilon \cdot \sigma \cdot (T_{m2}^4 - T_w^4) \qquad \text{(A8-3)}$$

For simplicity, assume that right hand side of the equation is known for Conduction and Radiation calculation from COBRA-SFS and we want to solve for T_{m1} (Otherwise, we have to solve a fourth-order equation for T_{m2} if given T_{m1}.) and compare this maximum temperature with COBRA-SFS results.

From COBRA-SFS, we have $\varepsilon_{rod} = 0.80$ (Table 7-6), $\varepsilon_{w} = 0.30$ (Table 7-7), L = 0.12 m (Figure 5-1), $T_w = 96°C$ (Figure 7-8) and $T_{m2} \approx 400°C$ (Table 7-5). Hence

$$\frac{T_{m2} + T_w}{2} = 248°C \ = \ 478.4°F$$

$$k_2\Big|_{\frac{T_{m2}+T_w}{2}} = 0.0227 \text{Btu} / \text{hr} \cdot \text{ft} \cdot °F = \ 0.0399 \ W / m \cdot °C$$

where

k_2 is taken from COBRA-SFS input deck at specified temperature

To evaluate T_{m1} from Equation A8-3, we need to know k_1, which itself is a function of T_{m1}, so we need to guess a value for T_{m1}. Assuming T_{m1} = 1089 °C, we can evaluate k_2 from the COBRA-SFS input deck.

$$\frac{T_{m1} + T_w}{2} = 592.5°C \ = \ 1098.5°F$$

$$k_1\Big|_{\frac{T_{m1}+T_w}{2}} = 0.0334 \text{Btu} / \text{hr} \cdot \text{ft} \cdot °F = \ 0.0588 \ W / m \cdot °C$$

Substituting these values into Equation A8-3

$$0.0588 \cdot \frac{T_{m1} - 96}{0.12} = 0.0399 \cdot \frac{400 - 96}{0.12} + \varepsilon \cdot 5.67 \times 10^{-8} \cdot [(400 + 273)^4 - (96 + 273)^4]$$

or

$$T_{m1} = 302.3 + 21592.3 \ \varepsilon \ \ (°C) \qquad \text{(A8-4)}$$

Using a simple model, i.e., Equation 7-90 and assuming $A_1 = A_2$, to evaluate effective emissivity, ε

$$\varepsilon = \frac{1}{\frac{1}{\varepsilon_{rod}} + \frac{1}{\varepsilon_{wall}} - 1} \qquad \text{(A8-5)}$$

$$= \frac{1}{\frac{1}{0.8} + \frac{1}{0.3} - 1}$$

$$= 0.279$$

Using $\varepsilon = 0.279$, Equation A8-4 yields

$$T_{m1} = 302.3 + 21592.3 \times 0.279$$
$$= 6326.6\ °C$$

This temperature is too high which indicates that the simple radiation model such as the one described in Equation A8-5 is inadequate, i.e., the model neglects the effect of thermal shielding of the outer rods to the inner rods in a fuel bundle by assuming only two surfaces (that of the rods and that of the wall), hence increases the effective emissivity. If the effective emissivity is assumed to 0.04, i.e., by incorporating the effect of Figure 7-7, then

$$T_{m1} = 302.3 + 21592.3 \times 0.04$$
$$= 1166.0\ °C$$

This value is about 7.1 % different from COBRA-SFS's 1089.0°C. Therefore simple hand method shows similar results to Table 7-9 and Figure 7-6, and radiation is dominant in dry spent fuel bundle calculation.

APPENDIX 9

17x17 BUNDLE ANALYSIS—INPUT FILE FOR COBRA-SFS (Cycle 2)

```
 3000
    1              THERMAL ANALYSYS OF KSC-7 CASK (N2 17X17 ARRAY 1 ASS'Y)
prop     11     1
         1.        100.      133.9      .0154        .240       14.08       .0463
         2.        200.      157.9      .0174        .241       16.67       .0518
         3.        300.      182.1      .0193        .243       19.23       .0580
         4.        400.      206.5      .0212        .245       21.74       .0630
         5.        500.      231.1      .0231        .247       24.27       .0680
         6.        600.      256.0      .0250        .250       26.81       .0720
         7.        700.      281.1      .0268        .253       29.33       .0770
         8.        800.      306.7      .0286        .256       31.85       .0810
        10.        900.      332.5      .0303        .259       34.36       .0850
        15.       1000.      358.6      .0319        .262       36.90       .0889
        20.       2000.      617.2      .0471        .286       62.11       .1242
    1STEEL                              1.E8
chan      1    15
     160.0       90.0
    1     1   324     0
    1     1     0     0    1
    1.28511.412.2938    2.3720.5276    19.3720.5276
    2.22241.084.5875    3.3720.4961    20.1220.5276
    3.22241.084.5875    4.3720.4961    21.1220.5276
    4.22241.084.5875    5.3720.4961    22.1220.5276
    5.22241.084.5875    6.3720.4961    23.1220.5276
    6.22241.084.5875    7.3720.4961    24.1220.5276
    7.22241.084.5875    8.3720.4961    25.1220.5276
    8.22241.084.5875    9.3720.4961    26.1220.5276
    9.22241.084.5875   10.3720.4961    27.1220.5276
   10.22241.084.5875   11.3720.4961    28.1220.5276
   11.22241.084.5875   12.3720.4961    29.1220.5276
   12.22241.084.5875   13.3720.4961    30.1220.5276
   13.22241.084.5875   14.3720.4961    31.1220.5276
   14.22241.084.5875   15.3720.4961    32.1220.5276
   15.22241.084.5875   16.3720.4961    33.1220.5276
   16.22241.084.5875   17.3720.4961    34.1220.5276
   17.22241.084.5875   18.3720.5276    35.1220.5276
   18.28511.412.2938   36.3720.5276
   19.22241.084.5875   20.1220.5276    37.3720.4961
   20.13621.1751.175   21.1220.4961    38.1220.4961
   21.13621.1751.175   22.1220.4961    39.1220.4961
   22.13621.1751.175   23.1220.4961    40.1220.4961
   23.13621.1751.175   24.1220.4961    41.1220.4961
   24.13621.1751.175   25.1220.4961    42.1220.4961
   25.13621.1751.175   26.1220.4961    43.1220.4961
   26.13621.1751.175   27.1220.4961    44.1220.4961
   27.13621.1751.175   28.1220.4961    45.1220.4961
   28.13621.1751.175   29.1220.4961    46.1220.4961
   29.13621.1751.175   30.1220.4961    47.1220.4961
   30.13621.1751.175   31.1220.4961    48.1220.4961
   31.13621.1751.175   32.1220.4961    49.1220.4961
   32.13621.1751.175   33.1220.4961    50.1220.4961
   33.13621.1751.175   34.1220.4961    51.1220.4961
```

34.13621.1751.175	35.1220.4961	52.1220.4961
35.13621.1751.175	36.1220.5276	53.1220.4961
36.22241.084.5875	54.3720.4961	
37.22241.084.5875	38.1220.5276	55.3720.4961
38.13621.1751.175	39.1220.4961	56.1220.4961
39.13621.1751.175	40.1220.4961	57.1220.4961
40.13621.1751.175	41.1220.4961	58.1220.4961
41.13621.1751.175	42.1220.4961	59.1220.4961
42.13621.1751.175	43.1220.4961	60.1220.4961
43.13621.1751.175	44.1220.4961	61.1220.4961
44.13621.1751.175	45.1220.4961	62.1220.4961
45.13621.1751.175	46.1220.4961	63.1220.4961
46.13621.1751.175	47.1220.4961	64.1220.4961
47.13621.1751.175	48.1220.4961	65.1220.4961
48.13621.1751.175	49.1220.4961	66.1220.4961
49.13621.1751.175	50.1220.4961	67.1220.4961
50.13621.1751.175	51.1220.4961	68.1220.4961
51.13621.1751.175	52.1220.4961	69.1220.4961
52.13621.1751.175	53.1220.4961	70.1220.4961
53.13621.1751.175	54.1220.5276	71.1220.4961
54.22241.084.5875	72.3720.4961	
55.22241.084.5875	56.1220.5276	73.3720.4961
56.13621.1751.175	57.1220.4961	74.1220.4961
57.13621.1751.175	58.1220.4961	75.1220.4961
58.13621.1751.175	59.1220.4961	76.1220.4961
59.13621.1751.175	60.1220.4961	77.1220.4961
60.13621.1751.175	61.1220.4961	78.1220.4961
61.13621.1751.175	62.1220.4961	79.1220.4961
62.13621.1751.175	63.1220.4961	80.1220.4961
63.13621.1751.175	64.1220.4961	81.1220.4961
64.13621.1751.175	65.1220.4961	82.1220.4961
65.13621.1751.175	66.1220.4961	83.1220.4961
66.13621.1751.175	67.1220.4961	84.1220.4961
67.13621.1751.175	68.1220.4961	85.1220.4961
68.13621.1751.175	69.1220.4961	86.1220.4961
69.13621.1751.175	70.1220.4961	87.1220.4961
70.13621.1751.175	71.1220.4961	88.1220.4961
71.13621.1751.175	72.1220.5276	89.1220.4961
72.22241.084.5875	90.3720.4961	
73.22241.084.5875	74.1220.5276	91.3720.4961
74.13621.1751.175	75.1220.4961	92.1220.4961
75.13621.1751.175	76.1220.4961	93.1220.4961
76.13621.1751.175	77.1220.4961	94.1220.4961
77.13621.1751.175	78.1220.4961	95.1220.4961
78.13621.1751.175	79.1220.4961	96.1220.4961
79.13621.1751.175	80.1220.4961	97.1220.4961
80.13621.1751.175	81.1220.4961	98.1220.4961
81.13621.1751.175	82.1220.4961	99.1220.4961
82.13621.1751.175	83.1220.4961	100.1220.4961
83.13621.1751.175	84.1220.4961	101.1220.4961
84.13621.1751.175	85.1220.4961	102.1220.4961
85.13621.1751.175	86.1220.4961	103.1220.4961

86.13621.1751.175	87.1220.4961	104.1220.4961
87.13621.1751.175	88.1220.4961	105.1220.4961
88.13621.1751.175	89.1220.4961	106.1220.4961
89.13621.1751.175	90.1220.5276	107.1220.4961
90.22241.084.5875	108.3720.4961	
91.22241.084.5875	92.1220.5276	109.3720.4961
92.13621.1751.175	93.1220.4961	110.1220.4961
93.13621.1751.175	94.1220.4961	111.1220.4961
94.13621.1751.175	95.1220.4961	112.1220.4961
95.13621.1751.175	96.1220.4961	113.1220.4961
96.13621.1751.175	97.1220.4961	114.1220.4961
97.13621.1751.175	98.1220.4961	115.1220.4961
98.13621.1751.175	99.1220.4961	116.1220.4961
99.13621.1751.175	100.1220.4961	117.1220.4961
100.13621.1751.175	101.1220.4961	118.1220.4961
101.13621.1751.175	102.1220.4961	119.1220.4961
102.13621.1751.175	103.1220.4961	120.1220.4961
103.13621.1751.175	104.1220.4961	121.1220.4961
104.13621.1751.175	105.1220.4961	122.1220.4961
105.13621.1751.175	106.1220.4961	123.1220.4961
106.13621.1751.175	107.1220.4961	124.1220.4961
107.13621.1751.175	108.1220.5276	125.1220.4961
108.22241.084.5875	126.3720.4961	
109.22241.084.5875	110.1220.5276	127.3720.4961
110.13621.1751.175	111.1220.4961	128.1220.4961
111.13621.1751.175	112.1220.4961	129.1220.4961
112.13621.1751.175	113.1220.4961	130.1220.4961
113.13621.1751.175	114.1220.4961	131.1220.4961
114.13621.1751.175	115.1220.4961	132.1220.4961
115.13621.1751.175	116.1220.4961	133.1220.4961
116.13621.1751.175	117.1220.4961	134.1220.4961
117.13621.1751.175	118.1220.4961	135.1220.4961
118.13621.1751.175	119.1220.4961	136.1220.4961
119.13621.1751.175	120.1220.4961	137.1220.4961
120.13621.1751.175	121.1220.4961	138.1220.4961
121.13621.1751.175	122.1220.4961	139.1220.4961
122.13621.1751.175	123.1220.4961	140.1220.4961
123.13621.1751.175	124.1220.4961	141.1220.4961
124.13621.1751.175	125.1220.4961	142.1220.4961
125.13621.1751.175	126.1220.5276	143.1220.4961
126.22241.084.5875	144.3720.4961	
127.22241.084.5875	128.1220.5276	145.3720.4961
128.13621.1751.175	129.1220.4961	146.1220.4961
129.13621.1751.175	130.1220.4961	147.1220.4961
130.13621.1751.175	131.1220.4961	148.1220.4961
131.13621.1751.175	132.1220.4961	149.1220.4961
132.13621.1751.175	133.1220.4961	150.1220.4961
133.13621.1751.175	134.1220.4961	151.1220.4961
134.13621.1751.175	135.1220.4961	152.1220.4961
135.13621.1751.175	136.1220.4961	153.1220.4961
136.13621.1751.175	137.1220.4961	154.1220.4961
137.13621.1751.175	138.1220.4961	155.1220.4961

138.13621.1751.175	139.1220.4961	156.1220.4961
139.13621.1751.175	140.1220.4961	157.1220.4961
140.13621.1751.175	141.1220.4961	158.1220.4961
141.13621.1751.175	142.1220.4961	159.1220.4961
142.13621.1751.175	143.1220.4961	160.1220.4961
143.13621.1751.175	144.1220.5276	161.1220.4961
144.22241.084.5875	162.3720.4961	
145.22241.084.5875	146.1220.5276	163.3720.4961
146.13621.1751.175	147.1220.4961	164.1220.4961
147.13621.1751.175	148.1220.4961	165.1220.4961
148.13621.1751.175	149.1220.4961	166.1220.4961
149.13621.1751.175	150.1220.4961	167.1220.4961
150.13621.1751.175	151.1220.4961	168.1220.4961
151.13621.1751.175	152.1220.4961	169.1220.4961
152.13621.1751.175	153.1220.4961	170.1220.4961
153.13621.1751.175	154.1220.4961	171.1220.4961
154.13621.1751.175	155.1220.4961	172.1220.4961
155.13621.1751.175	156.1220.4961	173.1220.4961
156.13621.1751.175	157.1220.4961	174.1220.4961
157.13621.1751.175	158.1220.4961	175.1220.4961
158.13621.1751.175	159.1220.4961	176.1220.4961
159.13621.1751.175	160.1220.4961	177.1220.4961
160.13621.1751.175	161.1220.4961	178.1220.4961
161.13621.1751.175	162.1220.5276	179.1220.4961
162.22241.084.5875	180.3720.4961	
163.22241.084.5875	164.1220.5276	181.3720.4961
164.13621.1751.175	165.1220.4961	182.1220.4961
165.13621.1751.175	166.1220.4961	183.1220.4961
166.13621.1751.175	167.1220.4961	184.1220.4961
167.13621.1751.175	168.1220.4961	185.1220.4961
168.13621.1751.175	169.1220.4961	186.1220.4961
169.13621.1751.175	170.1220.4961	187.1220.4961
170.13621.1751.175	171.1220.4961	188.1220.4961
171.13621.1751.175	172.1220.4961	189.1220.4961
172.13621.1751.175	173.1220.4961	190.1220.4961
173.13621.1751.175	174.1220.4961	191.1220.4961
174.13621.1751.175	175.1220.4961	192.1220.4961
175.13621.1751.175	176.1220.4961	193.1220.4961
176.13621.1751.175	177.1220.4961	194.1220.4961
177.13621.1751.175	178.1220.4961	195.1220.4961
178.13621.1751.175	179.1220.4961	196.1220.4961
179.13621.1751.175	180.1220.5276	197.1220.4961
180.22241.084.5875	198.3720.4961	
181.22241.084.5875	182.1220.5276	199.3720.4961
182.13621.1751.175	183.1220.4961	200.1220.4961
183.13621.1751.175	184.1220.4961	201.1220.4961
184.13621.1751.175	185.1220.4961	202.1220.4961
185.13621.1751.175	186.1220.4961	203.1220.4961
186.13621.1751.175	187.1220.4961	204.1220.4961
187.13621.1751.175	188.1220.4961	205.1220.4961
188.13621.1751.175	189.1220.4961	206.1220.4961
189.13621.1751.175	190.1220.4961	207.1220.4961

190.13621.1751.175	191.1220.4961	208.1220.4961
191.13621.1751.175	192.1220.4961	209.1220.4961
192.13621.1751.175	193.1220.4961	210.1220.4961
193.13621.1751.175	194.1220.4961	211.1220.4961
194.13621.1751.175	195.1220.4961	212.1220.4961
195.13621.1751.175	196.1220.4961	213.1220.4961
196.13621.1751.175	197.1220.4961	214.1220.4961
197.13621.1751.175	198.1220.5276	215.1220.4961
198.22241.084.5875	216.3720.4961	
199.22241.084.5875	200.1220.5276	217.3720.4961
200.13621.1751.175	201.1220.4961	218.1220.4961
201.13621.1751.175	202.1220.4961	219.1220.4961
202.13621.1751.175	203.1220.4961	220.1220.4961
203.13621.1751.175	204.1220.4961	221.1220.4961
204.13621.1751.175	205.1220.4961	222.1220.4961
205.13621.1751.175	206.1220.4961	223.1220.4961
206.13621.1751.175	207.1220.4961	224.1220.4961
207.13621.1751.175	208.1220.4961	225.1220.4961
208.13621.1751.175	209.1220.4961	226.1220.4961
209.13621.1751.175	210.1220.4961	227.1220.4961
210.13621.1751.175	211.1220.4961	228.1220.4961
211.13621.1751.175	212.1220.4961	229.1220.4961
212.13621.1751.175	213.1220.4961	230.1220.4961
213.13621.1751.175	214.1220.4961	231.1220.4961
214.13621.1751.175	215.1220.4961	232.1220.4961
215.13621.1751.175	216.1220.5276	233.1220.4961
216.22241.084.5875	234.3720.4961	
217.22241.084.5875	218.1220.5276	235.3720.4961
218.13621.1751.175	219.1220.4961	236.1220.4961
219.13621.1751.175	220.1220.4961	237.1220.4961
220.13621.1751.175	221.1220.4961	238.1220.4961
221.13621.1751.175	222.1220.4961	239.1220.4961
222.13621.1751.175	223.1220.4961	240.1220.4961
223.13621.1751.175	224.1220.4961	241.1220.4961
224.13621.1751.175	225.1220.4961	242.1220.4961
225.13621.1751.175	226.1220.4961	243.1220.4961
226.13621.1751.175	227.1220.4961	244.1220.4961
227.13621.1751.175	228.1220.4961	245.1220.4961
228.13621.1751.175	229.1220.4961	246.1220.4961
229.13621.1751.175	230.1220.4961	247.1220.4961
230.13621.1751.175	231.1220.4961	248.1220.4961
231.13621.1751.175	232.1220.4961	249.1220.4961
232.13621.1751.175	233.1220.4961	250.1220.4961
233.13621.1751.175	234.1220.5276	251.1220.4961
234.22241.084.5875	252.3720.4961	
235.22241.084.5875	236.1220.5276	253.3720.4961
236.13621.1751.175	237.1220.4961	254.1220.4961
237.13621.1751.175	238.1220.4961	255.1220.4961
238.13621.1751.175	239.1220.4961	256.1220.4961
239.13621.1751.175	240.1220.4961	257.1220.4961
240.13621.1751.175	241.1220.4961	258.1220.4961
241.13621.1751.175	242.1220.4961	259.1220.4961

242.13621.1751.175	243.1220.4961	260.1220.4961
243.13621.1751.175	244.1220.4961	261.1220.4961
244.13621.1751.175	245.1220.4961	262.1220.4961
245.13621.1751.175	246.1220.4961	263.1220.4961
246.13621.1751.175	247.1220.4961	264.1220.4961
247.13621.1751.175	248.1220.4961	265.1220.4961
248.13621.1751.175	249.1220.4961	266.1220.4961
249.13621.1751.175	250.1220.4961	267.1220.4961
250.13621.1751.175	251.1220.4961	268.1220.4961
251.13621.1751.175	252.1220.5276	269.1220.4961
252.22241.084.5875	270.3720.4961	
253.22241.084.5875	254.1220.5276	271.3720.4961
254.13621.1751.175	255.1220.4961	272.1220.4961
255.13621.1751.175	256.1220.4961	273.1220.4961
256.13621.1751.175	257.1220.4961	274.1220.4961
257.13621.1751.175	258.1220.4961	275.1220.4961
258.13621.1751.175	259.1220.4961	276.1220.4961
259.13621.1751.175	260.1220.4961	277.1220.4961
260.13621.1751.175	261.1220.4961	278.1220.4961
261.13621.1751.175	262.1220.4961	279.1220.4961
262.13621.1751.175	263.1220.4961	280.1220.4961
263.13621.1751.175	264.1220.4961	281.1220.4961
264.13621.1751.175	265.1220.4961	282.1220.4961
265.13621.1751.175	266.1220.4961	283.1220.4961
266.13621.1751.175	267.1220.4961	284.1220.4961
267.13621.1751.175	268.1220.4961	285.1220.4961
268.13621.1751.175	269.1220.4961	286.1220.4961
269.13621.1751.175	270.1220.5276	287.1220.4961
270.22241.084.5875	288.3720.4961	
271.22241.084.5875	272.1220.5276	289.3720.4961
272.13621.1751.175	273.1220.4961	290.1220.4961
273.13621.1751.175	274.1220.4961	291.1220.4961
274.13621.1751.175	275.1220.4961	292.1220.4961
275.13621.1751.175	276.1220.4961	293.1220.4961
276.13621.1751.175	277.1220.4961	294.1220.4961
277.13621.1751.175	278.1220.4961	295.1220.4961
278.13621.1751.175	279.1220.4961	296.1220.4961
279.13621.1751.175	280.1220.4961	297.1220.4961
280.13621.1751.175	281.1220.4961	298.1220.4961
281.13621.1751.175	282.1220.4961	299.1220.4961
282.13621.1751.175	283.1220.4961	300.1220.4961
283.13621.1751.175	284.1220.4961	301.1220.4961
284.13621.1751.175	285.1220.4961	302.1220.4961
285.13621.1751.175	286.1220.4961	303.1220.4961
286.13621.1751.175	287.1220.4961	304.1220.4961
287.13621.1751.175	288.1220.5276	305.1220.4961
288.22241.084.5875	306.3720.4961	
289.22241.084.5875	290.1220.5276	307.3720.5276
290.13621.1751.175	291.1220.4961	308.1220.5276
291.13621.1751.175	292.1220.4961	309.1220.5276
292.13621.1751.175	293.1220.4961	310.1220.5276
293.13621.1751.175	294.1220.4961	311.1220.5276

```
294.13621.1751.175  295.1220.4961  312.1220.5276
295.13621.1751.175  296.1220.4961  313.1220.5276
296.13621.1751.175  297.1220.4961  314.1220.5276
297.13621.1751.175  298.1220.4961  315.1220.5276
298.13621.1751.175  299.1220.4961  316.1220.5276
299.13621.1751.175  300.1220.4961  317.1220.5276
300.13621.1751.175  301.1220.4961  318.1220.5276
301.13621.1751.175  302.1220.4961  319.1220.5276
302.13621.1751.175  303.1220.4961  320.1220.5276
303.13621.1751.175  304.1220.4961  321.1220.5276
304.13621.1751.175  305.1220.4961  322.1220.5276
305.13621.1751.175  306.1220.5276  323.1220.5276
306.22241.084.5875  324.3720.5276
307.28511.412.2938  308.3720.5276
308.22241.084.5875  309.3720.4961
309.22241.084.5875  310.3720.4961
310.22241.084.5875  311.3720.4961
311.22241.084.5875  312.3720.4961
312.22241.084.5875  313.3720.4961
313.22241.084.5875  314.3720.4961
314.22241.084.5875  315.3720.4961
315.22241.084.5875  316.3720.4961
316.22241.084.5875  317.3720.4961
317.22241.084.5875  318.3720.4961
318.22241.084.5875  319.3720.4961
319.22241.084.5875  320.3720.4961
320.22241.084.5875  321.3720.4961
321.22241.084.5875  322.3720.4961
322.22241.084.5875  323.3720.4961
323.22241.084.5875  324.3720.5276
324.28511.412.2938

rods      1     1     0     0     0
    1     1   289
    1.3740    1.     1   .25     2   .25    19   .25    20   .25
    2.3740    1.     2   .25     3   .25    20   .25    21   .25
    3.3740    1.     3   .25     4   .25    21   .25    22   .25
    4.3740    1.     4   .25     5   .25    22   .25    23   .25
    5.3740    1.     5   .25     6   .25    23   .25    24   .25
    6.3740    1.     6   .25     7   .25    24   .25    25   .25
    7.3740    1.     7   .25     8   .25    25   .25    26   .25
    8.3740    1.     8   .25     9   .25    26   .25    27   .25
    9.3740    1.     9   .25    10   .25    27   .25    28   .25
   10.3740    1.    10   .25    11   .25    28   .25    29   .25
   11.3740    1.    11   .25    12   .25    29   .25    30   .25
   12.3740    1.    12   .25    13   .25    30   .25    31   .25
   13.3740    1.    13   .25    14   .25    31   .25    32   .25
   14.3740    1.    14   .25    15   .25    32   .25    33   .25
   15.3740    1.    15   .25    16   .25    33   .25    34   .25
   16.3740    1.    16   .25    17   .25    34   .25    35   .25
   17.3740    1.    17   .25    18   .25    35   .25    36   .25
   18.3740    1.    19   .25    20   .25    37   .25    38   .25
```

19.3740	1.	20	.25	21	.25	38	.25	39	.25
20.3740	1.	21	.25	22	.25	39	.25	40	.25
21.3740	1.	22	.25	23	.25	40	.25	41	.25
22.3740	1.	23	.25	24	.25	41	.25	42	.25
23.3740	1.	24	.25	25	.25	42	.25	43	.25
24.3740	1.	25	.25	26	.25	43	.25	44	.25
25.3740	1.	26	.25	27	.25	44	.25	45	.25
26.3740	1.	27	.25	28	.25	45	.25	46	.25
27.3740	1.	28	.25	29	.25	46	.25	47	.25
28.3740	1.	29	.25	30	.25	47	.25	48	.25
29.3740	1.	30	.25	31	.25	48	.25	49	.25
30.3740	1.	31	.25	32	.25	49	.25	50	.25
31.3740	1.	32	.25	33	.25	50	.25	51	.25
32.3740	1.	33	.25	34	.25	51	.25	52	.25
33.3740	1.	34	.25	35	.25	52	.25	53	.25
34.3740	1.	35	.25	36	.25	53	.25	54	.25
35.3740	1.	37	.25	38	.25	55	.25	56	.25
36.3740	1.	38	.25	39	.25	56	.25	57	.25
37.3740	1.	39	.25	40	.25	57	.25	58	.25
38.3740	1.	40	.25	41	.25	58	.25	59	.25
39.3740	1.	41	.25	42	.25	59	.25	60	.25
40.3740	1.	42	.25	43	.25	60	.25	61	.25
41.3740	1.	43	.25	44	.25	61	.25	62	.25
42.3740	1.	44	.25	45	.25	62	.25	63	.25
43.3740	1.	45	.25	46	.25	63	.25	64	.25
44.3740	1.	46	.25	47	.25	64	.25	65	.25
45.3740	1.	47	.25	48	.25	65	.25	66	.25
46.3740	1.	48	.25	49	.25	66	.25	67	.25
47.3740	1.	49	.25	50	.25	67	.25	68	.25
48.3740	1.	50	.25	51	.25	68	.25	69	.25
49.3740	1.	51	.25	52	.25	69	.25	70	.25
50.3740	1.	52	.25	53	.25	70	.25	71	.25
51.3740	1.	53	.25	54	.25	71	.25	72	.25
52.3740	1.	55	.25	56	.25	73	.25	74	.25
53.3740	1.	56	.25	57	.25	74	.25	75	.25
54.3740	1.	57	.25	58	.25	75	.25	76	.25
55.3740	1.	58	.25	59	.25	76	.25	77	.25
56.3740	1.	59	.25	60	.25	77	.25	78	.25
57.3740	1.	60	.25	61	.25	78	.25	79	.25
58.3740	1.	61	.25	62	.25	79	.25	80	.25
59.3740	1.	62	.25	63	.25	80	.25	81	.25
60.3740	1.	63	.25	64	.25	81	.25	82	.25
61.3740	1.	64	.25	65	.25	82	.25	83	.25
62.3740	1.	65	.25	66	.25	83	.25	84	.25
63.3740	1.	66	.25	67	.25	84	.25	85	.25
64.3740	1.	67	.25	68	.25	85	.25	86	.25
65.3740	1.	68	.25	69	.25	86	.25	87	.25
66.3740	1.	69	.25	70	.25	87	.25	88	.25
67.3740	1.	70	.25	71	.25	88	.25	89	.25
68.3740	1.	71	.25	72	.25	89	.25	90	.25
69.3740	1.	73	.25	74	.25	91	.25	92	.25
70.3740	1.	74	.25	75	.25	92	.25	93	.25

71.3740	1.	75	.25	76	.25	93	.25	94	.25
72.3740	1.	76	.25	77	.25	94	.25	95	.25
73.3740	1.	77	.25	78	.25	95	.25	96	.25
74.3740	1.	78	.25	79	.25	96	.25	97	.25
75.3740	1.	79	.25	80	.25	97	.25	98	.25
76.3740	1.	80	.25	81	.25	98	.25	99	.25
77.3740	1.	81	.25	82	.25	99	.25	100	.25
78.3740	1.	82	.25	83	.25	100	.25	101	.25
79.3740	1.	83	.25	84	.25	101	.25	102	.25
80.3740	1.	84	.25	85	.25	102	.25	103	.25
81.3740	1.	85	.25	86	.25	103	.25	104	.25
82.3740	1.	86	.25	87	.25	104	.25	105	.25
83.3740	1.	87	.25	88	.25	105	.25	106	.25
84.3740	1.	88	.25	89	.25	106	.25	107	.25
85.3740	1.	89	.25	90	.25	107	.25	108	.25
86.3740	1.	91	.25	92	.25	109	.25	110	.25
87.3740	1.	92	.25	93	.25	110	.25	111	.25
88.3740	1.	93	.25	94	.25	111	.25	112	.25
89.3740	1.	94	.25	95	.25	112	.25	113	.25
90.3740	1.	95	.25	96	.25	113	.25	114	.25
91.3740	1.	96	.25	97	.25	114	.25	115	.25
92.3740	1.	97	.25	98	.25	115	.25	116	.25
93.3740	1.	98	.25	99	.25	116	.25	117	.25
94.3740	1.	99	.25	100	.25	117	.25	118	.25
95.3740	1.	100	.25	101	.25	118	.25	119	.25
96.3740	1.	101	.25	102	.25	119	.25	120	.25
97.3740	1.	102	.25	103	.25	120	.25	121	.25
98.3740	1.	103	.25	104	.25	121	.25	122	.25
99.3740	1.	104	.25	105	.25	122	.25	123	.25
100.3740	1.	105	.25	106	.25	123	.25	124	.25
101.3740	1.	106	.25	107	.25	124	.25	125	.25
102.3740	1.	107	.25	108	.25	125	.25	126	.25
103.3740	1.	109	.25	110	.25	127	.25	128	.25
104.3740	1.	110	.25	111	.25	128	.25	129	.25
105.3740	1.	111	.25	112	.25	129	.25	130	.25
106.3740	1.	112	.25	113	.25	130	.25	131	.25
107.3740	1.	113	.25	114	.25	131	.25	132	.25
108.3740	1.	114	.25	115	.25	132	.25	133	.25
109.3740	1.	115	.25	116	.25	133	.25	134	.25
110.3740	1.	116	.25	117	.25	134	.25	135	.25
111.3740	1.	117	.25	118	.25	135	.25	136	.25
112.3740	1.	118	.25	119	.25	136	.25	137	.25
113.3740	1.	119	.25	120	.25	137	.25	138	.25
114.3740	1.	120	.25	121	.25	138	.25	139	.25
115.3740	1.	121	.25	122	.25	139	.25	140	.25
116.3740	1.	122	.25	123	.25	140	.25	141	.25
117.3740	1.	123	.25	124	.25	141	.25	142	.25
118.3740	1.	124	.25	125	.25	142	.25	143	.25
119.3740	1.	125	.25	126	.25	143	.25	144	.25
120.3740	1.	127	.25	128	.25	145	.25	146	.25
121.3740	1.	128	.25	129	.25	146	.25	147	.25
122.3740	1.	129	.25	130	.25	147	.25	148	.25

123.3740	1.	130	.25	131	.25	148	.25	149	.25
124.3740	1.	131	.25	132	.25	149	.25	150	.25
125.3740	1.	132	.25	133	.25	150	.25	151	.25
126.3740	1.	133	.25	134	.25	151	.25	152	.25
127.3740	1.	134	.25	135	.25	152	.25	153	.25
128.3740	1.	135	.25	136	.25	153	.25	154	.25
129.3740	1.	136	.25	137	.25	154	.25	155	.25
130.3740	1.	137	.25	138	.25	155	.25	156	.25
131.3740	1.	138	.25	139	.25	156	.25	157	.25
132.3740	1.	139	.25	140	.25	157	.25	158	.25
133.3740	1.	140	.25	141	.25	158	.25	159	.25
134.3740	1.	141	.25	142	.25	159	.25	160	.25
135.3740	1.	142	.25	143	.25	160	.25	161	.25
136.3740	1.	143	.25	144	.25	161	.25	162	.25
137.3740	1.	145	.25	146	.25	163	.25	164	.25
138.3740	1.	146	.25	147	.25	164	.25	165	.25
139.3740	1.	147	.25	148	.25	165	.25	166	.25
140.3740	1.	148	.25	149	.25	166	.25	167	.25
141.3740	1.	149	.25	150	.25	167	.25	168	.25
142.3740	1.	150	.25	151	.25	168	.25	169	.25
143.3740	1.	151	.25	152	.25	169	.25	170	.25
144.3740	1.	152	.25	153	.25	170	.25	171	.25
145.3740	1.	153	.25	154	.25	171	.25	172	.25
146.3740	1.	154	.25	155	.25	172	.25	173	.25
147.3740	1.	155	.25	156	.25	173	.25	174	.25
148.3740	1.	156	.25	157	.25	174	.25	175	.25
149.3740	1.	157	.25	158	.25	175	.25	176	.25
150.3740	1.	158	.25	159	.25	176	.25	177	.25
151.3740	1.	159	.25	160	.25	177	.25	178	.25
152.3740	1.	160	.25	161	.25	178	.25	179	.25
153.3740	1.	161	.25	162	.25	179	.25	180	.25
154.3740	1.	163	.25	164	.25	181	.25	182	.25
155.3740	1.	164	.25	165	.25	182	.25	183	.25
156.3740	1.	165	.25	166	.25	183	.25	184	.25
157.3740	1.	166	.25	167	.25	184	.25	185	.25
158.3740	1.	167	.25	168	.25	185	.25	186	.25
159.3740	1.	168	.25	169	.25	186	.25	187	.25
160.3740	1.	169	.25	170	.25	187	.25	188	.25
161.3740	1.	170	.25	171	.25	188	.25	189	.25
162.3740	1.	171	.25	172	.25	189	.25	190	.25
163.3740	1.	172	.25	173	.25	190	.25	191	.25
164.3740	1.	173	.25	174	.25	191	.25	192	.25
165.3740	1.	174	.25	175	.25	192	.25	193	.25
166.3740	1.	175	.25	176	.25	193	.25	194	.25
167.3740	1.	176	.25	177	.25	194	.25	195	.25
168.3740	1.	177	.25	178	.25	195	.25	196	.25
169.3740	1.	178	.25	179	.25	196	.25	197	.25
170.3740	1.	179	.25	180	.25	197	.25	198	.25
171.3740	1.	181	.25	182	.25	199	.25	200	.25
172.3740	1.	182	.25	183	.25	200	.25	201	.25
173.3740	1.	183	.25	184	.25	201	.25	202	.25
174.3740	1.	184	.25	185	.25	202	.25	203	.25

175.3740	1.	185	.25	186	.25	203	.25	204	.25
176.3740	1.	186	.25	187	.25	204	.25	205	.25
177.3740	1.	187	.25	188	.25	205	.25	206	.25
178.3740	1.	188	.25	189	.25	206	.25	207	.25
179.3740	1.	189	.25	190	.25	207	.25	208	.25
180.3740	1.	190	.25	191	.25	208	.25	209	.25
181.3740	1.	191	.25	192	.25	209	.25	210	.25
182.3740	1.	192	.25	193	.25	210	.25	211	.25
183.3740	1.	193	.25	194	.25	211	.25	212	.25
184.3740	1.	194	.25	195	.25	212	.25	213	.25
185.3740	1.	195	.25	196	.25	213	.25	214	.25
186.3740	1.	196	.25	197	.25	214	.25	215	.25
187.3740	1.	197	.25	198	.25	215	.25	216	.25
188.3740	1.	199	.25	200	.25	217	.25	218	.25
189.3740	1.	200	.25	201	.25	218	.25	219	.25
190.3740	1.	201	.25	202	.25	219	.25	220	.25
191.3740	1.	202	.25	203	.25	220	.25	221	.25
192.3740	1.	203	.25	204	.25	221	.25	222	.25
193.3740	1.	204	.25	205	.25	222	.25	223	.25
194.3740	1.	205	.25	206	.25	223	.25	224	.25
195.3740	1.	206	.25	207	.25	224	.25	225	.25
196.3740	1.	207	.25	208	.25	225	.25	226	.25
197.3740	1.	208	.25	209	.25	226	.25	227	.25
198.3740	1.	209	.25	210	.25	227	.25	228	.25
199.3740	1.	210	.25	211	.25	228	.25	229	.25
200.3740	1.	211	.25	212	.25	229	.25	230	.25
201.3740	1.	212	.25	213	.25	230	.25	231	.25
202.3740	1.	213	.25	214	.25	231	.25	232	.25
203.3740	1.	214	.25	215	.25	232	.25	233	.25
204.3740	1.	215	.25	216	.25	233	.25	234	.25
205.3740	1.	217	.25	218	.25	235	.25	236	.25
206.3740	1.	218	.25	219	.25	236	.25	237	.25
207.3740	1.	219	.25	220	.25	237	.25	238	.25
208.3740	1.	220	.25	221	.25	238	.25	239	.25
209.3740	1.	221	.25	222	.25	239	.25	240	.25
210.3740	1.	222	.25	223	.25	240	.25	241	.25
211.3740	1.	223	.25	224	.25	241	.25	242	.25
212.3740	1.	224	.25	225	.25	242	.25	243	.25
213.3740	1.	225	.25	226	.25	243	.25	244	.25
214.3740	1.	226	.25	227	.25	244	.25	245	.25
215.3740	1.	227	.25	228	.25	245	.25	246	.25
216.3740	1.	228	.25	229	.25	246	.25	247	.25
217.3740	1.	229	.25	230	.25	247	.25	248	.25
218.3740	1.	230	.25	231	.25	248	.25	249	.25
219.3740	1.	231	.25	232	.25	249	.25	250	.25
220.3740	1.	232	.25	233	.25	250	.25	251	.25
221.3740	1.	233	.25	234	.25	251	.25	252	.25
222.3740	1.	235	.25	236	.25	253	.25	254	.25
223.3740	1.	236	.25	237	.25	254	.25	255	.25
224.3740	1.	237	.25	238	.25	255	.25	256	.25
225.3740	1.	238	.25	239	.25	256	.25	257	.25
226.3740	1.	239	.25	240	.25	257	.25	258	.25

227.3740	1.	240	.25	241	.25	258	.25	259	.25
228.3740	1.	241	.25	242	.25	259	.25	260	.25
229.3740	1.	242	.25	243	.25	260	.25	261	.25
230.3740	1.	243	.25	244	.25	261	.25	262	.25
231.3740	1.	244	.25	245	.25	262	.25	263	.25
232.3740	1.	245	.25	246	.25	263	.25	264	.25
233.3740	1.	246	.25	247	.25	264	.25	265	.25
234.3740	1.	247	.25	248	.25	265	.25	266	.25
235.3740	1.	248	.25	249	.25	266	.25	267	.25
236.3740	1.	249	.25	250	.25	267	.25	268	.25
237.3740	1.	250	.25	251	.25	268	.25	269	.25
238.3740	1.	251	.25	252	.25	269	.25	270	.25
239.3740	1.	253	.25	254	.25	271	.25	272	.25
240.3740	1.	254	.25	255	.25	272	.25	273	.25
241.3740	1.	255	.25	256	.25	273	.25	274	.25
242.3740	1.	256	.25	257	.25	274	.25	275	.25
243.3740	1.	257	.25	258	.25	275	.25	276	.25
244.3740	1.	258	.25	259	.25	276	.25	277	.25
245.3740	1.	259	.25	260	.25	277	.25	278	.25
246.3740	1.	260	.25	261	.25	278	.25	279	.25
247.3740	1.	261	.25	262	.25	279	.25	280	.25
248.3740	1.	262	.25	263	.25	280	.25	281	.25
249.3740	1.	263	.25	264	.25	281	.25	282	.25
250.3740	1.	264	.25	265	.25	282	.25	283	.25
251.3740	1.	265	.25	266	.25	283	.25	284	.25
252.3740	1.	266	.25	267	.25	284	.25	285	.25
253.3740	1.	267	.25	268	.25	285	.25	286	.25
254.3740	1.	268	.25	269	.25	286	.25	287	.25
255.3740	1.	269	.25	270	.25	287	.25	288	.25
256.3740	1.	271	.25	272	.25	289	.25	290	.25
257.3740	1.	272	.25	273	.25	290	.25	291	.25
258.3740	1.	273	.25	274	.25	291	.25	292	.25
259.3740	1.	274	.25	275	.25	292	.25	293	.25
260.3740	1.	275	.25	276	.25	293	.25	294	.25
261.3740	1.	276	.25	277	.25	294	.25	295	.25
262.3740	1.	277	.25	278	.25	295	.25	296	.25
263.3740	1.	278	.25	279	.25	296	.25	297	.25
264.3740	1.	279	.25	280	.25	297	.25	298	.25
265.3740	1.	280	.25	281	.25	298	.25	299	.25
266.3740	1.	281	.25	282	.25	299	.25	300	.25
267.3740	1.	282	.25	283	.25	300	.25	301	.25
268.3740	1.	283	.25	284	.25	301	.25	302	.25
269.3740	1.	284	.25	285	.25	302	.25	303	.25
270.3740	1.	285	.25	286	.25	303	.25	304	.25
271.3740	1.	286	.25	287	.25	304	.25	305	.25
272.3740	1.	287	.25	288	.25	305	.25	306	.25
273.3740	1.	289	.25	290	.25	307	.25	308	.25
274.3740	1.	290	.25	291	.25	308	.25	309	.25
275.3740	1.	291	.25	292	.25	309	.25	310	.25
276.3740	1.	292	.25	293	.25	310	.25	311	.25
277.3740	1.	293	.25	294	.25	311	.25	312	.25
278.3740	1.	294	.25	295	.25	312	.25	313	.25

```
   279.3740   1.  295  .25  296  .25  313  .25  314  .25
   280.3740   1.  296  .25  297  .25  314  .25  315  .25
   281.3740   1.  297  .25  298  .25  315  .25  316  .25
   282.3740   1.  298  .25  299  .25  316  .25  317  .25
   283.3740   1.  299  .25  300  .25  317  .25  318  .25
   284.3740   1.  300  .25  301  .25  318  .25  319  .25
   285.3740   1.  301  .25  302  .25  319  .25  320  .25
   286.3740   1.  302  .25  303  .25  320  .25  321  .25
   287.3740   1.  303  .25  304  .25  321  .25  322  .25
   288.3740   1.  304  .25  305  .25  322  .25  323  .25
   289.3740   1.  305  .25  306  .25  323  .25  324  .25
  3.0 .059 655. .3224  10.  0.1 409..02241000. .374
 slab     1    2    8
     1                         5000.
     1     11.860               2    2    1    8    1
     2     11.860               1    3    1
     3     11.860               1    4    1
     4     11.860               1    5    1
     5     11.860               1    6    1
     6     11.860               1    7    1
     7     11.860               1    8    1
     8     11.860
     1       141.      .5591
     2       158.      .4961
     1    9    1    1    1    1    2    2    1    3    2    1    4    2
               1    5    2    1    6    2    1    7    2    1    8    2
               1    9    2
     2    9    1   10    2    1   11    2    1   12    2    1   13    2
               1   14    2    1   15    2    1   16    2    1   17    2
               1   18    1
     3    9    1   18    1    1   36    2    1   54    2    1   72    2
               1   90    2    1  108    2    1  126    2    1  144    2
               1  162    2
     4    9    1  180    2    1  198    2    1  216    2    1  234    2
               1  252    2    1  270    2    1  288    2    1  306    2
               1  324    1
     5    9    1  316    2    1  317    2    1  318    2    1  319    2
               1  320    2    1  321    2    1  322    2    1  323    2
               1  324    1
     6    9    1  307    1    1  308    2    1  309    2    1  310    2
               1  311    2    1  312    2    1  313    2    1  314    2
               1  315    2
     7    9    1  163    2    1  181    2    1  199    2    1  217    2
               1  235    2    1  253    2    1  271    2    1  289    2
               1  307    1
     8    9    1    1    1    1   19    2    1   37    2    1   55    2
               1   73    2    1   91    2    1  109    2    1  127    2
               1  145    2

radg      1    1
    1     1    8    1    2    3    4    5    6    7    8
heat      1    0    1
```

```
                 1.00                    1.00
 12.3
drag      1
 100. -1.0                 100. -1.0   .05
bdry      1    1    8    0
    1  1.00E+8
    1    2 0.0 204.8 1.0 204.8
    1    14.921    1
    1  1.0    1  1.0    1
    2    14.921    1
    1  1.0    1  1.0    1
    3    14.921    1
    1  1.0    1  1.0    1
    4    14.921    1
    1  1.0    1  1.0    1
    5    14.921    1
    1  1.0    1  1.0    1
    6    14.921    1
    1  1.0    1  1.0    1
    7    14.921    1
    1  1.0    1  1.0    1
    8    14.921    1
    1  1.0    1  1.0    1
calc      1
   0.                                                  0.25
        20
oper      1    0    3                                                       1
 0.0            400.     .0      .0073437       400.
   10
   0.  0.0.0499  0.0  .05 .706  .151.029  .251.206  .751.206
  .851.029.9499 .706  .95  0.0  1.0  0.0
outp 1101
endd
```

APPENDIX 10

17x17 BUNDLE ANALYSIS—INPUT FILE FOR RADGEN (Cycle 2)

```
     0
Korean Spent Fuel Cask -- KSC-7 (17*17)
     01.326    17    17
  .374 .372 .372 .372 .372
   0.8  0.3
    -1
     0
```